U.PORTO

MESTRADO
MEDICINA E ONCOLOGIA MOLECULAR

Evaluation of the role of genetic alterations and miRNA expression in the prognosis of thyroid neoplasms

Ana Soraia Barbosa Gonçalves

M

2020

Dissertação de candidatura ao grau de Mestre em Medicina e Oncologia Molecular,

apresentada à Faculdade de Medicina da Universidade do Porto

Evaluation of the role of genetic alterations and miRNA expression in the prognosis of thyroid neoplasms

Ana Soraia Barbosa Gonçalves

Supervisor:
Mafalda Pinto, MSc, PhD

IPATIMUP (http://www.ipatimup.pt)
Rua Júlio Amaral de Carvalho, 45 4200-135 Porto, Portugal
I3S - Instituto de Investigação e Inovação em Saúde, Universidade do Porto (www.i3s.up.pt), Rua Alfredo Allen, 208, 4200-135 Porto
E-mail: mafaldap@ipatimup.pt

Co-supervisor:
Paula Soares, MSc, PhD

Assistant Professor at Faculty of Medicine of the University of Porto
Alameda Prof. Hernâni Monteiro, 4200-319 Porto, Portugal, Telf: 22 551 3600
Group leader of the Cancer Signaling and Metabolism group at Institute of Pathology and Immunology of the University of Porto/ Institute of Research and Innovation in Health of the University of Porto (IPATIMUP/i3S)
Senior Investigator at IPATIMUP/i3S
Rua Alfredo Allen, 208 | 4200-135 Porto, Portugal, Telf: +351 220 408 800
E-mail: psoares@ipatimup.pt

‘’Sans la curiosité de l'esprit, que serions-nous? Telle est bien la beauté et la noblesse de la science: désir sans fin de repousser les frontières du savoir, de traquer les secrets de la matière et de la vie sans idée préconçue des conséquences éventuelles.’’

Marie Curie

Agradecimentos

A vida é feita de etapas. Estes últimos dois anos foram prova disso. Grandes mudanças, escolhas e um turbilhão de emoções.

A vida também é feita de agradecimentos e eu tenho muito a agradecer. Obrigada professora Paula Soares, por me ter aceite no seu grupo de investigação e pela sua orientação.

Mafalda, obrigada pela sua orientação e paciência. Obrigada por partilhar momentos comigo, por me animar e dizer que sou capaz.

Obrigada MJ, por naquele dia perguntares "Queres almoçar connosco?" e tornares esta aventura mais feliz. Graças a ti fiz um grupo de amigas incríveis. MJ, Riquinha, Mila, Bela, Aninha, obrigada pela amizade! Pelos bons momentos que passamos juntas, pelas risadas até doer a barriga, pelas conversas, por tudo.

Um agradecimento muito especial para a Sule, Paula Boaventura e Rui pela vossa ajuda, atenção e disponibilidade. Sou-vos muito grata.

Obrigada Elisabete. Obrigada pelas tuas palavras. Obrigada pela tua calma, pela tua ajuda e pela tua amizade.

Obrigada Sofia e Tiago pela vossa amizade, companhia e pelas gargalhadas. Obrigada por me ajudarem. Por relativizarem e mostrarem que a vida é bela!

Carol e Catarina, companheiras nesta aventura, obrigada. Agradeço a vossa companhia, as conversas, as gargalhadas e os chocolates de sexta-feira!

Agradeço aos meus pais e irmão. Obrigada por estarem sempre do meu lado. Por nunca me prenderem e por alimentarem sempre as minhas aventuras. "Vai, força! Se não correr bem, sabes sempre onde voltar!"

Agradeço à minha família todo o apoio. Toda a ajuda nestes dois anos. Obrigada por sacrificarem as vossas férias num projeto maior da minha vida. Obrigada por

tentarem aliviar as minhas preocupações dizendo: “Vai descansada! Se tens de ir trabalhar, vai! Nós cá continuamos para te ajudar.” Sou-vos eternamente grata.

Agradeço aos meus amigos, companheiros de uma vida, por terem sempre uma palavra de carinho nos momentos mais difíceis. Por ficarem felizes com os meus passos. Caminhamos juntos, sempre.

Merci mon petit bout de chou pour illuminer ma vie. J’espère un jour, que tu seras fière de Tata. Je t’aime très fort.

Merci à tous les amis, en France, qui m’ont soutenue les dernières années. Merci pour votre amitié, votre confiance et votre gentillesse.

Merci á toi, pour tout ce que tu m’as donnée. Pour l’opportunité. Pour tout ce que j’ai réussi dans la vie. Je te serais reconnaissante pour le reste de ma vie.

Obrigada, a ti, meu companheiro. Por caminhares junto comigo, sem nunca desistir. Por seres o responsável disto tudo e acreditares em mim. És luz na minha vida.

Table of Contents

Figures index

Table index

Supplementary tables

Abbreviations List

A

AJCC	American joint committee on cancer
ATC	Anaplastic thyroid carcinoma

B

BCL-2	B-cell lymphoma 2
BRAF	V-raf murine sarcoma viral oncogenes homolog B1

C

cAMP	Cyclic adenosine monophosphate
cDNA	Complementary deoxyribonucleic acid
c-PTC	Conventional PTC
CT	Threshold cycle

E

ERK	Extracellular-signal-regulated kinase
ETS	E-twenty-six
EV-PTC	Encapsulated variant of papillary thyroid carcinoma

F

FFPE	Formalin-fixed paraffin-embedded
FNAB	Fine-needle aspiration biopsy
FTA	Follicular thyroid adenoma
FTC	Follicular thyroid carcinoma
FV-PTC	Follicular variant of papillary thyroid carcinoma

G

GF	Growth factor

H

h*TERT*	Human telomerase reverse transcriptase
HCC	Hürthle cell carcinoma
HPF	High power fields
HR	Histological review

I

IARC	International agency for research on cancer

L

LNM	Lymph node metastasis

M

MAPK	Mitogen-activated protein kinase
MEK	Mitogen-activated protein kinase kinase

microPTC	Papillary thyroid microcarcinoma
MTC	Medullary thyroid carcinoma

N

ND	Non-diagnostic
NIFTP	Noninvasive follicular thyroid neoplasm with papillary-like nuclear features
NTC	Non-template control

O

OV-PTC	Oncocytic variant of papillary thyroid carcinoma

P

PCR	Polymerase chain reaction
PTC	Papillary thyroid carcinoma
PDTC	Poorly differentiated thyroid carcinoma
PI3K	Phosphoinositide 3-kinase

R

RAI	Radioactive iodine
RAS	Rat sarcoma viral oncogenes homologue
RET	Rearranged during transfection
RT	Reverse transcription

S

SCNs	Solid cell nests
SV-PTC	Solid variant of papillary thyroid carcinoma

T

TC-PTC	Tall cell variant of papillary thyroid carcinoma
TKR	Tyrosine kinase receptor
T3	Triiodothyronine
T4	Thyroxine
TH	Thyroid hormones
TPC-1	Thyroid papillary carcinoma cell line
TRH	Thyrotropin-releasing hormone
TSH	Thyroid-stimulating hormone
TSHR	Thyroid-stimulating hormone receptor
TREs	Thyroid hormone response elements
TC	Thyroid cancer

W

WDTC	Well differentiated thyroid carcinoma
WDT-UMP	Well differentiated tumor with uncertain malignant potential
WHO	World health organization
WT	Wild-type

Resumo

O cancro da tiróide é a neoplasia endócrina mais comum no mundo. A sua incidência tem aumentado nas últimas décadas, afetando com maior frequência as mulheres. O cancro da tiróide apresenta uma grande variedade de lesões benignas e malignas, levando a diferenças no prognóstico. O aumento da incidência é mais prevalente no carcinoma papilar da tiróide (CPT), a neoplasia maligna mais comum. Antes da cirurgia, os métodos de diagnóstico existentes para o cancro de tiróide são a ultrassonografia, seguido da punção aspirativa por agulha fina (PAAF). A PAAF é o teste pré-cirúrgico mais preciso, económico e minimamente invasivo para diagnóstico, diferenciando nódulos benignos e malignos, o que permite um encaminhamento mais preciso de cada paciente. No entanto, cerca de 30% das PAAF são classificadas como nódulos indeterminados ou lesões "grey zone", o que torna que a decisão do diagnóstico de extrema importância para o seguimento do paciente por forma a evitar cirurgias desnecessárias.

Vários estudos recomendam o uso de testes moleculares para um diagnóstico preciso de malignidade. O desenvolvimento do cancro da tiróide tem sido associado à ativação de oncogenes, (*TERT*p, *BRAF* e *RAS* (*NRAS*, *HRAS* e *KRAS*)), que levam à ativação de vias de sinalização celular, interferindo no desenvolvimento do tumor e no prognóstico do doente. Também o envolvimento de microRNAs no cancro da tiróide foi recentemente reconhecido como tendo um papel importante no desenvolvimento e progressão do tumor.

Este estudo tem como objetivo avaliar o papel de alterações genéticas (*TERT*p, *BRAF* e *RAS* (*NRAS*, *HRAS* e *KRAS*)) e da expressão de miRNAs (miR146b, miR221, miR222 e miR15a), em PAAF e tecido cirúrgico fixado em formol e embebido em parafina (FFPE) correspondente, numa série consecutiva de tumores da tiróide para perceber o valor de diagnóstico destas alterações em PAAFs.

A série neste estudo foi composta por uma amostra de PAAF e pelo tecido FFPE correspondente de 90 pacientes consecutivos com tumor da tiróide. As alterações genéticas foram avaliadas por reação em cadeia da polimerase (PCR), seguida pela

sequenciação de DNA. A expressão de miRNAs foi avaliada utilizando a PCR quantitativo em tempo real (qRT-PCR). As associações entre as alterações genéticas e as características histopatológicas foram avaliadas.

As percentagens de mutações encontradas para as amostras de citologia e histologia foram, respetivamente: *TERT*p: 6.7% e 9.1%; *BRAF*: 24.7% e 24.4%; *NRAS*: 5.6% e 5.6%; *HRAS*: 3.3% e 4.4%; e *KRAS*: 0% e 2.2%. Os resultados obtidos demonstraram uma boa correlação cito-histológica (76.7%). Os nossos dados apresentam várias associações estatisticamente significativas entre as características clinico-patológicas e moleculares dos tumores. As mutações do *BRAF* foram associadas com características clinico-patológicas de mau prognóstico e o mesmo foi observado com a presença de mutações concomitantes na *TERT*p+*BRAF*. Ao contrário, as mutações no *RAS* foram associadas com um melhor prognóstico do doente. Demonstramos uma tendência para uma sobre-expressão em todos os miRNAs analisados sendo esta sobre-expressão estatisticamente significativa para o miR221 e miR222 ($p<0.001$).

Palavras-chave: Cancro da tiróide, Carcinoma Papilar da Tiróide, Marcadores moleculares, Punção aspirativa por agulha fina, Tecidos fixados em formol e embebidos em parafina, microRNAs.

Abstract

Thyroid cancer (TC) is the most common endocrine malignancy worldwide. Its incidence has been increasing over the last decades, affecting more frequently women. TC comprises a large range of benign and malignant lesions, leading to prognostic differences. The increased incidence is more prevalent in the papillary thyroid carcinoma (PTC) subtype, the most common thyroid malignancy. Before surgery, the existing diagnostic tools for thyroid cancer are ultrasonography, followed by a fine-needle aspiration biopsy (FNAB). FNAB is the most accurate, cost-effective and minimal invasive preoperative test to distinguish benign from malignant thyroid nodules, aiming to resolve patient management. However, up to 30% of FNABs are classified as indeterminate nodules or "grey zone" lesions, making the decision on patient management crucial to avoid unnecessary surgeries.

Several studies recommend the use of molecular tests for a complete diagnosis of malignancy. The development of TC has been associated with the activation of oncogenes (*TERT*p, *BRAF* and *RAS* (*NRAS*, *HRAS* and *KRAS*)), that are implicated in the cell signaling pathway, interfering in cancer promotion and outcome. Moreover, the involvement of microRNAs in TC has been recently identified as being important in tumor development and progression.

This study aims to evaluate the value of genetic alterations (*TERT*p, *BRAF* and *RAS* (*NRAS*, *HRAS* and *KRAS*)) and miRNAs (miR146b, miR221, miR222 and miR15a) expression in the improvement of TC diagnosis and prognosis by using correspondent FNAB and formalin-fixed paraffin embedded (FFPE) samples. It also aims to establish a detection method for miRNA extraction in FNAB samples as well and to validate the diagnostic value of FNABs by tumor's cyto-histologic molecular correlation.

The series in this study was composed by one FNAB and corresponding FFPE tissue from 90 consecutive patients. The genetic alterations were examined by polymerase chain reaction (PCR), followed by DNA sequencing. The miRNA expression was detected using quantitative reverse transcriptase-polymerase chain reaction (qRT-

PCR). The association of the genetic alterations with clinicopathologic features was evaluated.

We found mutation frequencies in cytology and histology specimens, as follow, *TERT*p: 6.7% and 9.1%; *BRAF*: 24.7% and 24.4%; *NRAS*: 5.6% and 5.6%; *HRAS*: 3.3% and 4.4%; and *KRAS*: 0% and 2.2%, respectively. A good cyto-histologic correlation was obtained (76.7%). Our data presents several statistically significant associations between the clinicopathological and molecular features of the tumors. *BRAF* mutations were associated with poor clinicopathological features and the same was observed for the presence of concomitant *TERT*p+*BRAF* mutations. On contrary, *RAS* mutations were associated with a better patient outcome. We show a tendency for all analyzed miRNAs to be upregulated and that reached statistical significance for miR221 and miR222 (p<0.001).

Keywords: Thyroid cancer, Papillary thyroid cancer, Molecular markers, FNAB, FFPE tissue, miRNAs.

Introduction

1. Thyroid gland: anatomy, function, and physiology

The growth and development of the thyroid gland begins at the third week of gestation [1]. The thyroid's name originated from the Greek word *thyreoeidos* (Thyreos – sheild, eidos – from), due to its similarity to a shield [2, 3].

The thyroid gland is a highly vascularized organ, composed by two lobes connected by a isthmus and is placed at the base of the throat anterior to the trachea [2, 4]. The gland weighs approximately 15g to 25g and the lobes measure about 4 cm in length, 2 cm in width, and 2–3 cm in thickness [3].

Thyroid gland is composed by two types of endocrine cells: follicular and parafollicular cells (Figure 1). Follicular cells or thyrocytes form a large number of close follicles, which are filled by colloid, surrounded by a monolayer of epithelial cells [2, 4]. These cells are responsible for the production and storage of thyroid hormones (TH) *triiodothyronine* (T3) and *thyroxine* (T4), which are vital for the development and growth, having important functions in body weight, metabolic regulation and thermogenesis [2, 5].

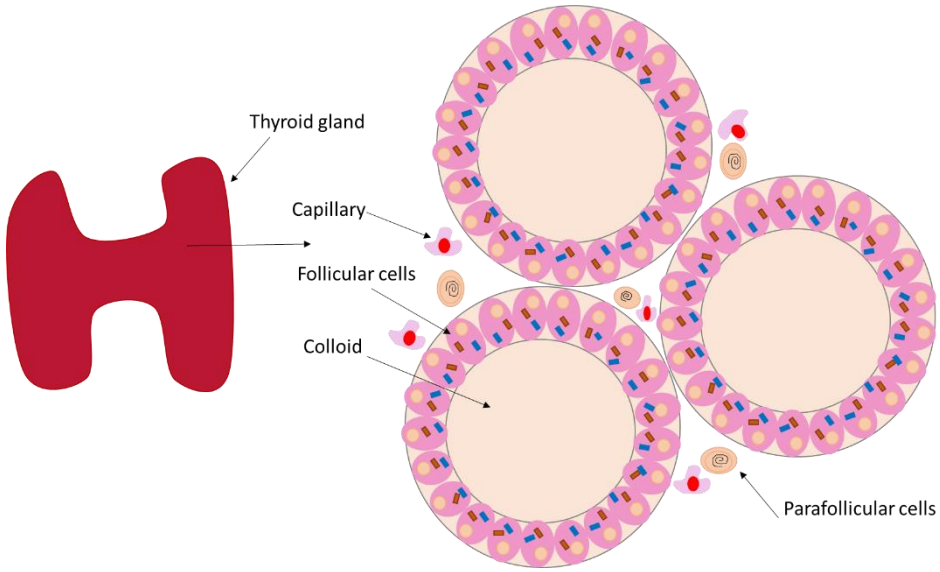

Figure 1. Illustration of thyroid gland cells and tissue organization.

The thyroid basal function is mediated by a homeostasis between the hypothalamus, the pituitary gland and the thyroid itself. This regulation involves the release of thyrotropin-releasing hormone (TRH) by the hypothalamus, which promotes the secretion of thyroid-stimulating hormone (TSH) by the pituitary. TSH binds to its receptor (TSHR), leading to a conformational change that causes the activation of G proteins, increases the levels of cyclic adenosine monophosphate (cAMP), promoting cellular differentiation and function, and culminating in the release of T3 and T4 into the bloodstream. This process is also regulated by a negative feedback loop since high levels of thyroid hormones suppress the secretion of TSH (Figure 2) [4, 6]. The interaction of T3 and T4 with the thyroid hormone receptor (TR) forms a complex that migrates into the nucleus and binds to the thyroid hormone response elements (TREs) to initiate the transcription of target genes.

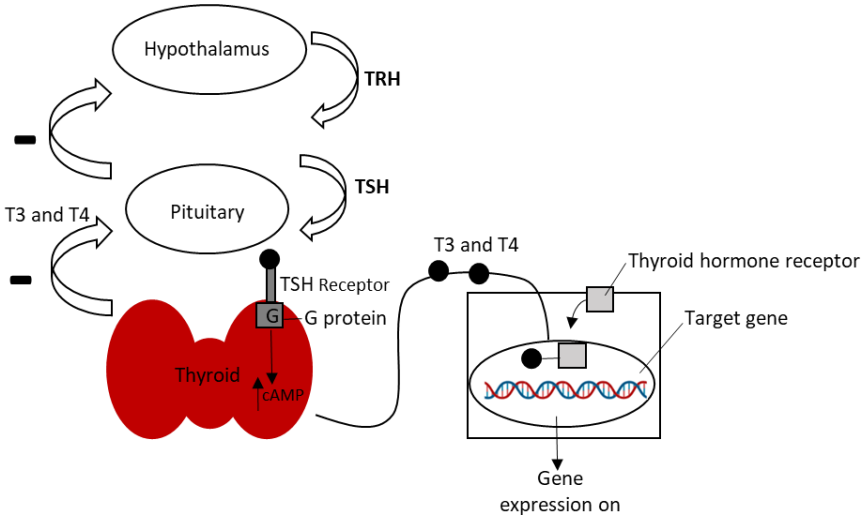

Figure 2. Mechanism of synthesis and function of thyroid hormones T3 and T4.

Parafollicular cells or C cells, located between the follicles, are responsible for the production and secretion of a hypocalcemic hormone: calcitonin [7].

Thyroid diseases include structural and functional thyroid abnormalities. The most frequent are hypo and hyperthyroidism which are characterized by a deficiency and an excessive production of thyroid hormone, respectively, and nodular lesions. Thyroid nodular lesions are the focus of this study and will be explored below [4, 8].

2. Thyroid Cancer: Epidemiology

Cancer is one of the leading causes of death in the 21st century mostly due to growth and aging of the population, particularly in developed countries. According to the International Agency for Research on Cancer (IARC), in 2018 about 18 million new patients were diagnosed with cancer and almost 10 million patients died worldwide [9].

Concerning endocrine organs, thyroid cancer (TC) is the most common malignancy and its incidence has increased worldwide over the last decades [10]. As documented by the IARC, TC ranks ninth in terms of cancer incidence with 567.233 (3.1%) new cases and 41.071 (0.4%) deaths worldwide in 2018 [9, 11]. Concerning gender, 77% (436.344) occurred in females and 23% (130.889) in males displaying a predominance in women with an incidence 3-folds higher than in men (Figure 3) [11].

In Portugal the incidence of TC ranks eighth with 1701 (2.9%) new cases in 2018: 1400 in women and 301 in men, while the mortality rates stayed relatively constant [12]. However, in Portugal, women TC is the third most frequent malignancy according to the Oncologic Regional Registry of the North database [*Registo Oncológico Regional do Norte* (RORENO)] [13] and the numbers are expected to rise during the next decades, due to the increased diagnosis intensity and lifestyle habits (further explained below) [14].

It is also estimated by the IARC that in 2030 there will be an increase of about 100 thousand new cases worldwide and almost 16 thousand deaths from TC and this might be due to the indolence of this pathology.

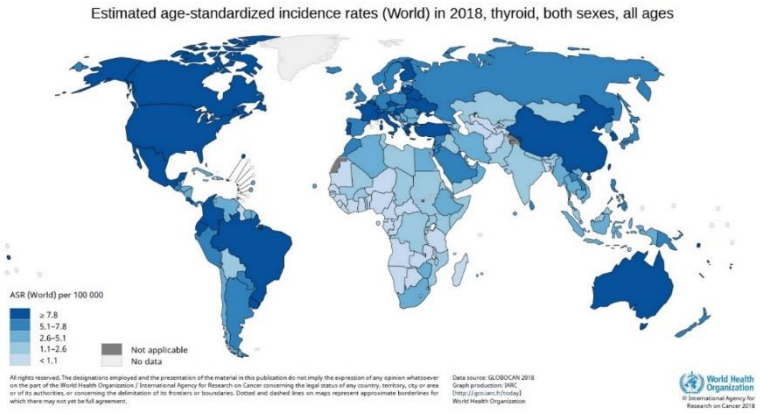

Figure 3. Thyroid cancer distribution around the world.

This pathology can occur at any age, being its incidence peak between 45 to 49 years in women and 65 to 69 in men [15, 16].

3. Thyroid Cancer: Etiology

The incidence of thyroid tumors is increasing. It is mandatory to understand if this boost is due to the improved imaging diagnostic methods, overdiagnosis or lifestyle habits [17, 18].

3.1 Radiation exposure

Radiation causes DNA double-strand breaks and somatic mutations which makes it a risk factor for cancer development. The location of the thyroid in the body makes it vulnerable to irradiation when compared to other organs. Moreover, the exposure of the gland to different diagnostics procedures like x-rays, computed tomography scan, as well as the use of iodinated contrast agents, contributes to a higher absorption of radiation [19]. The radiosensitivity of the thyroid gland is higher at early ages. Children exposed to ionizing radiation have been associated with a higher risk of developing TC, more specifically papillary thyroid carcinoma (PTC), as seen after Chernobyl accident in 1986. This nuclear accident released excessive amount of radioactive iodine to the atmosphere resulting a peak of PTC cases in children [20, 21].

3.2 Iodine Intake

Iodine is important for the production of thyroid hormones and in a healthy human body it is concentrated in the thyroid. Iodine intake can influence TSH levels as well as the development and histotype of TC. In areas of iodine sufficiency, the TSH serum levels decrease and increases the PTC incidence. On contrary, iodine deficit causes a high TSH serum levels which are associated with development of follicular thyroid carcinoma (FTC) [22, 23].

3.3 Environmental factors

It as has been described that lifestyle, reproductive factors, nutrition, obesity, and smoking can promote cancer in thyroid gland.

The excessive weight of people can lead to insulin resistance and hyperinsulinemia. These features are linked to TC since the proliferation and differentiation of thyrocytes are regulated by insulin. However, the influence of insulin resistance on the promotion of TC are not well established [21, 24].

4. Thyroid Cancer: Prognostic factors

The prognosis of TC patient's is known usually excellent with a 10 year survival rate of more than 90% [25]. However, there are several clinical factors influencing the prognosis of TC such as patients' age and gender, histology and size of the tumor, presence of lymph node metastasis (LNM) and molecular alterations.

The age of the patient at diagnosis is an important prognostic factor. According to the last update of the American Joint Committee on Cancer (AJCC/TNM 8th edition) the age cutoff has been updated from 45 to 55 years, proposing more accurate prognosis [26]. Females have an earlier onset and a 3-fold higher rate of TC than men. However, thyroid malignancies in male gender are associated with a worst prognosis and higher mortality rates [27].

Tumor size and histologic features as well as the presence of LNM are factors with an important role on prognosis and with a high clinical impact [28].

Molecular alterations in genes involved in different pathways have been described as prognostic factors increasing the risk for development of LNM, and higher risk for disease specific mortality [28]. This subject will be further explored in this study.

5. Thyroid Cancer: Histotypes

As previously mentioned, thyroid gland is composed by two types of cells (Figure 1): follicular cells and parafollicular cells and both give rise to tumors with different clinical and histological features.

Follicular cells give rise to benign lesions, the follicular adenomas (FTA), and to malignant lesions, comprising the well differentiated thyroid carcinoma (WDTC), poorly differentiated (PDTC) and anaplastic thyroid carcinoma (ATC). WDTC includes papillary thyroid carcinoma (PTC), follicular thyroid carcinoma (FTC) and Hürthle cell carcinoma

(HCC). Parafollicular cells give rise to medullary thyroid carcinoma (MTC) [29, 30] (Figure 4).

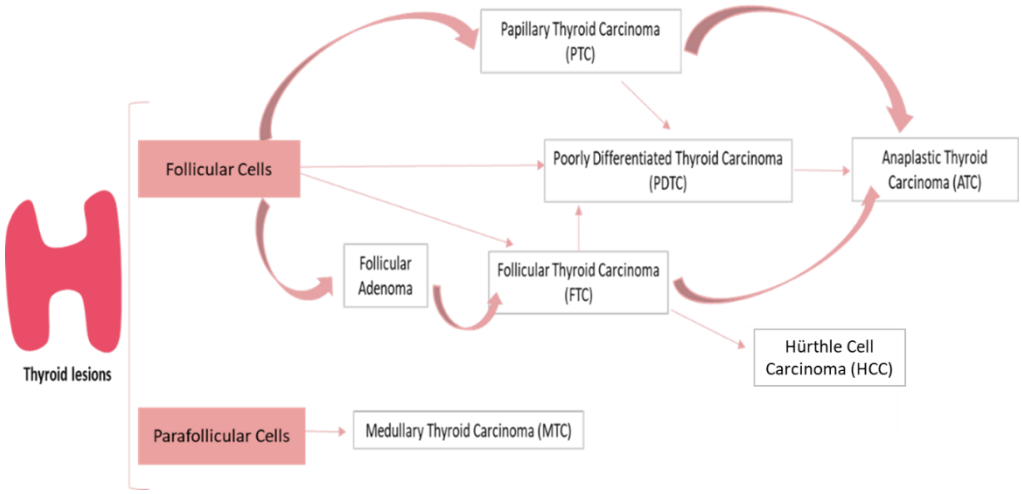

Figure 4. Thyroid Cancer histotypes - Representative scheme**.**

5.1 Follicular Thyroid Adenoma (FTA)

FTA are benign encapsulated lesions, without invasion and show evidence of follicular cells differentiation [29]. Follicular adenoma has a homogenous shape, enclosed by a thin fibrous capsule and easily identified when compared to the normal thyroid tissue. It is possible to discover thyroid adenomas by thyroid imaging and/or by incidental palpation and most of patients are euthyroid. The tumors measure about 1-3cm although they can be much larger. Exposure to radiation and deficit in iodine intake are risk factor for thyroid adenomas. The radiation exposure during childhood and adolescence increases exponentially the risk of follicular adenoma [29]. Follicular adenomas do not invade or metastasize. Yet they must be removed surgically for exclusion of malignancy [4, 29].

5.2 Encapsulated follicular-patterned thyroid tumors

a) Well differentiated tumor with uncertain malignant potential (WDT- UMP)

WDT-UMP is an encapsulated follicular-patterned neoplasm of the thyroid with borderline nature. It has questionable capsular invasion. Generally, the tumor presents as a single nodule, with 1-4 cm and similar appearance to that of follicular adenoma, in most cases behaving in an indolent manner. *NRAS* mutation is present in about 14% of WDT-UMP cases [29, 31].

b) Noninvasive follicular thyroid neoplasm with papillary-like nuclear features (NIFTP)

Recently a new category of non-invasive and encapsulated neoplasm was defined, the NIFTP. NIFTP has a follicular growth pattern and nuclear features of papillary thyroid carcinoma [29, 32, 33]. NIFTPs are considered as an indolent neoplasm with a good prognosis and account for up to 20% of the tumors previously classified as PTCs [29]. Like other thyroid neoplasms, this lesion affects more women than man, in their fourth to sixty decade of life. Normally this neoplasm is asymptomatic, can be identified in any part of thyroid and is painless. Morphologically it is a solid and homogeneous lesion, well circumscribed and hypoechoic. To establish the diagnosis of NIFTP four histologically features were defined: (1) encapsulation, (2) the presence of follicular growth pattern, (3) nuclear features of PTC and (4) lack of invasion. On the other hand, there are criteria for exclusion of NIFTP diagnosis, namely the presence of papillae, psammoma bodies and high mitotic activity. These characteristics allows distinction between NIFTP and PTC diagnosis [29, 33].

5.3 Thyroid Carcinomas (TC)

5.3.1 Papillary Thyroid Carcinoma (PTC)

WDTC - including PTC and FCT - accounts for 95% of all thyroid tumors - in which approximately 80% are PTC [29, 34]. The incidence of PTC is increasing [35].

Generally, PTC tend to be indolent showing a good prognosis and a survival rate of 96% at 5 years. Patients present a normal thyroid function, are painless and the tumor can appear in either lobe as well as in the isthmus. The probability of PTC increases with age (from third to fifth decades), although it can occur at any age, being females more frequently affected than man (2:1 to 4:1) [29, 36].

A typical PTC can be present as a single or a multinodular lesion, in general measuring 2-3cm, although smaller or larger lesions can occur. There are some general pathological features that can be seen in PTC: the undefined margins, calcification, cystic formation, and the capacity of invasion, which leads to regional metastases.

Microscopically, a set of nuclear features and papillae changes become the diagnostic hallmarks for PTC although for some variants of PTC, these features are less representative (diffuse sclerosing and columnar cell variant, for instance). The change in

the size and shape of nuclei cells (irregular contours), its empty appearance, the alterations in the chromatin and membrane can distinguish the tumor cells from thyroid normal cells. The papillae, composed by a fibro vascular tissue, surrounded by a neoplastic epithelial layer can in several cases be combined with neoplastic follicles. The presence of psammoma bodies (calcium salt deposits presents in about 50% of cases) and metaplasia (present in 20-40% of cases) are also common in PTC [29]. Distant metastases, in 5-7% of the PTCs cases, occur to bones or lungs. In other hand, regional metastases are present in more than 50% of initial cases of PTC [29, 36, 37]

Standard methods for PTC diagnosis are ultrasonography, to detect suspicious nodules and select the area of interest in order to perform FNAB (fine needle aspiration biopsy), a rapid and minimal invasive diagnostic method. The FNAB smear can expose typical nuclear features, as previously explained, to establish the diagnosis of PTC with an accuracy around 90% [38, 39].

The first line for treatment is surgery (total thyroidectomy for nodules with more than 1cm). Radiodine (RAI) therapy is used in selected cases in postoperative condition to eliminate eventual remaining thyroid cells (low doses from 30–100 mCi for low-risk patients and doses ranges from 150–200 mCi for high-risk patients). An adjuvant treatment is thyroid hormone suppression (TSH suppression) [40].

The survival rate of PTC is excellent, however recurrences represents 15-35% of thyroid neoplasms [29]. Therefore, it is necessary to better understand thyroid cancer emergence to prevent cancer and, hopefully, allow a more efficient treatment of TC.

PTCs have several subtypes, each with specific features, cell types and stroma changes (Table 1). They also present characteristic genetic alterations [29, 41, 42]. The most common variants present in our study are conventional PTC, follicular variant of PTC and papillary microcarcinoma.

Table 1. Variants of PTC

Different subtypes of PTC	
• Papillary microcarcinoma	• Cribriform-morular
• Follicular	• Hobnail
• Oncocytic	• Papillary thyroid carcinoma with fibromatosis/fasciitis-like stroma
• Encapsulated	• Diffuse sclerosing
• Solid/trabecular	• Spindle cell
• Tall cell	• Clear cell
• Columnar cell	• Warthin-like

a) Papillary microcarcinoma (microPTC)

Papillary microcarcinoma or papillary micro tumor measures ≤ 1cm in diameter [29, 41, 42]. The incidence of these tumors in autopsy series vary between 5.6 and 35.6% and shows an excellent prognosis, with up to 90% of the patients free of disease during follow-up [29]. Due to their small size, the detection of these lesions can easily be missed on gross examination [29]. Microscopically, microPTC are characterized by the typical nuclear alterations of PTC, the presence of psammoma bodies, fibrosis, and the formation of papillae. Several authors have described the presence of LNM and genetic alterations in microPTC. In the presence of *BRAF* mutations a minority of these tumors can exhibit a poor behavior [29, 41].

b) Follicular variant (FV-PTC)

The follicular variant of PTC (FV-PTC) presents an exclusive or almost exclusively follicular growth pattern. This variant can be divided into infiltrative (the most typical form) or encapsulated with invasion. The infiltrative subtype shows the typical nuclear features of PTC [29]. Histologically, this lesion is composed by follicles of different sizes and the colloid is hyper eosinophilic compared with healthy follicles [29, 41]. The diagnosis of FV-PTC can be complex and controversial because this lesion can be easily misdiagnosed with follicular adenoma or follicular carcinoma or the new entity NIFTP. Immunohistochemistry and molecular markers are important for the correct diagnosis

of FV-PTC. The incidence of this lesion is about 20% to 30% of all PTCs and shows a good prognosis. Genetic alterations like *RAS*, Rat sarcoma viral oncogenes homologue, are frequently present in FV-PTC [29, 30, 41, 42].

c) Encapsulated variant of PTC (EV-PTC)

This variant shows typical features of PTC being completely delimited by a fibrous capsule. EV-PTC accounts for about 10% of all cases of PTC and has an excellent prognosis with a survival rate of 100% [29].

d) Oncocytic variant (OV-PTC)

These tumors are variants of PTC and are extremely rare. OV-PTCs have papillary features and present massive numbers of mitochondria. Histologically, this subtype is often encapsulated, invasive and composed by oncocytes [29, 41, 43]. This lesion may have a papillary or follicular architecture and its diagnosis is based on the presence of oncocytes and the nuclear features of PTC [41, 43].

e) Solid variant of PTC (SV-PTC)

The SV-PTC is an uncommon variant of PTC, accounting for approximately 1-3% of PTC cases. This subtype is described as more common in young patients, which were associated with exposition to ionizing radiation. Histologically, presents the nuclear features of PTC and solid and/or trabecular growth patterns. The distinction between PDTC and SV-PTC must be established since both can have the same solid growth pattern [29, 44].

f) Tall cell variant of PTC (TC-PTC)

The TC-PTC is an aggressive subtype, composed by tall columnar cells and an eosinophilic cytoplasm. In the literature it represents 1.3 to 13% of all diagnosed PTCs [45]. These cells are characterized by their height and width, needing to be at least 2-3 times taller than wide and be predominant in ≥ 30% of all tumor cells to establish the diagnosis of TC-PTC. This variant occurs in older patients, has a large size (5-45mm), presents frequently extrathyroidal invasion, and consequently a poor prognosis. Mutations of *TERT* promoter and *BRAF* are described in this variant [29, 46].

5.3.2 Follicular thyroid carcinoma (FTC)

FTC is a well-differentiated thyroid malignancy derived from the follicular cells. This lesion is defined as an epithelial tumor and shows lack of PTC nuclear features [29, 47]. FTC accounts for about 6-10% of thyroid cancer, are more prevalent in areas with iodine deficiency and occur more frequent in women than man (ratio 3:1) [30]. Usually, FTC appear as a painless neck mass and the first symptom can be the presence of metastasis, which are most common in the lung followed by bone [29]. Microscopically, FTC varies in appearances. Usually FTC is an encapsulated tumor and its cytoarchitecture is like those of follicular adenoma. However, for a correct diagnosis the presence of capsular and/or vascular invasion is required [29, 47]. Minimal invasive FTC without vascular invasion have an excellent prognosis. For this malignancy the treatment consists of thyroidectomy followed by radioactive iodine and a positive response is expected (70% to 80% long term survival) [29].

5.3.3 Hürthle cell carcinoma (HCC)

HCC is composed by oncocytic cells in a percentage above 75% and has a follicular pattern of growth. They show capsular and/or vascular invasion and tend to be encapsulated. It is described that HCC are large tumors (normally ≥ 2cm), and presents areas of necrosis [29, 48]. HCC can metastasize to the liver, lung and bones and generally affects older patients [29].

5.3.4 Poorly differentiated thyroid carcinoma (PDTC)

PDTC is a rare thyroid malignancy, accounting for up to 10% of all thyroid neoplasms [49]. This entity is characterized as a malignant neoplasm with poor evidence of follicular cell differentiation and is placed biologically between WDTC (PTC or FTC) and anaplastic thyroid carcinoma (ATC) [29]. PDTC was accepted and introduced in the 2004 World Health Organization (WHO) classification as a malignant neoplasm of the thyroid. In a 2006 meeting in Turin, Italy, with international thyroid experts, a uniform diagnostic algorithm was developed for PDTC based on two main characteristics of malignancy: high grade features and growth pattern. More specifically, PDTC must show a solid, trabecular or insular growth pattern, lack of nuclear features of PTC and it should

present at least one of the following characteristics: convoluted nuclei, mitotic activity of 3x10 high power fields (HPF) or higher and/or tumor necrosis [29, 49, 50].

Macroscopically, PDTC is a solitary, large (median size about 5cm) and brown to grey mass. Microscopically, it shows mitoses and necrosis, high-grade features indicative of poor prognosis. PDTCs are invasive and the presence of distant metastases at presentation accounts for approximately 15% of the cases [29]. There is no consistent treatment for PDTC and usually, the response to radioiodine treatment is poor. The overall 5-years survival of these lesions is about 60-70% and recurrences generally develop in the first 3 years [29].

5.3.5 Anaplastic Thyroid Carcinoma (ATC)

ATC is described as the most aggressive thyroid malignancy and is composed by undifferentiated cells [29]. ATC accounts for <2% of all thyroid malignancies and is associated with a very poor prognosis [49]. Elderly patients are the most affected and usually present an advanced tumor staging. According to the American Joint Committee on Cancer (AJCC), ATC *per se* is classified as stage IV and is further divided in stage IVa, IVb and IVc. The IVc stage correspond to any T and M1 and affects approximately 20-40% of all ATC [26]. Distant metastases may occur in lung, bone and brain [29]. Microscopically, these lesions present necrosis, high mitotic levels, giant and squamoid cells and vascular invasion [51]. Current treatments for ATC are surgical resection, radiotherapy, and chemotherapy. A second line of treatment includes target therapies such as, tyrosine kinase inhibitors and anti-angiogenic drugs. Palliative care is also needed due to the aggressiveness of this malignancy and its highly lethal behavior. The overall survival of this malignancy is very poor and for most cases it is fatal [51].

5.3.6 Medullary Thyroid Carcinoma (MTC)

MTC is a malignant tumor, arising from the parafollicular cells of the thyroid gland. It accounts for 1-2% of all thyroid malignancies [29, 52]. Almost 75% of these cases are sporadic and 25% are hereditary [29]. Sporadic tumors are lightly predominant in females and the clinical presentation is in fourth to sixth decades of life [29]. The disease in young patients is usually hereditary [29]. Sporadic MTC presents as a single

lesion while hereditary MTC presents as a bilateral and multicentric lesion. Both vary in size and present a greyish tan to yellow mass [52]. Microscopically, the tumor cells can be round, polygonal and with a variable size. The nuclei are usually round with small nucleoli. Mitotic activity is rare and 90% of MTC cases show stromal amyloid deposits with calcitonin as the main component [29]. In a palpable nodule of sporadic MTC, up to 70% of the patients present cervical node metastases and 10% have distant metastases, typically in the lung, bone and/or liver [29, 52]. Total thyroidectomy with central lymph node dissection is the first line of treatment. Chemotherapy is administered to the patients although with a limited response rate [52].

6. Molecular Markers of Papillary Thyroid Carcinoma

Novel diagnostic and prognostic tools are required to better treat patients as well as to avoid unnecessary surgeries. The study and identification of molecular markers in thyroid will lead to a more personalized and effective treatment of the patients.

In recent years, a significant knowledge in molecular mechanisms of thyroid carcinogenesis has been achieved. The development and progression of TC is due to a gradual accumulation of genetic and epigenetic events, which includes activating and inactivating somatic mutations and alterations in gene expression patterns. These changes are associated with specific tumor phenotypes and implicated in the disease etiology. Plus, molecular alterations induce the activation of different pathways such as the mitogen-activated protein kinase (MAPK) and phosphoinositide 3-kinase (PI3K) signaling pathways (Figure 5) [53].

6.1 The Mitogen-activated protein kinase (MAPK) signaling pathway

The MAPK signaling pathway (Figure 5) activation is frequently involved in tumor initiation. This pathway involves a set of proteins that have a fundamental role in the regulation of cell growth, proliferation, differentiation, migration and apoptosis through the regulation of gene expression. These mechanisms are highly conserved in eukaryotes and the members of signaling cascade (RAS/RAF/MEK/ERK) acts as a signal transducer between the extracellular environment and the nucleus [54].

MAPK pathway is initiated by an external stimulus such as a hormone, growth factor or cytokine, which interacts with its receptor on the cell membrane, leading to a conformational change that results in Rat sarcoma viral oncogene homologue (RAS) activation. RAS will then activate RAF proteins, following by phosphorylation and activation of MEK (MAPK kinase), which in turn activates ERK (extracellular-signal-regulated kinase) that migrates into the nucleus to induce a range of cellular processes. It is described that about 30% of all cancers have mutations in genes coding for proteins of the MAPK pathway [54]. This pathway is important in thyroid cancer development, particularly in WDTC, PTC and FTC.

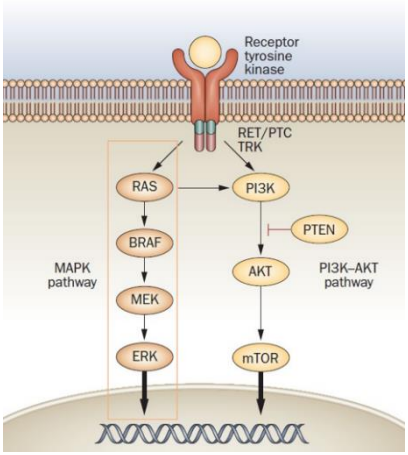

Figure 5. The MAPK pathway in thyroid cancer.

(Adapted from Nikiforov, Y.E., Nature Reviews Endocrinology, 2011 after permission request).

In PTC, the presence of genetic alterations is well described and in most of the cases leads to the activation of the MAPK signaling pathway. Lu *et al.* (2017), reveal that 69.6% of PTCs have genetic alterations (such as in V-raf murine sarcoma viral oncogenes homolog B1 (*BRAF*) (58%), *KRAS* and *HRAS* (2.9%) genes) that lead to the constitutive activation of the MAPK signaling pathway [55].

Others described that about 75% of PTCs present point mutations in *BRAF* and *NRAS* genes (36-69% if only *BRAF*); gene fusion, such as RET (Rearranged during transfection)/PTC rearrangements, are present in about 15% of the cases and copy number variations in 7% of the cases [29, 56]. To corroborate this findings, Fakhruddin N. *et al.* (2017), have shown that the incidence of *BRAF* mutations is approximately 60%

and of *NRAS* is 11% [56], and Soares, P. *et al.* (2003) show in their series that 18% had RET/PTC rearrangement [57].

6.1.1 *BRAF* mutations

BRAF encodes a serine–threonine kinase of the MAPK signaling pathway [58]. When mutated, this gene is no longer dependent on RAS, promoting the activation of the MEK–ERK–MAP kinase pathway in a constitutive manner and promoting tumorigenesis [59]. This gene is associated with human carcinogenesis due to its high mutation frequency in a wide range of neoplastic lesions such as melanoma (40-70%), thyroid (45%) and colorectal cancer (10%) [53, 54].

BRAF gene is located at 7q24 and is a member of RAF kinase family that consists of 3 kinases: ARAF, *BRAF* and CRAF (RAF-1) [54, 60]. The most common point mutation in *BRAF* arises from a thymine to adenine transversion in the nucleotide 1799, resulting in a substitution of a valine by a glutamic acid at position 600 in exon 15 (Val600Glu) and accounts for about 98-99% of all *BRAF* mutations found in TC [53].

BRAF mutations are the most common molecular alterations in PTC, being found in about 36-69% of the cases [61, 62]. It is also present in PDTC (20-40%) and ATC (30-40%), suggesting that *BRAF* mutated PTCs can progress to less differentiated thyroid cancers [53, 63]. Trovisco, V. *et al.* (2004), have shown that $BRAF^{V600E}$ mutation is almost exclusively present in conventional PTC and variants with a predominant papillary architecture, such as the Warthin-like variant, and are rare in the follicular variants of PTC [63, 64]. Fakhruddin, N. *et al.* (2017) also demonstrated the predominance of $BRAF^{V600E}$ mutation in the conventional PTC cases of their cohort (56.8%) [56].

Studies of Nikiforova, M. *et al.* (2004) [65] and Lima, J. *et al.* (2004) [66], have shown that *BRAF* mutations are more common in PTC of adults, than in PTC from children, and are rare in radiation-induced PTCs.

In about 1-2% of PTCs, *BRAF* can be activated by other point mutations such as $BRAF^{K601E}$, by small in-frame insertions or deletions surrounding codon 600, as well as by chromosomal rearrangements, for instance the fusion gene AKAP9-*BRAF* that is linked with radiation exposure [67]. The $BRAF^{K601E}$ missense mutation, consists of an

adenine to guanine transversion at the position 1801, leading to a lysine to glutamic acid substitution at the 601 amino acid position (Lys601Glu) [68]. This mutation has been described in follicular variant of PTC [53, 67, 69] and, in 2016, Torregrossa, L. *et al.* have corroborate this data in a large cohort of PTCs [68]. A total of 2961 PTCs were evaluated and *BRAF* mutations were found in 40% of the PTC cases. Particularly, the *BRAF*^{V600E} mutation was found in 95.3% of the cases and the *BRAF* ^{K601E} was found in 3%. The majority of PTCs harboring *BRAF* ^{K601E} mutations were of the FV-PTC supporting the idea that *BRAF* ^{K601E} is associated with this less aggressive variant [68, 70].

Different studies have shown an association between *BRAF*^{V600E} and extrathyroidal extension, tumor multifocality, lack of tumor capsule and the presence of LMN, all predicting a poor prognosis [68, 70, 71]. Xing *et al.* (2005) have shown that these features are present in different variants of PTC (TC-PTC and conventional PTC) but are less frequent in the follicular variant. Nevertheless, it is important to recognize that it is not accurate to base the diagnosis on the molecular evaluation of a single gene (*BRAF*). The specificity of this alteration in the diagnosis of PTC is almost 100% but its sensitivity is under 35% and, most important, may have other drivers of malignancy [63]. Therefore, it is necessary to establish a panel of genes for better risk stratification.

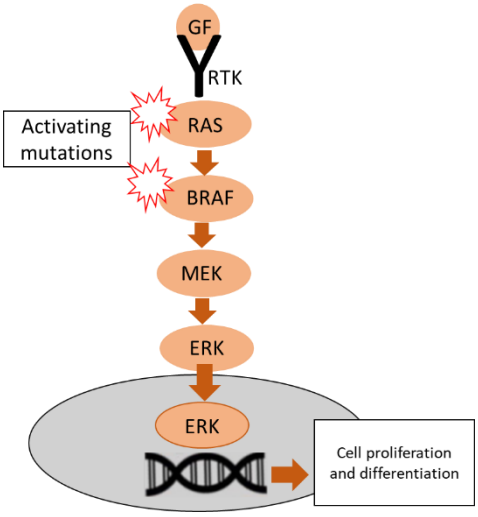

Figure 6. Mutations of the MAPK signaling pathway members promotes its constitutive activation.

The pathway is activated by the binding of a growth factor (GF) to a tyrosine kinase receptor (TKR), which activates the RAS, *BRAF*, MEK and ERK phosphorylation cascade.

The RAS protein belongs to a family of GTPases that regulates cell growth via the MAPK and PI3K-AKT pathways (Figure 6). They encode highly related G proteins that are

placed at the inner surface of the cell membrane and diffuse signals arising from the cell membrane TKR and G-protein–coupled receptors along the MAPK, PI3K/AKT and other signaling pathways [72].

RAS exists in a guanosine triphosphate (GTP)-bound active state or a guanosine diphosphate (GDP)-bound inactive state. When mutated, RAS proteins are unable to perform their GTPase activity, by hydrolyzing GTP to GDP. Consequently, mutated RAS are in a constitutive active GTP-bound state and are described as the second most common alteration in thyroid cancer [53, 61].

There are three members of the RAS gene family (*NRAS*, *HRAS* and *KRAS*). All of them have been shown to be mutated in TC. *HRAS* is located at 11p15.5, *KRAS* at 12p12.1 and *NRAS* at 1p13.2 genomic regions [61, 73]. They become constitutively activated by mutations that increase their affinity for GTP (codons 12/13) or decrease their intrinsic GTPase function (codon 61). Yet, both mechanisms have the same effect on the signaling pathways, which is the constitutive activation of RAS [74].

RAS activating mutations normally arise in codons 12, 13, 61. The most frequent mutations affect codon 61 of *NRAS* (about 95%) and less commonly codon 61 of *HRAS*. For *KRAS*, about 66% of the mutations affect codon 12 [75]. A few studies associate RAS mutations in TC with tumor dedifferentiation and anaplastic transformation that leads to a less favorable prognosis [53, 67, 76]. RAS mutations affects benign lesions as well as a variety of thyroid tumors and were shown to be more frequent in FTA (26%), FTC (30%–45%), FV-PTC (30%–45%), PDTC (33%) and ATC (20-40%) [53, 61, 74, 77].

Tumors with RAS mutations are associated with a good prognosis [77]. However, there is evidence that RAS mutations may be an early event in tumorigenesis that potentiates the development of the malignancy and consequent dedifferentiation of the cells [74, 77]. Detecting RAS mutations in thyroid samples provides improvement on risk stratification with solid evidence for neoplasia (about 80%) and has the potential patient management guidance [77].

6.2 h*TERT* mutations

Telomerase activation has been described as a hallmark of cancer. Its function is to extend and preserve telomeric DNA. In recent years, the importance of telomerase in cancer has increased, but not necessarily correlated with telomere integrity [78].

Telomeres are repetitive non-coding sequences that preserve the end of chromosomes from degradation. Telomerase, a ribonucleoprotein with reverse transcriptase activity, promotes the extension of telomeres by adding hexameric 5'-TTAGGG-3' tandem repeats at the end of the chromosome [79]. Telomerase is composed by two subunits: *TERT* and TERC. *TERT*, (telomerase reverse transcriptase) constitutes the catalytic subunit and TERC, a RNA component, gives the template for telomerase elongation [80]. The catalytic part of human telomerase (h*TERT* - Human telomerase reverse transcriptase) gene is located on chromosome 5p15.33, includes 16 exons spanning 35kb.

At each round of cell division, telomeres are shortened, reaching the replication limit that leads to a loss of genomic information and cell senescence or cell death [79]. Cancer cells manage to achieve immortalization and proliferation without restriction, by reactivating telomerase. The presence of telomerase in malignant tumors is in approximately 80-90% of the cancers and upregulation of *TERT* is well described [81, 82]. Several mechanisms for *TERT* activation have been proposed, including epigenetic changes, h*TERT* promoter mutations, h*TERT* amplification and alternative splicing [80, 83].

Thyroid tissue is a conditional-renewal tissue, which has low rates of proliferation and a stem cell population is not well-defined [80]. Preto, A. *et al.* (2004) advanced that the so-called Solid Cell Nests (SCNs) - a embryonic remnant of the ultimobranchial body – of human thyroid express markers of self-renewal capacity, namely telomerase which may represent the pool of the thyroid stem cells [84]. High telomerase activity is reported in thyroid tumors but it is rare in normal thyroid tissues [85]. So, in the presence of telomerase activation, h*TERT* may potentially be considered a useful molecular marker for thyroid cancer.

TERT promoter mutations are a common event in several cancer types. Vinagre, J. *et al.* (2013), described the presence of *TERT*p mutations in bladder cancer (59%), central nervous system (43%), melanoma (29%) and thyroid cancer (10%), suggesting it act as an enhancer of telomerase expression [86, 87]. These mutations occur in two hotspot positions, -124 and -146 bp upstream of the ATG start site of h*TERT*. They represent nucleotide changes of G>A (C>T in complementary strand). Both mutations are mutually exclusive, and comprehends the creation of a consensus binding site, (GGAA), for E-twenty six (ETS) transcription factors, offering biological significance of these mutations [85].

In TC, h*TERT* mutations have been observed particularly in follicular cell derived carcinomas, such as WDTC, PDTC and ATC. In medullary thyroid carcinoma, benign lesions (FTA, thyroiditis and nodular goiter), or normal adjacent thyroid tissue *TERT* mutations were rarely detected [85].

In 2014, Melo, M. *et al.* reported the presence of h*TERT* in 7.5% of PTCs, 17.1% of FTCs, 29% of PDTCs and 33.3% of ATCs, showing the clinical importance of these mutations for patient management [85]. Recently, Panebianco, F. *et al.* (2019) studied a large cohort of thyroid carcinomas, showing similar results in which *TERT* mutations were found in 7% of PTC, 18% of FTC and 86% for both PDTC/ATC [83]. Several studies have reported that -124 G>A mutation was most common than the -146 G>A mutation [83, 85, 88]. Relatively to PCT variants, h*TERT* has been reported more prevalent in conventional PTC than in other variants, being also found in FV-PTC [85].

Several authors suggested that *TERT* mutations are strongly associated with worse pathological features (older age, tumor size and stage), aggressive behavior (worse response to treatment), distant metastases, poor prognosis and higher risk for disease-specific mortality [83, 85, 88, 89]. Furthermore, h*TERT* mRNA expression is also associated with extrathyroidal extension and vascular invasion [88, 89].

A better understanding of the presence of these mutations in TC, particularly in WDTC, may lead to a promising prognostic indicator and have impact in the management of patients namely for individualized treatments [85, 88].

6.3 MicroRNAs (miRNAs)

A promising area of study in cancer is the assessment of microRNAs (miRNAs) expression and role. miRNAs are an important class of small non-coding RNAs, with a length of approximately 22 nucleotides. They have a key role in posttranscriptional regulation of gene expression by reducing the stability of the target messenger RNA (mRNA) and/or repressing its translation [90]. These events may have influence in intracellular regulatory processes implicated in carcinogenesis, including differentiation, proliferation and apoptosis [72, 90]. Several studies report that miRNAs are involved in multiple types of cancer, such as thyroid, breast, ovarian, lung, colorectal and chronic lymphocytic leukemia [91-93].

When mRNA has enough complementarity with the miRNA, miRNA induce the cleavage of mRNA acting as a small interfering RNA (siRNA). Insufficiency of complementarity between mRNA-miRNA induces blocking of translation [93].

When TC growth occurs due to the action of oncogenes, a set of alterations on miRNAs biogenesis is displayed. The activation of oncogenic miRNAs occurs, leading to a constitutive activation of MAPK pathway [94, 95]. miRNAs can act as tumor promoters (oncomiRs) which downregulates tumor suppressor genes or act as tumor suppressors leading to upregulation of oncogenes with consequences in tumor progression and growth [90].

In 2008 Nikiforova *et al.* described the biological importance and diagnostic value of miRNAs analysis in normal and tumor thyroid tissue. In thyroid tumors 32% of miRNAs are upregulated while 38% are downregulated [96].

When compared with thyroid normal tissue, specific up and downregulated miRNAs are involved in the progression of PTC such as miR-146b, miR-221, miR-222 (upregulated) and miR-15a (downregulated). The miRNA expression is tissue specific, varying among the different types of TC [93].

Upregulated miR-146b, miR-221 and miR-222 downregulate proto-oncogene receptor tyrosine kinase (KIT), which is involved in cell differentiation and growth, while miR-15a downregulates B-cell lymphoma 2 (BCL-2) and controls the proliferation and

apoptosis of PTC through AKT pathway [90, 92, 93]. Pallante, P. *et al.* (2006) shows that miR-221 and miR-222 are overexpressed in PTC, and the authors also validate that these miRNAs downregulate c-KIT levels in PTC [90, 91, 93]. Castagna, M. G. *et al.* (2019) have shown, in a series of fine-needle aspiration cytology samples, that miR-146b, miR-221 and miR-222 are overexpressed in malignant or suspicious of malignancy nodules confirming the utility of these miRNAs in the classification of thyroid nodules (Figure 7) [97]. The overexpression of these miRNA is correlated with tumor aggressiveness, high TMN stage, extrathyroidal extension, recurrence and metastases, representing a real signature of PTC [72, 91, 95, 98]. Therefore, the study of miRNA expression can be useful in the early and accurate diagnosis, as well as in the evaluation of progression of PTC [99].

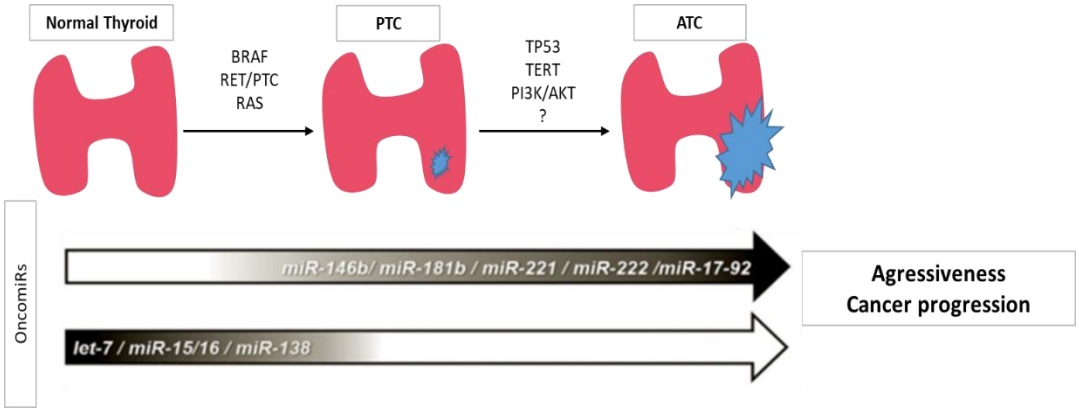

Figure 7. Oncogene activation induces thyroid cancer and deregulation of miRNA expression (loss or gain of expression), which also contributes to cancer progression.

Darker regions in the arrow represent higher expression levels.

Aims

The general aim of this project is to evaluate the value of genetic alterations and miRNA expression in the improvement of TC diagnosis and its contribution to establish a more assertive diagnosis/prognosis of patients with thyroid neoplasms. For that, we intend to perform the genetic characterization of a series of thyroid tumors, establish methods for miRNA isolation and expression analysis, and the correlation between its expression and the clinicopathological features of the tumors.

More specifically, the aims include:

(1) Characterization of the genetic alterations in a series of thyroid tumors using paired FNAB and FFPE samples.
(2) Validation of the diagnostic value of a FNAB in thyroid cancer by establishing the tumor's cyto-histologic molecular correlation.
(3) Establishment of isolation and detection methods for miRNA expression in FNAB samples.
(4) Evaluation of the expression levels of miR-146b, miR-221 miR-222 and miR-15a in both FNAB and FFPE samples and establish its correlation with clinicopathological features of thyroid lesions.

Material and Methods

1. Biological samples

The samples analyzed in this study were collected at Centro Hospitalar de Lisboa Central - Hospital Curry Cabral and belong to a consecutive series of patients with thyroid nodules referred for surgical excision from 2016 to 2018, inclusive. Two hundred and sixty-six samples, including fine needle aspiration biopsy (FNAB) (n=111) and formalin-fixed paraffin embedded tissues (FFPE) (n=155), belonging to 97 patients, were available and analyzed for molecular characterization in this study. For the sake of this thesis, a total of 180 samples belonging to 90 patients were afterwards selected for a retrospective evaluation, totalizing 90 FNABs and the corresponding 90 FFPE tissues. The selection/exclusion criteria were the availability, for each of the patients enrolled, of one cytology sample and corresponding FFPE material. Patients from whom either the FNAB or the FFPE tissue sample were not available were excluded, as well as different FFPE samples from the same patient that did not correspond to the cytology.

2. Microtome cuts

FFPE tissue blocks were cut in a microtome (Micron HM 335 E). Three cuts were made per case one for hematoxylin-eosin staining (3µm), one for DNA extraction (10µm) and another for miRNAs extraction (10µm).

3. Hematoxylin-eosin (H&E) staining

Three µm thick sections of FFPE samples for each case were used for H&E staining. This procedure is based in 5 steps: dewaxing paraffin sections, hydration, coloration with hematoxylin and eosin, dehydration and diaphanization.

Deparaffination of the slides was obtained by two consecutive rinses of the slides in xylol for 10 minutes (Enzymatic, Portugal), followed by hydration with a decreasing concentration of ethanol (Enzymatic, Portugal): two consecutive passages in 100% ethanol for 5 minutes, one passage in 96% ethanol for 5 minutes and, one passage in 70% ethanol for 5 minutes, followed by a washing step in running water for 5 minutes. The slides were then stained with hematoxylin for 4.5 minutes (DIAPATH, Italy) and

washed in running water for 5 minutes before a passage in 70% ethanol. After this procedure, the slides were stained with eosin-Y alcoholic (Thermo Scientific, USA) for 3 minutes and the tissue dehydration was established through increasing concentrations of ethanol (Enzymatic, Portugal): one passage in 96% ethanol and two passages in 100% ethanol for 5 minutes each. For diaphanization, two rinses in xylol for 10 minutes were performed and all slides were assembled with mounting medium (Thermo Scientific, USA). All slides, two cytologies and one histology per patient, were reviewed by a pathologist at *Instituto de Investigação e Inovação em Saúde* (i3S) to select the tumor area for manual microdissection in histology and to confirm the diagnosis.

4. DNA extraction, quantification, and quality assessment

4.1 FFPE Tissues

DNA extraction was performed with the GRiSP kit (GRiSP, Portugal) following the manufacturer's instructions. The kit contains all reagents and material needed for the extraction.

The slides with a 10µm cut of each paraffin block sample were deparaffinized in two rinses of xylol (Enzymatic, Portugal) for 10 minutes each, followed by two passages in 100% ethanol (Enzymatic, Portugal) for 5 minutes each, and then left to air dry for 15 minutes at room temperature. The tumor area of each sample was manually microdissected and collected to a 1.5mL eppendorf tube. Cell lysis and protein digestion was performed overnight at 60°C in 200 µL of Buffer BR1 provided by the kit and with 10 µL of proteinase K (200mg/mL). When necessary, due to incomplete digestion, 5 µL extra of proteinase K (200mg/mL) were added to the samples. After complete protein digestion, 200 µL of Buffer BR2 and 200 µL of absolute ethanol were added to each sample before vortexing, for approximately 10 seconds. Precipitated DNA was transferred to gDNA plus spin column. The samples were centrifuged (Sorvall Legend Micro 21R centrifuge, Thermo Scientific, USA) at 16000 g for 1 minute at room temperature. The columns were transferred to new collection tubes. Two washes were performed, one with 400 µL of wash Buffer 1 and another with 600 µL of wash Buffer 2, both provided by the kit, followed by a centrifugation at 16000 g for 30 seconds (Sorvall Legend Micro 21R centrifuge, Thermo Scientific, USA). Each column was transferred to

a new previously labeled eppendorf tube and DNA was eluted with 50 µL of Elution Buffer by centrifugation. Samples were stored at 4°C. DNA was quantitively and qualitatively analyzed in a NanoDrop (ND-1000, Thermo Fisher Scientific, Lithuania) spectrophotometer.

4.2 FNAB Samples

DNA extraction from FNABs was performed with the QIAmp® DNA Investigator Kit (Qiagen, Germany) following the manufacturer's instructions. The kit contains all reagents and material needed for the extraction.

Initially, the slides were left in xylol (Enzymatic, Portugal) for approximately 5 days for coverslips removal. Then, the slides were rinsed in 100% ethanol (Enzymatic, Portugal) for 10 minutes, followed by one passage in 96% ethanol (Enzymatic, Portugal) for 10 minutes and a drying period of 15 minutes at room temperature. Approximately 10 µL of ATL lysis Buffer was added to each sample, before they were manually scraped and cells were collected to a labelled 1.5mL eppendorf tube. Cell lysis and protein digestion was performed in 300 µL of ATL Buffer and with 20 µL of proteinase K (200mg/mL) at 56°C for 1 hour. To ensure efficient lysis, 300 µL of AL Buffer was added to each sample before vortexing for 10 seconds, followed by another incubation at 70°C for 10 minutes with shaking (900 rpm). 150 µL of 100% ethanol was added and then vortexed for 15 seconds. Precipitated DNA was transferred to the QIAmp MinElute column (2mL collection tube) and then centrifuged (Sorvall Legend Micro 21R centrifuge, Thermo Scientific, USA) for 1 minute at 8000 rpm. The columns were transferred to new collection tubes and 500 µL of AW1 Buffer and 700 µL of AW2 Buffer were added, followed by two centrifugations (Sorvall Legend Micro 21R centrifuge, Thermo Scientific, USA) at 8000 rpm for 1 minute. The columns were transferred to new collection tubes, and 700 µL of 100% ethanol was added followed by a centrifugation at 8000 rpm for 1 minute. The columns were transferred to a new collection tube and centrifuged at 14000 rpm for 3 minutes. The columns were then transferred to a new previously labelled eppendorf tube and were incubated at 56°C for 3 minutes. DNA was eluted with 30 µL of ATE Buffer by centrifugation at 14000 rpm for 1 minute. Samples

were stored at 4°C. DNA was quantified in a NanoDrop (ND-1000, Thermo Fisher Scientific, Lithuania) spectrophotometer.

5. Genetic characterization

All samples were evaluated for the presence of hotspot mutations in *TERT*p, *BRAF* and *RAS* (*NRAS*, *HRAS*, *KRAS*) genes.

5.1 Polymerase Chain Reaction (PCR)

All samples were amplified by Polymerase Chain Reaction (PCR) (SimpliAmp™ Thermalcycler, Applied Biosystems, USA) to identify the presence of hotspot mutations.

Multiplex PCR was performed to amplify regions harboring the hotspot mutations of h*TERT* (mutations at -124 and -146 positions, both G>A), *BRAF* (p.V600E mutation) and *NRAS* (p.Q61R mutation) genes. PCR was performed using the QIAGEN multiplex PCR kit (USA) following the instructions given by the manufacturer. The thermocycler (SimpliAmp™ Thermalcycler, Applied Biosystems, USA) and reaction conditions used for amplification are described in Figure 8. Primers are described in Table 2. About 30 to 50 ng of DNA were used per reaction.

(A)

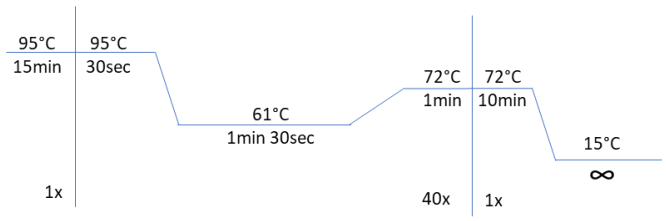

(B)

Multiplex PCR Master Mix	
Buffer	6,25 µL
Q Solution	1,25 µL
Primer Forward	0,125 µL
Primer Reverse	0,125 µL
H2Od	3,5 µL
DNA	-
Total	**11,75 µL**

Figure 8. (A) Thermocycler programme and (B) reaction conditions used for multiplex PCR of h*TERT*, *BRAF* and *NRAS* genes.

For the amplification of hotspot mutation regions of *HRAS* and *KRAS* (codons 12, 13 and 61) genes, a touchdown PCR was adopted due to the inability to optimize amplification of all genes in multiplex reaction. The Bioline PCR Kit (MyTaq HS Mix 2X, USA) was used following the manufacturer's instructions. The thermocycler (SimpliAmp™ Thermalcycler, Applied Biosystems, USA) conditions and mix composition are described in Figure 9. Primers are described in Table 2. About 30 to 50 ng of DNA were used per reaction.

(A)

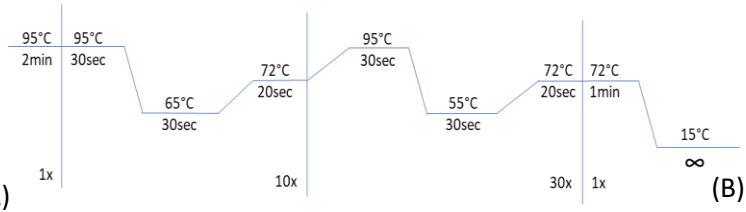

(B)

Bioline PCR Mix	
MyTaq	5 µL
Primer Forward	0,25 µL
Primer Reverse	0,25 µL
H2Od	3,5 µL
DNA	-
Total	**9 µL**

Figure 9. (A) Thermocycler programme and (B) reaction mix composition of the touchdown PCR used for: *HRAS* and *KRAS* gene amplification.

Table 2. Primer sequences used in the PCR reactions

Gene	Primers (5' – 3')		Fragment size (bp)
	Forward	Reverse	
hTERT	CAGCGCTGCCTGAAACTCG	GTCCTGCCCCTTCACCTTC	166
BRAF	TTCCTTTACTTACTACACCTCAG	CATCCACAAAATGGATCCAGAC	133
NRAS	CAGAAAACAAGTGGTTATAGATGG	GTCCTCATGTATTGGTCTCTCA	110
HRAS (codon 12 and 13)	CAGGAGACCCTGTAGGAGG	TCGTCCACAAAATGGTTCTG	139
HRAS (codon 61)	GGAGACGTGCCTGTTGGA	GGTGGATGTCCTCAAAAGAC	140
KRAS (codon 12 and 13)	GGCCTGCTGAAAATGACTG	GGTCCTGCACCAGTAATATG	163
KRAS (codon 61)	CCAGACTGTGTTTCTCCCTT	CACAAAGAAAGCCCTCCCCA	155

5.2 Agarose gel and PCR products purification

PCR products were run on a 1% agarose gel electrophoresis (GRS Agarose LE, GRiSP, Portugal) in 0.5 X concentrated SGTB buffer (20 X SGTB agarose electrophoresis buffer, GRiSP, Portugal) to assess for PCR efficacy and eventual presence of contaminants. 2.5 µL of PCR products were mixed with 1 µL of Loading Buffer dye containing Gel Red. A Ladder (Invitrogen, CA, USA) was used in each run, to evaluate the molecular weight of the PCR bands. The gel was exposed to UV light using the ChemiDoc™ XRS+ System, BIORAD (Universal Hood II, Hercules, CA, USA – 50/60 Hz) and a picture was taken.

Purification of the PCR samples was performed by adding 2-3 µL of a mixture of Exonuclease I and Shrimp Alkaline Phosphatase enzymes (Thermo Fisher Scientific, Lithuania), and incubating the samples at 37°C for 30 minutes followed by an incubation at 85°C for 15 minutes for enzyme inactivation. This procedure removes excess of

primers, primer dimer and DNA not processed during the PCR reaction. The reaction was performed in the SimpliAmp Thermalcycler, Applied Biosystems.

6. Sanger sequencing

To determine the presence or absence of mutations in the amplified regions of the analyzed genes a Sanger sequencing reaction was performed. All PCR products were sequenced using BigDye v3.1 Sequencing Kit (Applied Biosystems, Washington). The reaction was performed in the BIORAD MyCycler™ Thermal Cycler System (Hercules, California, USA), with the conditions described in Figure 10.

(A)

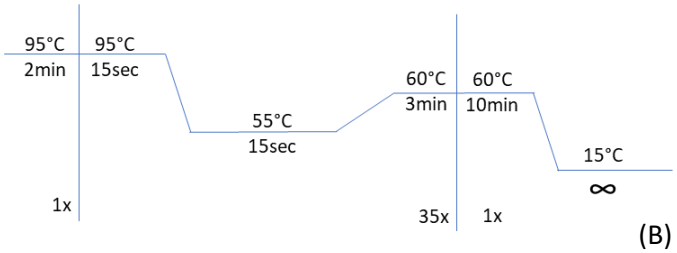

(B)

Sequencing Mix	
BigDye	0,4 µL
Buffer	3,4 µL
H2Od	3,5 µL
Primer	0,3 µL
DNA	-
Total	**7,6 µL**

Figure 10. (A) Thermocycler programme and (B) reaction conditions for the sequencing reaction.

6.1 Sanger Sequencing Products Purification

The purification of the sequencing products was achieved using Sephadex™ G-50 resin fine columns (GE Healthcare Life Sciences, UK) to eliminate residual contaminants (dNTPs and ddNTPs not incorporated in DNA) which could interfere with the correct interpretation of the signal. The sequencing products were transferred to the top of Sephadex columns and centrifuged at 3200 rpm for 4 minutes at 4°C (Centrifuge 5417R, Eppendorf, Germany). After the purification, 15 µL of Hi-Di™ Formamide (Applied Biosystems, USA) was added to each sample to maintain the DNA denaturated. Samples were analyzed by capillary electrophoresis using the Applied Biosystems 3130/3130xl Genetic Analysers (California, USA). All mutations found were double checked with a new PCR and sequencing reaction to validate the results.

7. MicroRNA extraction from FFPE tissues and FNAB samples

microRNA extraction was performed with the miRNeasy Mini kit (Qiagen, Germany) following the manufacturer's instructions. The kit contains all reagents and material needed for the extraction.

The initial step is different for FFPE tissues and FNAB samples.

For FFPE tissues, a slide with a 10 µm cut of each paraffin block sample was deparaffinized in two rinses of xylol (Enzymatic, Portugal) for 10 minutes each, followed by two passages in 100% ethanol (Enzymatic, Portugal) for 5 minutes each and then left to air dry for 15 minutes at room temperature. The tumor area of each sample was manually microdissected and collected into a 1.5 mL labelled eppendorf tube.

For FNAB samples, the slides were left in xylol (Enzymatic, Portugal) for approximately 5 days for coverslips removal. Then, the slides were rinsed in 100% ethanol (Enzymatic, Portugal) for 10 minutes, followed by a passage in 96% ethanol (Enzymatic, Portugal) for 10 minutes and a drying period of 15 minutes at room temperature. The material was manually scraped, and cells were collected into a 1.5 mL labelled eppendorf tube.

The next steps are common for both FFPE tissues and FNAB samples. Cell lysis was performed in 700 µL of QIAzol Lysis Reagent after vortexing, followed by incubation at room temperature for 5 minutes. Then, 140 µL of chloroform was added, followed by a vigorously agitation for 15 seconds and an incubation for 3 minutes at room temperature. After this incubation, the samples were centrifuged (Sorvall Legend Micro 21R centrifuge, Thermo Scientific, USA) for 15 minutes at 12000 g at 4°C and the upper aqueous phase was carefully transferred into a new collection tube. RNA precipitation was performed by adding 525 µL of 100% ethanol. Precipitated RNA was transferred into a RNeasy® Mini column in a 2 mL collection tube, centrifuged (Sorvall Legend Micro 21R centrifuge, Thermo Scientific, USA) at 8000 g for 15 seconds at room temperature and the contaminants were discarded. Three washes were performed by centrifugation (Sorvall Legend Micro 21R centrifuge, Thermo Scientific, USA). First wash was carried out by adding 700 µL of Buffer RWT and centrifugation at 8000 g for 15 seconds; second

and third washes were performed with 500 µL of Buffer RPE and centrifugation at 8000 g for 15 seconds and 2 minutes, respectively. The RNeasy Mini column was transferred into a new 2 mL collection tube and centrifuged at full speed to dry the membrane. The RNeasy Mini column was then transferred into a final labelled eppendorf tube and RNA was eluted in 40 µL of RNase free water in a final centrifugation for 1 minute at 8000 g. Samples were stored at -80°C. RNA concentration was determined using the NanoDrop (ND-1000, Thermo Fisher Scientific, Lithuania) spectrophotometer. RNA handling was always performed on ice.

8. Reverse transcription

Complementary deoxyribonucleic acid (cDNA) synthesis was achieved with TaqMan® Advanced miRNA cDNA Synthesis Kit (Applied biosystems, USA) following the manufacturer's instructions. The kit contains all reagents and material needed for the reactions.

To prepare cDNA templates a series of reactions were performed: polyadenylation (Poly(A)) tailing, adaptor ligation, reverse transcription (RT) and miR-Amp reaction. All components were thaw on ice, mixed and briefly centrifuged prior to use.

A mix for Poly(A) reaction was prepared using 10X Poly(A) Buffer, ATP, Poly(A) Enzyme and RNase-free water. The mix was vortexed and pipetted to each reaction tube. Two µL, containing about 5 ng of RNA of each sample, were added to each reaction tube, followed by a centrifugation. The reaction was carried out in a thermocycler (SimpliAmp™ Thermalcycler, Applied Biosystems, USA) using the following conditions: 45 minutes at 37°C for polyadenylation, and 10 minutes at 65°C to stop reaction (Figure 11).

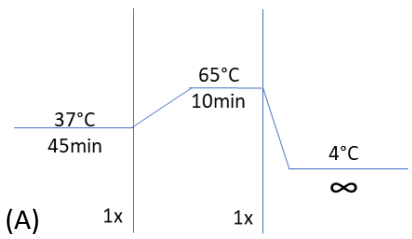

(B)

Poly(A) tailing reaction mix	
10X Poly(A) Buffer	0.5 µL
ATP	0.5 µL
Poly(A) Enzyme	0.3 µL
RNase-free water	1.7 µL
Total	**3 µL**

Figure 11. (A) Thermocycler programme and (B) mix composition for the Poly(A) tailing reaction.

This procedure was followed by an adaptor ligation reaction. For that a mix was prepared using 5X DNA Ligase Buffer, 50% PEG 8000, 25X Ligation Adaptor, RNA Ligase, and RNase-free water. The mix was briefly vortexed and then centrifuged before being transferred into the reaction tube containing the preceding reaction mix. After vortexing samples were incubated in a thermocycler (SimpliAmp™ Thermalcycler, Applied Biosystems, USA) for 60 minutes at 16°C for ligation (Figure 12).

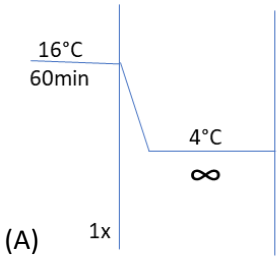

(B)

Adaptor ligation reaction mix	
5X DNA Ligase Buffer	3 µL
50% PEG 8000	4.5 µL
25X Ligation Adaptor	0.6 µL
RNA Ligase	1.5 µL
RNase-free water	0.4 µL
Total	10 µL

Figure 12. (A) Thermocycler programme and (B) mix composition for the adaptor ligation reaction.

The reverse transcription reaction was performed using 5X RT Buffer, dNTP Mix, 20X Universal RT Primer, 10X RT Enzyme Mix, and RNase-free water. The contents were vortexed and centrifuged before being transferred into the reaction tube containing the above reaction products. The reverse transcription reaction (30 µL total volume) was carried out in a thermocycler (SimpliAmp™ Thermalcycler, Applied Biosystems, USA) using the following conditions: 15 minutes at 42°C for reverse transcription and 5 minutes at 85°C to stop reaction (Figure 13).

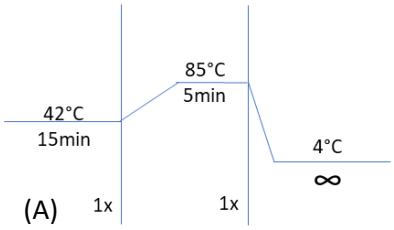

(B)

Reverse Transcription reaction mix	
5X RT Buffer	6 µL
dNTP Mix	1.2 µL
20X Universal RT Primer	1.5 µL
10X RT Enzyme Mix	3 µL
RNase-free water	3.3 µL
Total	**15 µL**

Figure 13. (A) Thermocycler programme and (B) mix composition for the reverse transcription reaction.

For the miR-Amp reaction a mix was performed with 2X miR-Amp Master Mix, 20X miR-Amp Primer Mix and RNase free water. The mix of each sample was vortexed and centrifuged before being transferred into a new labelled reaction tube. Five µL of

RT reaction product was transferred into this new reaction tube, mixed and centrifuged. The reaction took place in a thermocycler (SimpliAmp™ Thermalcycler, Applied Biosystems, USA) using the following conditions: 5 minutes at 95°C for enzyme activation followed by 14 cycles of 3 seconds at 95°C for denaturation and 30 seconds at 60°C for annealing, followed by a final step of 10 minutes at 99°C to stop reaction (Figure 14).

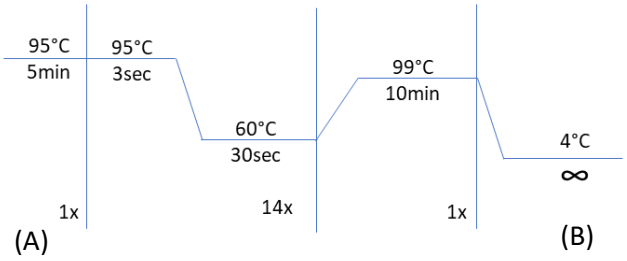

miR-Amp reaction mix	
2X miR-Amp Master Mix	25 µL
20X miR-Amp Primer Mix	2.5 µL
RNase free water	17.5 µL
Total	**45 µL**

Figure 14. (A) Thermocycler programme and (B) mix composition for the miR-Amp reaction.

9. Quantitative real time PCR (RT-qPCR)

RT-qPCR was performed to evaluate the relative expression levels of miR-146b, miR-221, miR-222 and miR-15a, previously reported to be altered in thyroid cancer [100]. miR-16 was used as an endogenous control for normalization of the expression values [101]. For each analyzed sample, the relative quantity of miRNA was determined as ΔCT. The ΔCT value is the subtraction of the endogenous control gene CT (threshold cycle) from the target gene CT. The relative quantification of gene expression was attained using the $2^{-\Delta\Delta CT}$ method. The ΔΔCT value is determined by subtracting the average control group ΔCT (benign tumors) from each sample (malignant tumors) ΔCT [102].

RT-qPCR was performed using TaqMan® Fast Advanced Master Mix (2X), TaqMan® Advanced miRNA Assay (20X) and RNase-free water in a final volume of 15 µL. The mix was vortexed followed by a short spin and 15 µL of the PCR reaction mix was transferred into a well of a 96-well PCR reaction plate. 5 µL of diluted cDNA was added to each reaction well before a short centrifugation. The reaction was incubated for 20 seconds at 95°C for enzyme activation followed by 40 cycles of 1 second at 95°C for denaturation, 20 seconds at 60°C for annealing, using the QuantStudio 5 Real-Time PCR System (ThermoScientific, USA) (Figure 15). Duplicates were done for all samples, and a non-template control (NTC) was used to verify the presence of contamination.

(A)

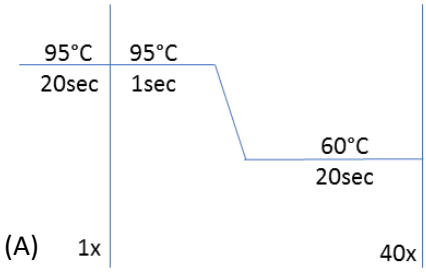

(B)

RT-qPCR mix	
TaqMan® Fast Advanced Master Mix (2X)	10 µL
TaqMan® Advanced miRNA Assay (20X)	1 µL
RNase-free water	4 µL
Total	**15 µL**

Figure 15. (A) QuantStudio programme and (B) reaction conditions for the RT-qPCR.

10. Statistical Analysis

Statistical analysis was performed using the Software IBM SPSS Statistics 26 (IBM, New York, USA). Proportions were compared using $\chi 2$ test or Fisher's exact test when appropriate (Yates correction in cases of multiple entries). McNemar's test was used to compare the mutation status between the cytology and the corresponding histology. The differences between means were assessed by Student's unpaired t-test for independent samples. Differences were considered statistically significant when $p<0.05$.

Results

1. Database construction

A database for all samples was created in which the clinicopathological features of patients and tumors were gathered based on the information available in the clinic and histopathologic reports from the Hospital Curry Cabral, as well as all revised histological features from the tumors, after a careful revision of the H&E slides by an experienced pathologist at our institute. All molecular and miRNA expression data obtained from practical work were added to the same database, which was later used for statistical analysis (IBM SPSS Statistics version 26) (IBM, New York, USA).

2. Series description

2.1 Clinicopathological characteristics

We have evaluated a series of 90 consecutive patients referred for surgical excision from 2016 to 2018 at Hospital Curry Cabral, from which one thyroid cytology (FNAB) and respective histology (FFPE tissue) was available. A molecular and diagnostic cyto-histologic correlation was determined.

The 90 histology samples were composed by 2 (2.22%) normal thyroid tissues, 13 (14.44%) benign lesions, 2 (2.22%) cases of WDT-UMP, 2 (2.22%) cases of NIFTP, and 71 (78.9%) tumor lesions, comprising 66 (73.33%) cases of PTC, 3 (3.33%) cases of HCC, 1 (1.11%) case of FTC and 1 (1.11%) of PDTC (Table 3).

Cytology samples were distributed according to Bethesda classification as follow: 24 (26.7%) samples were benign (B), 10 (11.1%) samples were atypia of undetermined significance/follicular lesion of undetermined significance (AUS/FLUS), 6 (6.7%) samples were suspicious for follicular neoplasm (SFN), 19 (21.1%) suspicious for malignancy (SM) and 25 (27.8%) samples were considered malignant (M) (Table 3). The diagnostic of six (6.7%) samples was not determined due to lack of material in the FNAB slide being classified as non-diagnostic (ND). The distribution of the cytology within each histology category is represented in table 4.

Table 3. Distribution of the cytology and histology specimens within the series

Series composition	
Cytology (n=90)	**Histology** (n=90)
6 ND 24 Benign 10 AUS/FLUS 6 SFN 19 SM 25 M	2 Normal thyroid tissue 13 Benign 2 WDT-UMP 2 NIFTP 66 PTC 3 HCC 1 FTC 1 PDTC

Abbreviations: ND: Non-diagnostic, B: Benign, AUS/FLUS: Atypia of undetermined significance/Follicular lesion of undetermined significance, SFN: Suspicious for a follicular neoplasm, SM: Suspicious for malignancy, M: Malignant.

Table 4. Distribution of the cytology within each histological subtype

Histology diagnosis (n=90)	**Normal Thyroid tissue** n=2 (2.22%)	**Benign** n=13 (14.44%)	**WDT-UMP** n=2 (2.22%)	**NIFTP** n=2 (2.22%)	**PTC** n=66 (73.33%)	**HCC** n=3 (3.33%)	**FTC** n=1 (1.11%)	**PDTC** n=1 (1.11%)
Cytology diagnosis (n=90)	1 B 1 SM	12 B 1 M	1 B 1 AUS/FLUS	1 ND 1 SFN	5 ND 9 B 9 AUS/FLUS 3 SFN 17 SM 23 M	1 B 1 SFN 1 M	1 SFN	1 SM

Abbreviations: ND: Non-diagnostic, B: Benign, AUS/FLUS: Atypia of undetermined significance/Follicular lesion of undetermined significance, SFN: Suspicious for a follicular neoplasm, SM: Suspicious for malignancy, M: Malignant.

The clinicopathological features of the 90 cases are described in tables 5 and 6. All primary lesions were evaluated for several parameters, both concerning patient´s characteristics (age and gender) (Table 5), as well as tumor's clinicopathological features (tumor size, extrathyroidal invasion, capsule invasion, vascular, venous and lymphatic invasion, presence of fibrosis, inflammatory infiltrate, tall cell, oncocytic component, psammoma bodies, calcification, necrosis, LNM, as well as focality and laterality (Table 6).

From the 90 patients, 75 (83.3%) were female, with mean age of 52.31 ± 15.93, ranging between 18 to 84 years, and 15 (16.7%) were male, with mean age of 53.6 ± 13.74 ranging between 35 to 79 years (Table 5).

Table 5. Series distribution: age and sex

Series distribution (n=90)		
Sex	**N (%)**	**Mean age (± SD)**
Female	75 (83.3%)	52.31 ± 15.93
Male	15 (16.7%)	53.6 ± 13.74

The majority of the tumor samples were PTCs (66/90, 73.3%). The mean tumor size of all series was 27.85 ± 14.99 mm, ranging from 3 to 70 mm, and PTC, FTC and PDTC tended to be larger. Aggressive tumors were more prevalent in older patients. Extrathyroidal invasion, capsule invasion, fibrosis, and inflammatory infiltrate were predominant in PTCs as well as absence of vascular, venous, lymphatic invasion, tall cell and oncocytic component. All cases of HCC, FTC and PDTC presented capsule invasion. Psammoma bodies and calcification were only observed in PTCs. The presence of necrosis was observed only in 3 cases, in two PTCs and one PDTC. Malignant tumors tended to be unifocal whereas benign samples tended to be multifocal. The majority of the lesions were unilateral. LNM were mainly present in PTCs (Table 6).

Table 6. Patient's and tumors clinicopathological features

Clinicopathological characteristics	Histology Diagnosis							
	Normal thyroid tissue n=2	**Benign** n=13	**WDT-UMP** n=2	**NIFTP** n=2	**PTC** n=66	**HCC** n=3	**FTC** n=1	**PDTC** n=1
Mean age ± Std (n=90)	46.5 ± 7.78	49.92 ± 14.77	49 ± 4.24	40 ± 2.83	53.27 ± 16.23	49.67 ± 9.45	61 ± 0.00	81 ± 0.00
Mean tumor size ± Std (mm) (n=83)	-	21.25 ± 14.82	42.5 ± 10.61	21 ± 12.73	27.11 ± 14.56	24.33 ± 5.13	60 ± 0.00	65 ± 0.00
Gender (n=90)								
Male	0 (0.0%)	3 (23.1%)	0 (0.0%)	0 (0.0%)	10 (15.2%)	1 (33.3%)	1 (100%)	0 (0.0%)
Female	2 (100%)	10 (76.9%)	2 (100%)	2 (100%)	56 (84.8%)	2 (66.7%)	0 (0.0%)	1 (100%)
Extrathyroidal invasion (n=67)								
Absent	-	2 (100%)	2 (100%)	1 (100%)	34 (59.6%)	2 (66.7%)	1 (100%)	0 (0.0%)
Present	-	0 (0.0%)	0 (0.0%)	0 (0.0%)	23 (40.4%)	1 (33.3%)	0 (0.0%)	1 (100%)
Capsule invasion (n=49)								
Absent	-	1 (100%)	-	2 (100%)	5 (12.2%)	0 (0.0%)	0 (0.0%)	0 (0.0%)
Present	-	0 (0.0%)	-	0 (0.0%)	36 (87.8%)	3 (100%)	1 (100%)	1 (100%)
Vascular invasion (n=74)								
Absent	-	2 (100%)	2 (100%)	2 (100%)	54 (84.4%)	0 (0.0%)	1 (100%)	0 (0.0%)
Present	-	0 (0.0%)	0 (0.0%)	0 (0.0%)	10 (15.6%)	2 (100%)	0 (0.0%)	1 (100%)
Venous invasion (n=66)								
Absent	-	2 (100%)	2 (100%)	2 (100%)	55 (96.5%)	0 (0.0%)	1 (100%)	0 (0.0%)
Present	-	0 (0.0%)	0 (0.0%)	0 (0.0%)	2 (3.5%)	1 (100%)	0 (0.0%)	1 (100%)
Lymphatic invasion (n=66)								
Absent	-	2 (100%)	2 (100%)	2 (100%)	46 (78%)	1 (100%)	-	-
Present	-	0 (0.0%)	0 (0.0%)	0 (0.0%)	13 (22%)	0 (0.0%)	-	-
Fibrosis (n=72)								
Absent	-	-	1 (100%)	0 (0.0%)	17 (26.2%)	2 (66.7%)	-	0 (0.0%)
Present	-	-	0 (0.0%)	2 (100%)	48 (73.8%)	1 (33.3%)	-	1 (100%)

Table 6. Continued

Clinicopathological characteristics	Histology Diagnosis							
	Normal thyroid tissue n=2	**Benign** n=13	**WDT-UMP** n=2	**NIFTP** n=2	**PTC** n=66	**HCC** n=3	**FTC** n=1	**PDTC** n=1
Inflammatory infiltrate (n=73)								
Absent	-	0 (0.0%)	1 (100%)	2 (100%)	37 (56.9%)	2 (66.7%)	-	0 (0.0%)
Present	-	1 (100%)	0 (0.0%)	0 (0.0%)	27 (41.5%)	1 (33.3%)	-	1 (100%)
Chronic	-	0 (0.0%)	0 (0.0%)	0 (0.0%)	1 (1.5%)	0 (0.0%)	-	0 (0.0%)
Tall cell (n=72)								
Absent	-	-	1 (100%)	2 (100%)	53 (81.5%)	3 (100%)	-	1 (100%)
< 50%	-	-	0 (0.0%)	0 (0.0%)	10 (15.4%)	0 (0.0%)	-	0 (0.0%)
≥ 50%	-	-	0 (0.0%)	0 (0.0%)	2 (3.0%)	0 (0.0%)	-	0 (0.0%)
Oncocytic component (n=72)								
Absent	-	-	1 (100%)	2 (100%)	39 (60.0%)	0 (0.0%)	-	1 (100%)
< 75%	-	-	0 (0.0%)	0 (0.0%)	23 (35.3%)	0 (0.0%)	-	0 (0.0%)
≥ 75%	-	-	0 (0.0%)	0 (0.0%)	3 (4.6%)	3 (100%)	-	0 (0.0%)
Psammoma bodies (n=72)								
Absent	-	-	1 (100%)	2 (100%)	51 (78.5%)	3 (100%)	-	1 (100%)
Present	-	-	0 (0.0%)	0 (0.0%)	14 (21.5%)	0 (0.0%)	-	0 (0.0%)
Calcification (n=72)								
Absent	-	-	1 (100%)	2 (100%)	47 (72.3%)	3 (100%)	-	1 (100%)
Present	-	-	0 (0.0%)	0 (0.0%)	18 (27.7%)	0 (0.0%)	-	0 (0.0%)
Necrosis (n=72)								
Absent	-	-	1 (100%)	2 (100%)	63 (96.9%)	3 (100%)	-	0 (0.0%)
Present	-	-	0 (0.0%)	0 (0.0%)	2 (3.1%)	0 (0.0%)	-	1 (100%)
Focality (n=90)								
Unifocal	1 (50.0%)	1 (7.7%)	2 (100%)	2 (100%)	36 (54.5%)	1 (33.3%)	1 (100%)	0 (0.0%)
Multifocal	1 (50.0%)	12 (92.3%)	0 (0.0%)	0 (0.0%)	30 (45.5%)	2 (66.7%)	0 (0.0%)	1 (100%)
Laterality (n=90)								
Unilateral	1 (50.0%)	9 (69.2%)	2 (100%)	2 (100%)	43 (65.2%)	1 (33.3%)	1 (100%)	0 (0.0%)
Bilateral	1 (50.0%)	4 (30.8%)	0 (0.0%)	0 (0.0%)	23 (34.8%)	2 (66.7%)	0 (0.0%)	1 (100%)
Lymph node metastasis (n=46)								
Absent	0 (0.0%)	2 (100%)	2 (100%)	-	28 (71.8%)	1 (100%)	-	0 (0.0%)
Present	1 (100%)	0 (0.0%)	0 (0.0%)	-	11 (28.4%)	0 (0.0%)	-	1 (100%)

2.2 Genetic alterations

The molecular status of *TERT*p, *BRAF*, and *RAS* (*NRAS*, *HRAS* and *KRAS*) genes of the cytologies and histologies is summarized in tables 7 and 8, respectively.

Table 7. Mutational status of the cytology samples

	n=	WT	Mutated	Mutation type
***TERT*p**	90	84 (93.3%)	6 (6.7%)	124 (G>A)
BRAF	89*	67 (75.2%)	22 (24.7%)	21 p.V600E 1 p.K601E
NRAS	90	85 (94.4%)	5 (5.6%)	p.Q61R
HRAS	90	87 (96.7%)	3 (3.3%)	p.Q61R
KRAS	90	90 (100%)	0 (0.0%)	-

*One case missing due to technical issues.

Table 8. Mutational status of the histology samples

	n=	WT	Mutated	Mutation type
***TERT*p**	88*	80 (90.9%)	8 (9.1%)	7 (-124 G>A) 1 (-146 G>A)
BRAF	90	68 (75.6%)	22 (24.4%)	21 p.V600E 1 p.K601E
NRAS	90	85 (94.4%)	5 (5.6%)	p.Q61R
HRAS	90	86 (95.6%)	4 (4.4%)	3 p.Q61R 1 p.Q61K
KRAS	90	88 (97.8%)	2 (2.2%)	p.Q61R

*Two cases missing due to technical issues.

Thirty six of the 90 cytology samples were mutated. Six tumors (6.7%) were mutated for *TERT*p, 22 (24.7%) were mutated for *BRAF*, 5 (5.6%) for *NRAS* and 3 (3.3%) for *HRAS*. No mutations were found in *KRAS* gene (Table 7).

Concerning *TERT*p mutations, two hotspots were assessed (-124 and -146). All mutations were found in the -124 hotspot (G>A) (Figure 16). From the 22 *BRAF* mutations found, 21 were p.V600E and one was p.K601E (Figure 17). All 8 mutations found in the RAS genes (5 in *NRAS* and 3 in *HRAS*), were the p.Q61R mutation (Figures 18 and 19, respectively).

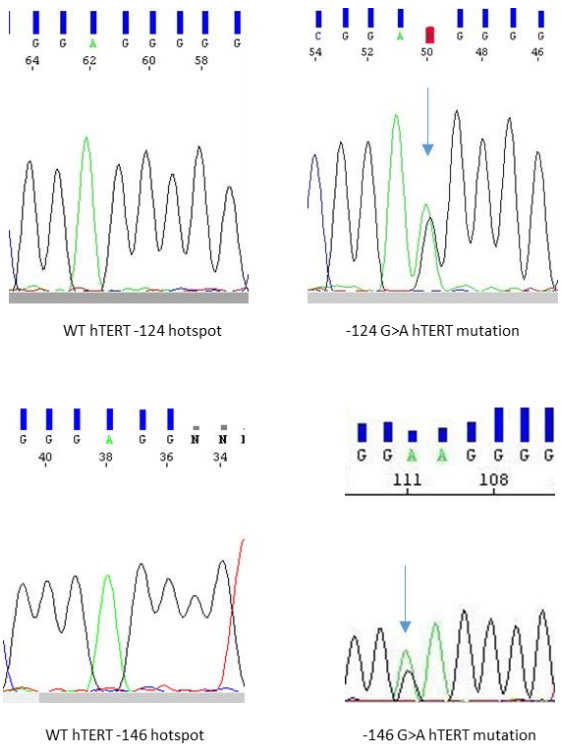

Figure 16. Representative chromatogram of WT and mutated (-124 and -146) h*TERT* hotspots.

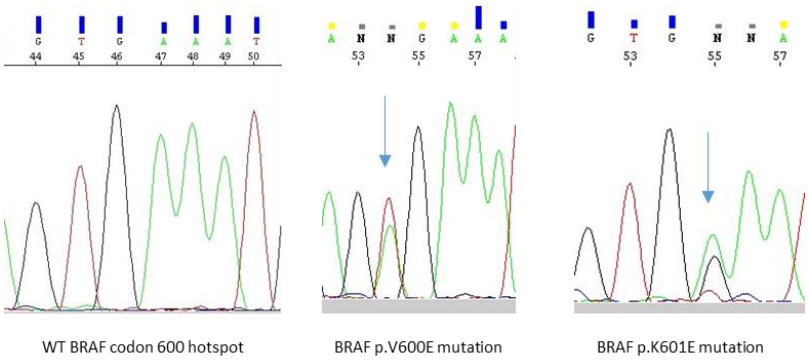

Figure 17. Representative chromatogram of WT and mutated (p.V600E and p.K601E) *BRAF*.

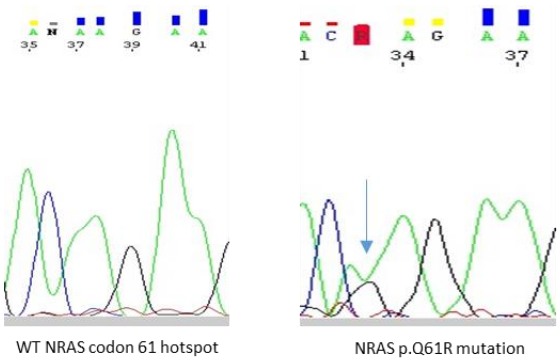

Figure 18. Representative chromatogram of WT and mutated (p.Q61R) *NRAS*.

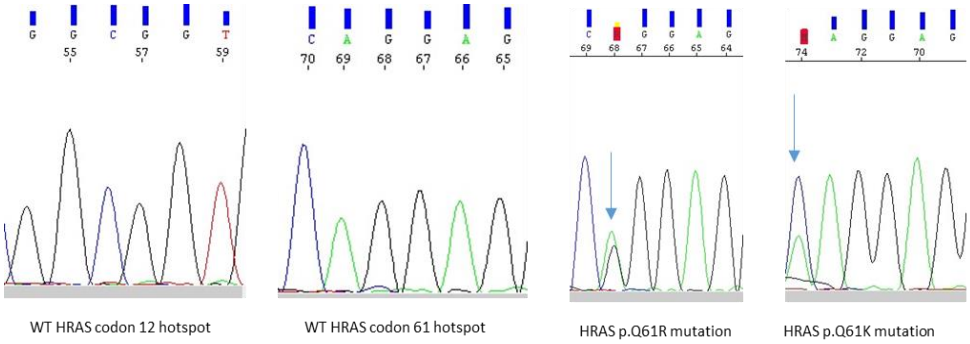

Figure 19. Representative chromatogram of WT and mutated (p.Q61R and p.Q61K) *HRAS*.

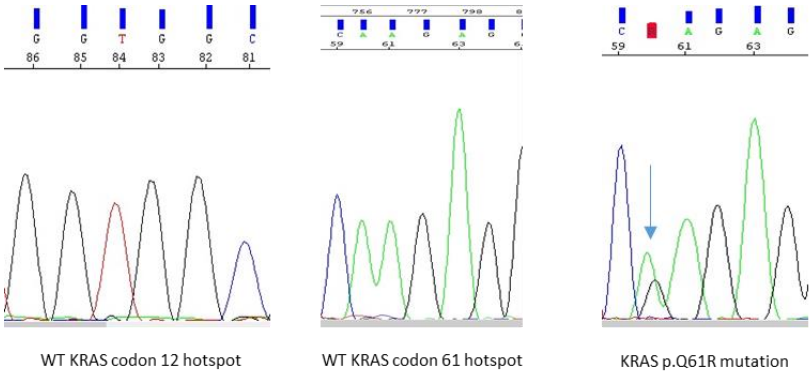

Figure 20. Representative chromatogram of WT and mutated (p.Q61R) *KRAS*.

In histology samples, 41 cases were mutated (Table 8). Eight cases (9.1%) have a *TERT*p mutation, 22 (24.4%) a *BRAF* mutation, 5 (5.6%) a *NRAS* mutation, 4 (4.4%) a *HRAS* and 2 (2.2%) a *KRAS* mutation (Table 8). From the 8 *TERT*p mutations, 7 (87.5%) cases presented the -124 (G>A) mutation, and 1 (12.5%) case had the -146 (G>A) mutation (Figure 16). Concerning *BRAF*, 21 (95.5%) samples have the p.V600E mutation and one (4.5%) has the p.K601E mutation (Figure 17). The 7 mutations found in both *NRAS* and *KRAS* are the p.Q61R mutation (Figure 18 and 20, respectively). For *HRAS*, 3 samples have the p.Q61R mutation and 1 sample the p.Q61K (Figure 19). All mutations were detected in PTCs which will be better described further in this study.

Globally, there was a good cyto-histologic molecular correlation (69/90, 76.7%). However, when we evaluate the paired correlation between the presence of mutations in cytology and respective histology (McNemar's test) and analyzing all genes individually, the cyto-histological correlations were not statistically significant (data not shown), as 21 cases presented discordant results (Table 9). The highest discordance was found for the presence of mutations in the *BRAF* gene (10/89 cases), representing 11.2% discordancy, followed by *TERT*p and *NRAS* genes (4 cases each; 4.5% and 4.4%, discordancy respectively), and by *KRAS* and *HRAS*, with 2.2% and 1.1% discordancy, respectively (2 and 1 case, respectively). It is worth to note that all these cases were repeated three to four times for confirmation.

In order to understand this genetic cyto-histologic discrepancy, we have looked more closely to these 21 cases (Table 9). In thirteen of 21 cases we had wild-type cytology, whereas mutations were present in the respective histology (3 cases for *TERT*, 5 cases for *BRAF* and 5 cases for *RAS* genes). On the other hand, 8 of the 21 cases that showed mutations in the cytology were wild-type in the respective histology (1 case for *TERT*, 5 cases for *BRAF* and 2 cases for *RAS* genes) (Table 9).

Table 9. Profile of the molecular cyto-histological discordant cases

Case number	Tumor size (mm)	Gene	Cytology		Histology	
			Diagnosis	Molecular status	Diagnosis	Molecular status
22	25	***TERT***	ND	WT	Invasive FV-PTC	-124 (G>A)
61	28	***TERT***	B	WT	c-PTC	-124 (G>A)
64	50	***TERT***	M	-124 (G>A)	OV-PTC	WT
82	35	***TERT***	M	WT	c-PTC	-146 (G>A)
6	19	***BRAF***	M	V600E	TC-PTC	WT
12	12	***BRAF***	M	WT	c-PTC	p.V600E
24	15	***BRAF***	M	V600E	Hashimoto's thyroiditis	WT
29	3	***BRAF***	SM	WT	microPTC	p.V600E
34	25	***BRAF***	SM	WT	c-PTC	p.V600E
47	15	***BRAF***	B	WT	c-PTC	p.V600E
52	20	***BRAF***	M	WT	Invasive FV-PTC	p.V600E
63	-	***BRAF***	SM	V600E	Normal thyroid tissue	WT
65	20	***BRAF***	ND	V600E	c-PTC	WT
80	30	***BRAF***	SM	V600E	c-PTC	WT
48	45	***NRAS***	B	WT	Invasive FV-PTC	p.Q61R
71	25	***NRAS***	SM	WT	Invasive FV-PTC	p.Q61R
39	14	***NRAS***	AUS/FLUS	p.Q61R	c-PTC	WT
29	3	***NRAS***	SM	p.Q61R	microPTC	WT
17	5	***HRAS***	AUS/FLUS	WT	microPTC	p.Q61K
43	15	***KRAS***	ND	WT	Infiltrative FV-PTC	p.Q61R
49	40	***KRAS***	SM	WT	c-PTC	p.Q61R

Abbreviations: ND: Non-diagnostic, B: Benign, AUS/FLUS: Atypia or follicular lesion of undetermined significance, SM: Suspicious for malignancy and M: Malignant.

According to the Bethesda classification, 3 of the discordant cases were ND, 3 were B, 2 were AUS/FLUS and 13 were SM or M. The benign, AUS/FLUS and ND cases were classified as malignant in the histology. The SM and M remained malignant, except for two cases that after histopathological review of the available slides were classified as Hashimoto thyroiditis and normal thyroid tissue (Table 9).

For 6 of the 90 cases, LNM were available for molecular characterization. Five of the LNM samples were wild-type for all genes and 1 case presented the p.V600E mutation, results that were concordant with the respective cytology and histology samples (data not shown).

2.3 Mutation frequency across the FNABs within the malignant histology

The histology slides were reviewed for all cases. In some of them there was divergence with the original histologic diagnosis. This was mainly due to the fact that some of the histologic slides we have access did not correspond to the reported diagnosis. The distribution of the mutations and their comparison between benign and malignant histology reviewed cases in each Bethesda category is shown in table 10. All ND cases were classified as malignant in the histological diagnosis. Concerning the B cytologies, 11 of 24 (45.8%) cases were classified as malignant in the histology. All AUS/FLUS (n=10) and all SFN (n=6) cytologies were classified as malignant in the histology. Within the SM (n=19) and M (n=25) cytologies, only one case of each was not classified as malignant in the histology.

From the 11 B cytologies classified as malignant in the histology, one (9.1%) has a *RAS* mutation; the 10 AUS/FLUS cytologies classified as malignant in the histology, two (20%) have a *RAS* mutation; from the 6 SFN cytologies, classified as malignant in the histology, one (16.7%) shows a *TERT*p mutation (Table 10).

In the histology, ND cytologies only presented mutations in *BRAF* gene in 2/6 (33.3%). Benign and AUS/FLUS lesions only show mutations in RAS gene in 1/11 (9.1%) and 2/10 (20%) cases, respectively. SFN lesions present only one (16.7%) *TERT*p mutation within the 6 malignant histological classified cases. SM cytologies show a *BRAF* mutation in the unique case that was classified as B in the histology, and in the malignant cases, both *BRAF* and *RAS* mutations were present in 7/18 (38.9%) and 2/18 (11.1%) lesions, respectively. For the M cytologies, a *BRAF* mutation was found in the unique case that was classified as B in the histology, and in the malignant cases *TERT*p+*RAS*, *RAS*, *TERT*p+*BRAF* and *BRAF* only mutations, were present in 1/24 (4.2%), 2/24 (8.3%), 4/24 (16.7%) and 7/24 (29.2%), respectively (Table 10). No statistical significances were observed in any of the groups (Figure 21).

Table 10. Mutational frequency through Bethesda categories in histology malignant cases

Bethesda	ND n=6		B n=24		AUS/FLUS n=10		SFN n=6		SM n=19		M n=25	
Histology malignancy	No (0)	Yes (6)	No (13)	Yes (11)	No (0)	Yes (10)	No (0)	Yes (6)	No (1)	Yes (18)	No (1)	Yes (24)
WT	0	4	13	10	0	8	0	5	0	9	0	10
TERTp only	0	0	0	0	0	0	0	**1**	0	0	0	0
BRAF only	0	**2**	0	0	0	0	0	0	1	**7**	1	**7**
TERTp+BRAF	0	0	0	0	0	0	0	0	0	0	0	**4**
RAS (NRAS, HRAS, KRAS)	0	0	0	**1**	0	**2**	0	0	0	**2**	0	**2**
TERTp+RAS (NRAS, HRAS, KRAS)	0	0	0	0	0	0	0	0	0	0	0	**1**

Abbreviations: ND: Non-diagnostic, B: Benign, AUS/FLUS: Atypia of Undetermined Significance/Follicular Lesion of Undetermined Significance, SFN: Suspicious for follicular neoplasm, SM: Suspicious for malignancy and M: Malignant.

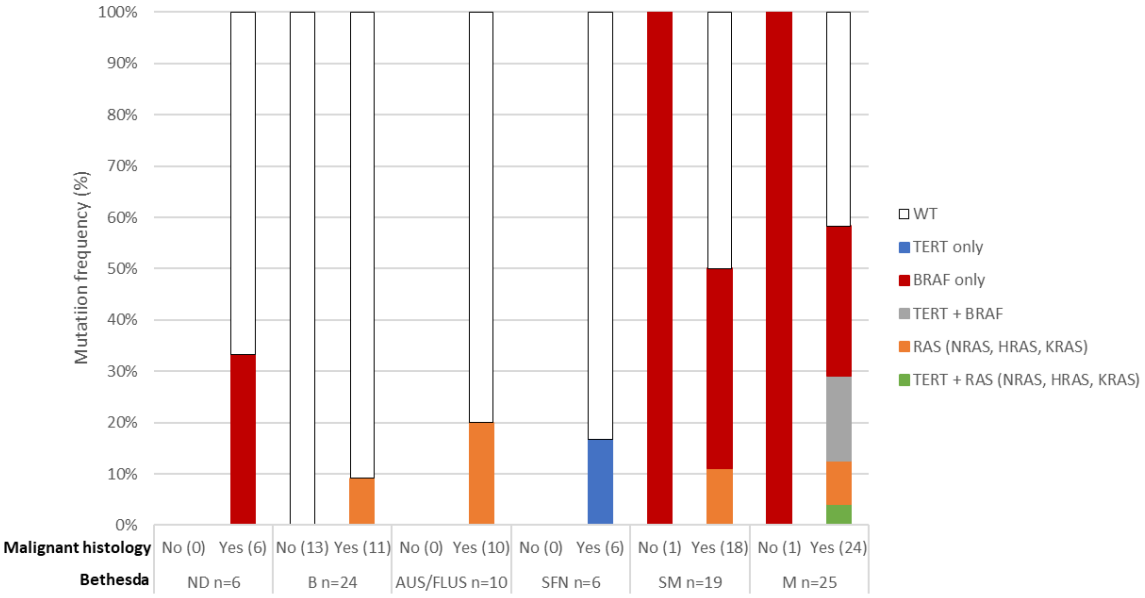

Figure 21. Mutational frequency in cytology samples according to Bethesda categories.

Diagnosis of malignancy was confirmed in the paired histology. No/Yes: Absence/Presence of malignancy, N: Number of cytologies in each Bethesda category. Chi-square tests were used to compare frequency between benign and malignant cases.

We have looked more closely to the results of each of the B, AUS/FLUS, SFN and SM (n=59) cytologies after histologic review (HR). Forty-five of these 59 lesions have a diagnosis of malignancy after histological evaluation and only 14 are benign. Due to the small numbers of mutations found, we have grouped all mutated cases independently from the type of mutated gene. Thus, from 45 cytologies that present malignancy in the histological evaluation, 13 (28.9%) presented genetic alterations: 1 (7.7%) *TERT*p, 5 (38.5%) *RAS* and 7 (53.8%) *BRAF* and 32 were wild-type for all the analyzed genes. From the 14 cases classified as B after histological evaluation, only one was mutated for *BRAF* gene. No statistical significances were found when comparing these groups (Table 11).

Table 11. Correlation between the diagnosis and mutational status of the cytologies

	Wild-type	Mutated
Histological malignant (n=45)	32	13
Histological benign (n=14)	13	1
Total (n=59)	45	14

2.4 Clinicopathological features of PTCs

For statistical analysis of the clinicopathological features of the cases, only PTCs were considered due to the reduced number of the other lesions (B, WDT-UMP, NIFTP, HCC, FTC and PDTC). Data on B, WDT-UMP, NIFTP, HCC, FTC and PDTC lesions is available in the supplementary section.

From the 90 patients, 66 (73.33%) were PTCs. PTCs were composed by 27 (40.9%) c-PTC, 20 (30.3%) FV-PTC, from which 18 (27.3%) cases were invasive FV-PTC and two (3%) cases were infiltrative FV-PTC, 2 (3%) cases of EV-PTC, 2 (3%) cases of SV-PTC and 2 (3%) of TC-PTC, 6 (9.1%) cases of OV-PTC and 7 (10.6%) were microPTCs (Table 12). The patient's characteristics and clinicopathological description are represented in table 13 and 14.

Table 12. Histological distribution of the PTC variants

PTC n=66
c-PTC n=27 (40.9%)
FV-PTC n=20 (30.3%)
EV-PTC n=2 (3%)
SV-PTC n=2 (3%)
TC-PTC n=2 (3%)
OV-PTC n=6 (9.1%)
microPTC n=7 (10.6%)

c-PTC (40.9%) and FV-PTC (30.3%, either invasive or infiltrative) were the most common PTC tumors, and less frequent were the EV-PTC (3%), SV-PTC (3%), TC-PTC (3%) OV-PTC (9.1%), and microPTCs (10.6%). Other less common variants such as diffuse sclerosing, spindle cell, whartin-like, columnar cell, cribriform-morular, hobnail, fibromatosis/fasciitis like and clear cell were not reported in this study.

From the 66 PTC, 10 (15.2%) were males and 56 (84.8%) females (Table 13). The mean age was 53.27 ± 16.23, ranging between 18 to 84 years. Mean tumor size was 27.11 ± 14.56mm, ranging from 3 to 70 mm (Table 13). EV-PTC, OV-PTC, SV-PTC and TC-PTC were found in females only (Table 14). Considering the clinicopathological features, about 88% of all PTCs presented capsule invasion with a higher trend in invasive FV-PTC (43.9%). The presence of fibrosis was observed in 73.8% of all PTCs and most of them were unifocal (54.5%) and unilateral (65.2%). LNM was observed in 11 (28.2%) cases, from which 8 (72.7%) were c-PTCs. Only 3.1% of the tumors presented necrosis (Table 14).

Table 13. Patient's age, tumor size and gender of all PTCs

Clinicopathological features of PTCs (n=66)	
Mean age ± Std	53.27 ± 16.23
Mean tumor size ± Std (mm)	27.11 ± 14.56
Gender	
Male	10 (15.2%)
Female	56 (84.8%)

Table 14. Patient's age and gender, and clinicopathological features of the PTC variants

Clinicopathological characteristics	**PTC variants**							
	c-PTC n=27 (40.9%)	**FV-PTC** n=20		**Encapsulated PTC** n=2 (3%)	**Oncocytic PTC** n=6 (9.1%)	**Solid PTC** n=2 (3%)	**Tall Cell PTC** n=2 (3.0%)	**microPTC** n=7 (10.6%)
		Invasive n=18 (27.3%)	**Infiltrative** n=2 (3%)					
Mean age ± Std (n=66)	49.78 ± 16.66	53.50 ± 17.49	50.50 ± 17.68	65.00 ± 2.83	61.33 ± 12.71	69.50 ± 9.19	43.50 ± 13.44	54.86 ± 16.15
Mean tumor size ± Std (mm) (n=66)	27.93 ± 13.69	28.11 ± 12.18	13.50 ± 2.12	42.50 ± 3.54	39.50± 15.96	36.50 ± 12.02	28.0 ± 12.73	7.29 ± 2.81
Gender (n=66)								
Male	3 (11.1%)	5 (27.8%)	1 (50.0%)	0 (0.0%)	0 (0.0%)	0 (0.0%)	0 (0.0%)	1 (14.3%)
Female	24 (88.9%)	13 (72.2%)	1 (50.0%)	2 (100%)	6 (100%)	2 (100%)	2 (100%)	6 (85.7%)
Extrathyroidal invasion (n=57)								
Absent	11 (45.8%)	13 (86.7%)	1 (100%)	1 (100%)	4 (66.7%)	1 (50.0%)	1 (50.0%)	2 (33.3%)
Present	13 (54.2%)	2 (13.3%)	0 (0.0%)	0 (0.0%)	2 (33.3%)	1 (50.0%)	1 (50.0%)	4 (66.7%)
Capsule invasion (n=41)								
Absent	1 (9.1%)	0 (0.0%)	-	2 (100%)	1 (25.0%)	0 (0.0%)	-	1 (25.0%)
Present	10 (90.9%)	18 (100%)	-	0 (0.0%)	3 (75.0%)	2 (100%)	-	3 (75.0%)
Vascular invasion (n=64)								
Absent	22 (84.6%)	14 (77.8%)	2 (100%)	2 (100%)	4 (80.0%)	1 (50.0%)	2 (100%)	7 (100%)
Present	4 (15.4%)	4 (22.2%)	0 (0.0%)	0 (0.0%)	1 (20.0%)	1 (50.0%)	0 (0.0%)	0 (0.0%)
Venous invasion (n=57)								
Absent	24 (96.0%)	14 (100%)	1 (100%)	2 (100%)	4 (80.0%)	1 (100%)	2 (100%)	7 (100%)
Present	1 (4.0%)	0 (0.0%)	0 (0.0%)	0 (0.0%)	1 (20.0%)	0 (0.0%)	0 (0.0%)	0 (0.0%)
Lymphatic invasion (n=59)								
Absent	15 (62.5%)	15 (93.8%)	2 (100%)	2 (100%)	2 (50.0%)	2 (100%)	1 (50.0%)	7 (100%)
Present	9 (37.5%)	1 (6.3%)	0 (0.0%)	0 (0.0%)	2 (50.0%)	0 (0.0%)	1 (50.0%)	0 (0.0%)
Fibrosis (n=65)								
Absent	4 (15.4%)	8 (44.4%)	1 (50.0%)	1 (50.0%)	1 (16.7%)	0 (0.0%)	0 (0.0%)	2 (28.6%)
Present	22 (84.6%)	10 (55.6%)	1 (50.0%)	1 (50.0%)	5 (83.3%)	2 (100%)	2 (100%)	5 (71.4%)
Inflammatory infiltrate (n=65)								
Absent	9 (34.6%)	16 (88.9%)	1 (50.0%)	2 (100%)	5 (83.3%)	1 (50.0%)	0 (0.0%)	3 (42.9%)
Present	16 (61.5%)	2 (11.1%)	1 (50.0%)	0 (0.0%)	1 (16.7%)	1 (50.0%)	2 (100%)	4 (57.1%)
Chronic	1 (3.8%)	0 (0.0%)	0 (0.0%)	0 (0.0%)	0 (0.0%)	0 (0.0%)	0 (0.0%)	0 (0.0%)

Table 14. (Continued)

Clinicopathological characteristics	PTC variants							
	c-PTC n=27 (40.9%)	**FV-PTC** n=20		**Encapsulated PTC** n=2 (3%)	**Oncocytic PTC** n=6 (9.1%)	**Solid PTC** n=2 (3%)	**Tall Cell PTC** n=2 (3.0%)	**microPTC** n=7 (10.6%)
		Invasive n=18 (27.3%)	**Infiltrative** n=2 (3%)					
Tall cell (n=65)								
Absent	19 (73.1%)	18 (100%)	2 (100%)	2 (100%)	5 (83.3%)	2 (100%)	0 (0.0%)	5 (71.4%)
< 50%	7 (26.8%)	0 (0.0%)	0 (0.0%)	0 (0.0%)	1 (16.7%)	0 (0.0%)	0 (0.0%)	2 (28.6%)
≥ 50%	0 (0.0%)	0 (0.0%)	0 (0.0%)	0 (0.0%)	0 (0.0%)	0 (0.0%)	2 (100%)	0 (0.0%)
Oncocytic component (n=65)								
Absent	14 (53.8%)	15 (83.3%)	1 (50.0%)	2 (100%)	0 (0.0%)	1 (50.0%)	0 (0.0%)	6 (85.7%)
< 75%	12 (45.9%)	3 (16.7%)	1 (50.0%)	0 (0.0%)	3 (50.0%)	1 (50.0%)	2 (100%)	1 (14.3%)
≥ 75%	0 (0.0%)	0 (0.0%)	0 (0.0%)	0 (0.0%)	3 (50.0%)	0 (0.0%)	0 (0.0%)	0 (0.0%)
Psammoma bodies (n=65)								
Absent	17 (65.4%)	17 (94.4%)	2 (100%)	2 (100%)	5 (83.3%)	2 (100%)	0 (0.0%)	6 (85.7%)
Present	9 (34.6%)	1 (5.6%)	0 (0.0%)	0 (0.0%)	1 (16.7%)	0 (0.0%)	2 (100%)	1 (14.3%)
Calcification (n=65)								
Absent	15 (57.5%)	16 (88.9%)	2 (100%)	2 (100%)	4 (66.7%)	2 (100%)	0 (0.0%)	6 (85.7%)
Present	11 (42.3%)	2 (11.1%)	0 (0.0%)	0 (0.0%)	2 (33.3%)	0 (0.0%)	2 (100%)	1 (14.3%)
Necrosis (n=65)								
Absent	25 (96.2%)	18 (100%)	2 (100%)	2 (100%)	5 (83.3%)	2 (100%)	2 (100%)	7 (100%)
Present	1 (3.8%)	0 (0.0%)	0 (0.0%)	0 (0.0%)	1 (16.7%)	0 (0.0%)	0 (0.0%)	0 (0.0%)
Focality (n=66)								
Unifocal	16 (59.3%)	9 (50.0%)	0 (0.0%)	2 (100%)	4 (66.7%)	2 (100%)	0 (0.0%)	3 (42.9%)
Multifocal	11 (40.7%)	9 (50.0%)	2 (100%)	0 (0.0%)	2 (33.3%)	0 (0.0%)	2 (100%)	4 (57.1%)
Laterality (n=66)								
Unilateral	19 (70.4%)	11 (61.1%)	0 (0.0%)	2 (100%)	4 (66.7%)	2 (100%)	1 (50.0%)	4 (57.1%)
Bilateral	8 (29.6%)	7 (38.9%)	2 (100%)	0 (0.0%)	2 (33.3%)	0 (0.0%)	1 (50.0%)	3 (42.9%)
Lymph node metastasis (n=39)								
Absent	12 (60.0%)	10 (100%)	1 (100%)	1 (100%)	1 (33.3%)	1 (100%)	0 (0.0%)	2 (100%)
Present	8 (40.0%)	0 (0.0%)	0 (0.0%)	0 (0.0%)	2 (66.7%)	0 (0.0%)	1 (100%)	0 (0.0%)

2.5 Genetic alterations of PTCs

The mutational status of the PTC variants was established for all cytology and histology samples. The detailed results are described in tables 15 and 16.

Concerning cytology samples, 6 (9.1%) *TERT*p mutations, located at -124 hotspot (G>A), were found (Table 15). One (16.7%) mutation was found in both c-PTC and TC-PTC, and two (33.3%) mutations were found in both invasive FV-PTC and OV-PTC. Twenty (30.3%) *BRAF* mutations were found, from which nineteen (28.8%) were p.V600E and one (1.5%) p.K601E (Table 15). From the nineteen p.V600E, ten (52.6%) were found in c-PTC, two (10.5%) in invasive FV-PTC, one (5.3%) in infiltrative FV-PTC, two (10.5%) in OV-PTC, two (10.5%) in TC-PTC and two (10.5%) in microPTC. The p.K601E mutation found was detected in an invasive FV-PTC. *NRAS* and *HRAS* p.Q61R mutation was found in five (7.6%) and three (4.5%) samples, respectively (Table 15). For *NRAS* 2/5 (40%) mutations were detected in c-PTC, and one (20%) mutation in invasive FV-PTC, OV-PTC and microPTC. Two of the three *HRAS* p.Q61R mutation were observed in invasive FV-PCR and one in c-PTC. No *HRAS* p.Q61K mutations nor any *KRAS* mutation was found.

Histology samples harbored eight mutations in *TERT*p, from which seven (10.8%) were at -124 hotspot (G>A) and one (1.5%) at -146 hotspot (G>A) (Table 16). Concerning the -124 hotspot, two (28.6%) mutations were present in c-PTC, three (42.9%) in invasive FV-PTC and one (14.3%) in both an OV- and a TC-PTC. The only -146 hotspot mutation found was present in a c-PTC. Twenty-two (33.3%) samples were positive for *BRAF* mutations, from which twenty-one (31.8%) were the p.V600E, eleven (52.4%) detected in c-PTCs, three (14.3%) in invasive FV-PTC and three in microPTC, two (9.5%) in OV-PTC and one (4.8%) in an infiltrative FV-PTC and one in a TC-PTC, and the only (1.5%) p.K601E mutation present was in invasive FV-PTC. *NRAS* and *KRAS* presented five (7.6%) and two (3%) p.Q61R mutations, respectively. For *NRAS* one of the five (20%) mutation was present in c-PTC and one in an OV-PTC, and three of the five (60%) in invasive FV-PTC. One (50%) mutation was detected in c-PTC and one (50%) in infiltrative FV-PTC for *KRAS* gene. Four cases harbored *HRAS* mutation: one (1.5%) p.Q61K and three (4.5%) p.Q61R. The only p.Q61K mutation (25%) was detected in a microPTC, while the p.Q61R mutation

was present in one (25%) c-PTC and in two (50%) invasive FV-PTC. *HRAS* and *KRAS* were wild-type at codon 12 for all samples (Table 16).

It is noteworthy to report that, in low-grade PTCs, the majority of *BRAF* (p.V600E) mutations present in both cytology and histology samples were predominant in c-PTCs, while *RAS* (p.Q61R) mutations were more associated with c-PTC and invasive FV-PTC. On the other hand, aggressive variants of PTC like TC-PTC were only positive for *TERT*p and *BRAF* mutations, while the two SV-PTC show no mutations (Table 15 and 16).

Table 15. Mutational status of cytology samples within PTC variants

Genetic alterations in cytology		**PTC variants**							
		c-PTC n=27	**FV-PTC** n= 20		**Encapsulated PTC** n=2	**Oncocytic PTC** n=6	**Solid PTC** n=2	**Tall Cell PTC** n=2	**microPTC** n=7
			Invasive n=18	**Infiltrative** n=2					
TERT (n=66)	**WT**	26 (96.3%)	16 (88.9%)	2 (100%)	2 (100%)	4 (66.7%)	2 (100%)	1 (50.0%)	7 (100%)
	-124	1 (3.7%)	2 (11.1%)	0 (0.0%)	0 (0.0%)	2 (33.3%)	0 (0.0%)	1 (50.0%)	0 (0.0%)
	-146	0 (0.0%)	0 (0.0%)	0 (0.0%)	0 (0.0%)	0 (0.0%)	0 (0.0%)	0 (0.0%)	0 (0.0%)
BRAF (n=66)	**WT**	17 (63.0%)	15 (83.3%)	1 (50.0%)	2 (100%)	4 (66.7%)	2 (100%)	0 (0.0%)	5 (71.4%)
	p.V600E	10 (37.0%)	2 (11.1%)	1 (50.0%)	0 (0.0%)	2 (33.3%)	0 (0.0%)	2 (100%)	2 (28.6%)
	p.K601E	0 (0.0%)	1 (5.6%)	0 (0.0%)	0 (0.0%)	0 (0.0%)	0 (0.0%)	0 (0.0%)	0 (0.0%)
NRAS (n=66)	**WT**	25 (92.6%)	17 (94.4%)	2 (100%)	2 (100%)	5 (83.3%)	2 (100%)	2 (100%)	6 (85.7%)
	p.Q61R	2 (7.4%)	1 (5.6%)	0 (0.0%)	0 (0.0%)	1 (16.7%)	0 (0.0%)	0 (0.0%)	1 (14.3%)
HRAS (n=66)	**WT**	26 (96.3%)	16 (88.9%)	2 (100%)	2 (100%)	6 (100%)	2 (100%)	2 (100%)	7 (100%)
	p.Q61R	1 (3.7%)	2 (11.1%)	0 (0.0%)	0 (0.0%)	0 (0.0%)	0 (0.0%)	0 (0.0%)	0 (0.0%)
	p.Q61K	0 (0.0%)	0 (0.0%)	0 (0.0%)	0 (0.0%)	0 (0.0%)	0 (0.0%)	0 (0.0%)	0 (0.0%)
KRAS (n=66)	**WT**	27 (100%)	18 (100%)	2 (100%)	2 (100%)	6 (100%)	2 (100%)	2 (100%)	7 (100%)
	p.Q61R	0 (0.0%)	0 (0.0%)	0 (0.0%)	0 (0.0%)	0 (0.0%)	0 (0.0%)	0 (0.0%)	0 (0.0%)

Table 16. Mutational status of histology samples within PTC variants

Genetic alterations in histology		PTC variants							
		c-PTC n=27	**FV-PTC** n= 20		**Encapsulated PTC** n=2	**Oncocytic PTC** n=6	**Solid PTC** n=2	**Tall Cell PTC** n=2	**microPTC** n=7
			Invasive n=18	**Infiltrative** n=2					
TERT (n=65)	**WT**	23 (88.5%)	15 (83.3%)	2 (100%)	2 (100%)	5 (83.3%)	2 (100%)	1 (50.0%)	7 (100%)
	-124	2 (7.7%)	3 (16.7%)	0 (0.0%)	0 (0.0%)	1 (16.7%)	0 (0.0%)	1 (50.0%)	0 (0.0%)
	-146	1 (3.8%)	0 (0.0%)	0 (0.0%)	0 (0.0%)	0 (0.0%)	0 (0.0%)	0 (0.0%)	0 (0.0%)
BRAF (n=66)	**WT**	16 (59.3%)	14 (77.8%)	1 (50.0%)	2 (100%)	4 (66.7%)	2 (100%)	1 (50.0%)	4 (57.1%)
	p.V600E	11 (40.7%)	3 (16.7%)	1 (50.0%)	0 (0.0%)	2 (33.3%)	0 (0.0%)	1 (50.0%)	3 (42.9%)
	p.K601E	0 (0.0%)	1 (5.6%)	0 (0.0%)	0 (0.0%)	0 (0.0%)	0 (0.0%)	0 (0.0%)	0 (0.0%)
NRAS (n=66)	**WT**	26 (96.3%)	15 (83.3%)	2 (100%)	2 (100%)	5 (83.3%)	2 (100%)	2 (100%)	7 (100%)
	p.Q61R	1 (3.7%)	3 (16.7%)	0 (0.0%)	0 (0.0%)	1 (16.7%)	0 (0.0%)	0 (0.0%)	0 (0.0%)
HRAS (n=66)	**WT**	26 (96.3%)	16 (88.9%)	2 (100%)	2 (100%)	6 (100%)	2 (100%)	2 (100%)	6 (85.7%)
	p.Q61R	1 (3.7%)	2 (11.1%)	0 (0.0%)	0 (0.0%)	0 (0.0%)	0 (0.0%)	0 (0.0%)	0 (0.0%)
	p.Q61K	0 (0.0%)	0 (0.0%)	0 (0.0%)	0 (0.0%)	0 (0.0%)	0 (0.0%)	0 (0.0%)	1 (14.3%)
KRAS (n=66)	**WT**	26 (96.3%)	18 (100%)	1 (50.0%)	2 (100%)	6 (100%)	2 (100%)	2 (100%)	7 (100%)
	p.Q61R	1 (3.7%)	0 (0.0%)	1 (50.0%)	0 (0.0%)	0 (0.0%)	0 (0.0%)	0 (0.0%)	0 (0.0%)

The presence of concomitant genetic alterations in the histology was found in seven cases (Table 17). Three of them were present in invasive FV-PTC, three in c-PTC and one in a TC-PTC. *TERT*p mutations (-124 and -146 hotspot) coexisted with *BRAF* (p.V600E and p.K601E) in five cases and with *HRAS* (p.Q61R) in two cases. The cytology molecular results accompany those encountered in the histology. No concomitant mutations were found involving *BRAF* and *RAS* genes.

Two cases (Table 17) diagnosed as c-PTC and TC-PTC, both with a -124 *TERT*p mutation and *BRAF* mutation (p.V600E) presented LMN. Of note both cases show extrathyroidal invasion, fibrosis and inflammatory infiltrate.

Table 17. PTC variants with concomitant molecular alterations

Case	Sex	Age	Tumor size (mm)	Tumor diagnosis	Genes	Genetic alterations		Lymph node metastasis
						Cytology	Histology	
22	M	66	25	Invasive FV-PTC	*TERT* and *BRAF*	p.K601E	-124 and p.K601E	Absent
55	M	79	25	Invasive FV-PTC	*TERT* and *HRAS* codon 61	-124 and p.Q61R	-124 and p.Q61R	Absent
77	M	51	35	Invasive FV-PTC	*TERT* and *BRAF*	-124 and p.V600E	-124 and p.V600E	Absent
41	F	55	35	c-PTC	*TERT* and *BRAF*	-124 and p.V600E	-124 and p.V600E	**Present**
61	F	45	28	c-PTC	*TERT* and *HRAS* codon 61	p.Q61R	-124 and p.Q61R	Absent
82	F	44	35	c-PTC	*TERT* and *BRAF*	p.V600E	-146 and p.V600E	Absent
53	F	53	37	TC-PTC	*TERT* and *BRAF*	-124 and p.V600E	-124 and p.V600E	**Present**

2.6 Relationship between the clinicopathological features and the molecular profile in PTCs

The correlation between the clinicopathological features and genetic alterations was evaluated for the PTC variants. The presence of *TERT*p mutations was significantly associated with vascular invasion (p=0.002) and with venous invasion (p=0.006) (Table 18 and Supplementary table 1). Even though no statistical significance was achieved with gender (p=0.098), the presence of *TERT*p mutations tended to be more prevalent in females (Supplementary table 1).

BRAF mutations have a significant association with the presence of extrathyroidal invasion (p=0.009), fibrosis (p=0.006), inflammatory infiltrate (p=0.009), tall cell component (p=0.001) and psammoma bodies (p=0.011) (Table 18 and Supplementary table 2).

Patients carrying *NRAS* mutations were younger (38.20 ± 8.53) than those with a wild-type *NRAS* (54.51 ± 16.12) (p=0.03) and their tumors were significantly larger (p=0.042). No other significant associations were observed (Table 18 and Supplementary table 3).

No statistically significant associations were observed between the presence of *HRAS* or *KRAS* mutations and any of the clinicopathological features (Supplementary tables 4 and 5, respectively).

The association between the presence of *BRAF* mutations in *TERT* wild-type cases with clinicopathological features was significant for the presence of extrathyroidal invasion (p=0.039), fibrosis (p=0.023), inflammatory infiltrate (p=0.003), tall cell component (p=0.027) and psammoma bodies (p=0.013) (Table 18 and Supplementary table 6). When both *BRAF*+*TERT*p mutations are present there is a significant association with the presence of extrathyroidal invasion (p=0.031), vascular invasion (p=0.023) and tall cell component (p=0.010) (Table 18 and Supplementary table 7). No other significant associations were established.

Patients harboring *RAS* mutations tend to be younger (44 ± 14.23) (p=0.037) than those without mutations (55.13 ± 16.08). There is also a significant association between the presence of *RAS* mutation and the absence of fibrosis (p=0.005) (Table 18). No other statistically significant associations were found (Supplementary table 8).

Table 18. Significant associations between mutations and clinicopathological features in PTCs

Mutations	Clinicopathological characteristics	WT	Mutated	*p*-value
***TERT*p**	**Vascular invasion** (n=63)			
	Absent	50 (90.9%)	3 (37.5%)	**0.002**
	Present	5 (9.1%)	5 (62.5%)	
	Venous invasion (n=56)			
	Absent	51 (100%)	3 (60.0%)	**0.006**
	Present	0 (0.0%)	2 (40.0%)	
BRAF	**Extrathyroidal invasion** (n=57)			
	Absent	28 (71.8%)	6 (33.3%)	**0.009**
	Present	11 (28.2%)	12 (66.7%)	
	Fibrosis (n=65)			
	Absent	16 (37.2%)	1 (4.5%)	**0.006**
	Present	27 (62.8%)	21 (95.5%)	
	Inflammatory infiltrate (n=65)			
	Absent	31 (72.1%)	6 (27.3%)	**0.009**
	Present	11 (25.6%)	16 (72.7%)	
	Chronic	1 (2.3%)	0 (0.0%)	
	Tall cell (n=65)			
	Absent	39 (90.7%)	14 (63.6%)	**0.001**
	< 50%	3 (7.0%)	7 (31.8%)	
	≥ 50%	1 (2.3%)	1 (4.5%)	
	Psammoma bodies (n=65)			
	Absent	38 (88.4%)	13 (59.1%)	**0.011**
	Present	5 (11.6%)	9 (40.9%)	
NRAS	**Mean age ± Std** (n=66)	54.51 ± 16.12	38.20 ± 8.53	**0.03**
	Mean tumor size ± Std (mm) (n=66)	26.07 ± 14.49	39.80 ± 8.67	**0.042**

Table 18. (Continued)

Mutations	Clinicopathological characteristics	WT	Mutated	*p*-value
***TERT*^{WT}/*BRAF*^{Mut}**	**Extrathyroidal invasion** (n=48)			
	Absent	26 (74.3%)	5 (38.5%)	**0.039**
	Present	9 (25.7%)	8 (61.5%)	
	Fibrosis (n=56)			
	Absent	14 (35.9%)	1 (5.9%)	**0.023**
	Present	25 (64.1%)	16 (94.1%)	
	Inflammatory infiltrate (n=56)			
	Absent	28 (71.8%)	5 (29.4%)	**0.003**
	Present	10 (25.6%)	12 (70.6%)	
	Chronic	1 (2.6%)	0 (0.0%)	
	Tall cell (n=56)			
	Absent	35 (89.7%)	12 (70.6%)	**0.027**
	< 50%	3 (7.7%)	5 (29.4%)	
	≥ 50%	1 (2.6%)	0 (0.0%)	
	Psammoma bodies (n=56)			
	Absent	34 (87.2%)	9 (52.9%)	**0.013**
	Present	5 (12.8%)	8 (47.1%)	
***TERT*^{Mut}/*BRAF*^{Mut}**	**Extrathyroidal invasion** (n=40)			
	Absent	26 (74.3%)	1 (20.0%)	**0.031**
	Present	9 (25.7%)	4 (80.0%)	
	Vascular invasion (n=44)			
	Absent	35 (89.7%)	2 (40.0%)	**0.023**
	Present	4 (10.3%)	3 (60.0%)	
	Tall cell (n=44)			
	Absent	35 (89.7%)	2 (40.0%)	**0.010**
	< 50%	3 (7.7%)	2 (40.0%)	
	≥ 50%	1 (2.6%)	1 (20.0%)	
RAS	**Mean age ± Std** (n=66)	55.13 ± 16.08	44.00 ± 14.23	**0.037**
	Fibrosis (n=65)			
	Absent	10 (18.5%)	7 (63.6%)	**0.005**
	Present	44 (81.5%)	4 (36.4%)	

3. MicroRNA analysis

The relative quantification of each miRNA (miR146b, miR221, miR222, and miR15a) expression was assessed by real-time qPCR, and the results were analyzed using the $2^{-\Delta\Delta CT}$ method. For statistical analysis, the IBM SPSS Statistics program version 26 (IBM, New York, USA) was used.

For the relative quantification of miRNAs expression, a total of 63 thyroid samples were evaluated, composed by FFPE material of 12 benign and 51 malignant tumors.

3.1 Comparison of the relative miRNA expression between benign and malignant tumors

All four analyzed miRNAs (miR146b, miR221, miR22 and miR15a) showed a tendency to be overexpressed in malignant tumors when compared with benign lesions (Figure 22), and overexpression reached statistical significancy for miR221 and miR222 (p<0.001) (Figure 22b and 22c). The mean $2^{-\Delta\Delta CT}$ values of miR146b, miR221, miR222 and miR15a in benign lesions were 1.68 ± 1.79, 1.23 ± 1.01, 1.34 ± 1.15 and 1.20 ± 0.72, respectively, and 632.46 ± 2718.46, 5.31 ± 5.88, 9.14 ± 11.75 and 2.33 ± 2.39, respectively, for malignant tumors.

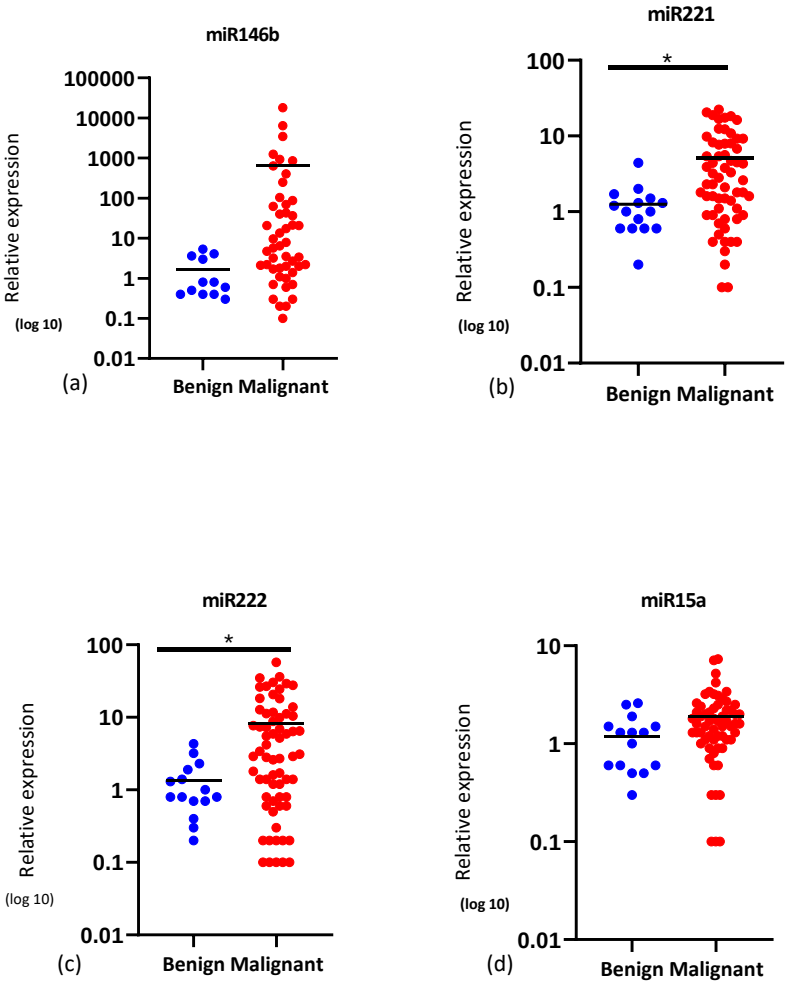

Figure 22. Relative expression levels of (a) miR146b, (b) miR221, (c) miR222, and (d) miR15a in benign vs malignant thyroid tumors. *p<0.001 (independent t-test)**.**

Discussion

The incidence of TC is rising all over the world and PTC is the most prevalent form of thyroid neoplasms [103]. Despite its favorable prognosis, some clinicopathological features, as well as the presence of some genetic alterations, influence the progression of TC leading to a patient's recurrences and/or death [103]. It is therefore important to improve the capacity of diagnostic methods, allowing a better risk stratification and a more efficient treatment for all individual patients, reducing unnecessary surgical procedures and mortality.

Our study was divided in two parts. In the first part we have performed the molecular characterization of thyroid cancer FNABs and correspondent FFPE tissues, in order to validate the diagnostic value of the FNAB. In the second part we aimed to establish a detection method for miRNA expression in the FNAB samples, to evaluate the expression levels of four different miRNAs, both in cytology and histology samples, and to assess their possible correlation.

It was possible to establish an association between the molecular alterations of the tumors and the clinicopathological features, being possible to identify the role of specific molecular alterations in tumor behavior and prognosis. For that, samples of 90 consecutive thyroid cancer patients who had surgical excision from 2016 to 2018 at Hospital Curry Cabral were evaluated, to determine the cyto-histologic correlation between each FNAB and the respective FFPE tissue.

The majority of the tumors in our series were PTCs (66 of 90 cases, 73.3%). As expected, our series was manly composed of females (83.3%), confirming a gender disparity in thyroid cancer [85, 103, 104]. Female patient's tumors were distributed through all histological subtypes, whereas male patients presented FV-PTCs, c-PTCs, and microPTC. This limited distribution is probably due to the reduced number of male patients in our series (n=15).

BRAF mutations were the most predominant mutation, either in cytology (24.7%) as well as in histology (24.4%) samples, followed by *RAS* mutations (8.9% and 12.2%, respectively) and by *TERT*p mutations, with 6.7% on cytologies and in 9.1% on histologies

cases. These findings are in accordance with other published studies [70, 86, 105], where they have found 36.6% mutated cases for *BRAF*, 15.9% and 6.2-10% for *RAS* and *TERT*p mutations, respectively.

By evaluating all the molecular results, it was possible to determine the degree of confidence for the diagnosis result given by the FNAB by analyzing the cyto-histologic molecular correlation of the cases and the possibility to predict malignancy. The mutational status of the FNABs and of the respective histologies was determined in our series.

Globally, a good correlation (76.7%) was found between the molecular results in cytologies and histologies. The gene showing more cyto-histologic molecular discrepancy was *BRAF*, with discordant results in 11.2% of the cases, although it was also the gene with a higher mutation rate, followed by *TERT*p results in 4.5% of the cases, *NRAS* in 4.4%, *KRAS* in 2.2% and *HRAS* in 1.1% of cases.

In order to understand these discrepancies, we have looked for possible reasons for this in all cases individually. It is important to refer that in the presence of discordant molecular cyto-histologic results the molecular analysis was repeated to exclude possible technical/human errors in the management of the samples.

It was not expected that one single patient would have a mutation in the cytology which is not present in the correspondent histology. This could be explained if the FFPE block was not representative of the biopsied lesion, as happened for cases #24 and #63 (Table 9), from which the available FFPE blocks do not correspond to the malignant tumor diagnosed but to adjacent Hashimoto's thyroiditis and to adjacent thyroid, respectively, explaining the discrepancy between the cytology and the histology of the same patient. Another example of an unexpected result is in the case diagnosed as microPTC with a *NRAS* mutation detected in the cytology and WT in the correspondent histology for *NRAS* (case #29, Table 9). In this case, the small nodule size (<1cm) could lead to a decrease in the capacity to detect mutations. However, another gene mutation in this same sample was detected (*BRAF*), invalidating the sample size theory for this specific sample. Eventually, the tumor heterogeneity, or lower allelic frequency in the tumor, could reduce the accuracy in Sanger sequencing and the alteration could be

missed. Small sample size, or inadequate selection of the histologic slide could be a reason to miss mutations in other samples though.

The opposite scenario (WT cytology and histology with a mutation) is, however, more understandable, since the nodule can be heterogeneous regarding the presence of the mutation. Three B FNAB cases with WT molecular result were classified as malignant in the histology and present a mutation. In these cases it could be that mutations were missed in the FNAB due to a biopsy sampling error or a misinterpretation of the biopsy, as also reported in previous studies [106-108]. Two cases were classified as ND in cytology samples. A FNAB with a ND result is a major limitation in cytology with consequences on a correct patient management. The reduced number of cells (acellular smear) or an insufficient fixation of the smear are possible explanations for inconsistency between molecular results in the histology and cytology [109]. Anand B. *et al.* (2020) related that the experience of the technician as well as all the steps to achieve the FNAB is directly related with ND results [107]. Seven cases have concordant results between the cytology and histology diagnostic, but were discrepant in the molecular analysis with mutations being found only in the histologic samples. A possible reason for this difference is the number and purity of tumor cells in the histology where only the tumor area was microdissected, when compared with the cytology sample where all cells were scraped diluting the amount of tumor cells.

FNABs have an important role in the evaluation of thyroid nodules, helping in the triage of patients for surveillance (if FNAB has a benign diagnosis) or surgery (if FNAB has a diagnosis of malignancy). It is a minimal invasive technique and cost-effective. However, up to 30% of FNABs have an undetermined diagnosis. AUS/FLUS and SFN categories remain difficult to manage due to the difficulty of correctly categorize these lesions – grey zone lesions. This uncertainty, for many patients, can lead to an unnecessary thyroidectomy. It is therefore important to be able to give a more confident diagnostic result on grey zone cytology lesions, in order to have more certainty on their future outcome, to manage these patients more adequately.

The presence of mutations increased from lower Bethesda category (B and AUS/FLUS) to higher Bethesda category (SM and M). Knowing the mutational status of

a FNAB, special from those categorized as grey zone lesions (AUS/FLUS and SFN), can improve the prognostic relevance of a cytology, allowing a better management of the patient.

In our series, the molecular cytology results of the grey zone lesions (AUS/FLUS and SFN, (n=16)) were 2.2% mutations for *RAS* and 1.1% for *TERT*p. Censi S. *et al.* (2017) evaluated a large cohort of indeterminate thyroid nodules (n=199) detecting *RAS* and *TERT*p mutations in 18% and 4% of all series, respectively [110]. The differences in mutation frequency may be due to the small numbers in our series. While the low rate of detected mutations and the predominance of WT cases, the malignancy rate of the grey zone was 100% and all patients underwent total thyroidectomy (11/16, 69%) or lobectomy (5/16, 31%), proving the importance of a prognostic certainty. Although in our series AUS/FLUS lesions were associated with *RAS* mutations, these patients were later on subjected to surgery (approximately nine months later).

Besides AUS/FLUS cases, benign samples were also associated with *RAS* mutation. On the other hand, higher risk molecular alterations, like *BRAF* and *TERT*p+*BRAF* mutations, were associated with SM and M categories that show higher risk of malignancy. These findings are consistent with the study developed by Bellevicine, C. *et al.* (2019) [111].

Tumors in the M category presented a high frequency of mutations in which *BRAF*, followed by *TERT*+*BRAF*, *RAS* and *TERT*+*RAS* were the most prevalent. This observation agrees with the study made by Decaussin-Petrucci, M. *et al*. (2017) [112]. However, no statistical significances were found when comparing these groups.

A limitation in our study is the low number of lesions other than PTCs, such as benign, WDT-UMP, NIFTP, HCC, FTC and PDTC, not allowing statistical comparisons. For that reason, we focused our study in PTCs. The three main variants of PTCs were the conventional, follicular and microPTCs that together accounted for 81.8% of all PTCs in our series. These numbers are similar to others previously reported [56, 113, 114].

The majority of PTCs presented capsule invasion (about 88%), especially in the invasive FV-PTC (43.9%), followed by the c-PTC (24.4%). On contrary, the studies

developed by Henke L. E. *et al.* (2018) and Estrada-Flórez A. P. *et al.* (2019), demonstrated a higher prevalence of capsule invasion in c-PTC (51.6% and 32%, respectively), than in FV-PTC (36.8% and 21.2%, respectively) [114, 115].

Liu, X. *et al.* (2018) show in their microPTC series that fibrosis contributes to a worse prognosis, being associated with age, tumor size and gender. In our series, the presence of fibrosis was observed in 73.8% of all PTCs, the majority in c-PTC (33.8%), being predominant in females (63.1%). However, no significant associations were established with tumor size and age [116].

Regarding the molecular results of the PTC's cytology, we saw a prevalence of mutations in *BRAF* (30.3%), and TERT (9.1%) genes. These findings are in accordance to those reported by Liu R. *et al.* (2014) that found 37.8% and 7% of *BRAF* and *TERT*p mutations, respectively [117].

The PTC mutation frequency for *TERT*p, *BRAF*, *NRAS*, *HRAS* and *KRAS*, in histology, was 12.3%, 33.3%, 7.6%, 6.1% and 3%, respectively. These mutations were mainly present in the c-PTC and FV-PTC, being *BRAF* mutations more prevalent in c-PTC while *RAS* mutations were predominant in FV-PTC. *TERT*p mutations were equally present in both variants. Insilla A. *et al.* (2017) published similar results, presenting 36.6%, 6.2% and 15.9% in *BRAF*, *TERT*p, and *RAS* mutations and the same tendency at histological level [70]. However, the study developed by Argyropoulou M. *et al.* (2018) in Greek population shows lower frequency of these mutations, with a prevalence of 3.4% for *TERT*p and *NRAS* and 17% for *BRAF* genes [118]. Finally, within the TC-PTCs, an aggressive variant of PTC, only *TERT*p and *BRAF* mutations were found, and these findings are in agreement with others studies from our group [88].

Xing, M. *et al.* (2014) observed that 6.9% of all PTCs have concomitant mutations in *TERT*p and *BRAF* gene, which are significantly associated with poor clinicopathological features and tumor progression, namely LNM, extrathyroidal and vascular invasion [119]. Estrada-Flórez A. P. *et al.* (2019) published similar results, with concomitant *TERT*p+*BRAF* mutations in 10% of their series and the same significant associations [115]. Corroborating with the above-mentioned studies, we observed *TERT*p+*BRAF* mutations in 7.6% of the cases and significant associations with clinicopathological

features related to a worst outcome (extrathyroidal and vascular invasion (p=0.031 and p=0.023, respectively). On the other hand, Melo M. *et al*. (2014) have not found this association in their series [85]. Plus, Ren H. *et al.* (2018) have found no associations with the presence of LNM but with extrathyroidal invasion, large tumors, and older patients [103]. The theory behind possible associations between the co-existence of *TERT*p+*BRAF* is not a consensus in the literature. However, the cooperation between both mutations can be explained by the activation of the MAPK signaling pathway that either generates new binding motifs for ETS leading to *TERT* expression, or once *BRAF* or *NRAS* genes are mutated, the MAPK signaling pathway is activated via ETS, which promotes *TERT* expression [80, 103]. Curiously, concomitant presence of *TERT*p+*BRAF* mutations was also observed in cytology sample.

No concomitant mutations were observed for *BRAF*+*RAS* and this was expected since these mutations are described as mutually exclusive events [120].

*TERT*p mutations were significantly associated with vascular invasion (p=0.002) as well as with venous invasion (p=0.006) in PTCs, as was observed in a previous study developed by our group [88]. The association between the presence of *TERT*p mutations with older patients has previously been described by our group [85, 104], although this was not seen in the present study.

We observed a significant association between the presence of *BRAF* mutations and poor clinicopathological features in PTCs, such as the presence of extrathyroidal invasion (p=0.009), fibrosis (p=0.006), inflammatory infiltrate (p=0.009), tall cell component (p=0.001) and psammoma bodies (p=0.011). These findings do not present a consensus among the literature. Although other authors have reported similar results [71, 121], a study developed by our group did not find any correlation between the presence of *BRAF* mutations and signs of clinicopathological aggressiveness [69].

The presence of *RAS* mutations was significantly associated with younger patients being in accordance with other published study [122].

The presence of LNM was significantly associated with invasive features such as extrathyroidal, lymphatic and vascular invasion (p=0.0003, p=0.0002 and p=0.021,

respectively). The presence of *BRAF* mutations in cytology specimens was associated with LNM (p=0.017) and, despite not statistically significant, a tendency for the association between *TERT*p mutations and LNM was also achieved (p=0.062). All these findings were previously reported by our group in different studies [104].

Dysregulated in cancer, microRNAs are implicated in cellular processes namely in cell differentiation, proliferation, migration and invasion [93]. Allied to the genetic alterations, microRNAs dysregulation has been described as a new biomarker in thyroid cancer and are pointed as possible therapeutic targets [92, 98, 123, 124].

The second part of this study aimed to determinate the expression levels of four microRNAs in malignant FNABs and respective histology and to compare it with benign lesions. We selected three miRNAs previously described in the literature as upregulated in TC, miR146b, miR221 and miR222, and one classified as downregulated (miR15a) [91, 92, 96].

Although our study had a small sample size, we found a wide range of variation concerning miRNA expression. We observed a tendency for miRNAs overexpression in malignant tumors when compared with benign lesions. Alterations of these specific miRNAs in TC have been already described in the literature, being responsible for thyroid cell transformation [91, 98].

Unexpectedly, although all miRNAs showed a tendency for overexpression, only the expression levels of miR221 and miR222 reached significance (p<0.001). We were expecting to see also significant overexpression values for miR146b, as it has been described elsewhere for TC [125, 126].

miR221 and miR222 are described to target CDKN1B (*p27Kip1* protein) and KIT. CDKN1B is an important regulator of the cell cycle, and KIT is involved in cell differentiation and growth. Visone R. *et al.* (2007) show that the overexpression of miR221 and miR222 induce the thyroid papillary carcinoma cell line (TPC-1) to progress into the S phase of cell cycle. Moreover, miR221 and miR222 can also play a role *in vivo* since they have an inverse correlation between their expression levels and downregulation of the *p27Kip1*. On the contrary, the inhibition of miR221 and miR222

expression increase the *p27Kip1* protein levels. This result support the influence of these miRNAs in the control of the cell cycle through the regulation of the *p27Kip1* protein levels [127]. Our findings are in accordance with previous studies [90, 91, 127].

Despite not statistically significant, we found a tendency for upregulation in miR146b being in line with other studies [96, 123]. Its upregulation is correlated with tumor aggressiveness and poor clinicopathological features (such as extrathyroidal and capsule invasion, presence of LMN as well with distant metastasis) [95].

Interestingly, the miR15a has been described as downregulated in thyroid cancer [92, 124]. However, in our series, we found a tendency for upregulation (p=0.074), suggesting a gain of function of this specific miRNA in PTCs. Jin J *et al.* (2019) has recently reported an association between miR15a low expression levels and human PTCs suggesting a possible influence of this miRNA in TC development by promoting proliferation, survival and invasion [92]. Moreover, in a *in vivo* study they found significant increase in the inhibition of cell proliferation and invasion promoting apoptosis when miR15a was upregulated [92]. They conclude that the overexpression of miR15a inhibit tumor progression via regulation of AKT pathway. With similar results Lu Z, *et al.* (2019), show that the upregulation of miR15a suppress the BCL-2 expression [124]. Based on these evidences, miR15a could be a potential therapeutic target in TC.

The above-mentioned studies show different results for miR15a expression when compared with our findings. It is important to refer that a limitation in our study, besides the small number of analyzed samples, is the absence of normal thyroid tissue for comparison. Our results were based on the comparison between benign and malignant tumors. Benign lesions, although not yet malignant, might already show small alterations, mainly in miRNA expression. In the future it will be interesting to compare these results with normal thyroid tissue.

Our preliminary data reveals a significant association between the expression levels of all miRNAs with the presence of *BRAF* mutations (data not shown). In accordance with our findings, Yang S. I. *et al.* (2020), show that the expression of miR146b is significantly associated with the presence of *BRAF* mutations [128]. Sun Y. *et al.* (2013), show that both miR221, miR222 and miR146b, together with miR181 are

upregulated in PTC patients with *BRAF* mutations. These findings suggest a connection or influence of the presence of *BRAF* mutations with miRNAs expression in the development of TC [129].

Our miRNA expression analysis has some limitations. One limitation is the number of cases studied, being important to increase sample size. Only a part of the FFPE tissues were evaluated and the analysis of the respective FNABs was not finished. Nevertheless, this is an ongoing work, and finishing the series of tumors might increase the statistical value of our results.

Conclusion

We have demonstrated a good correlation of the molecular results between cytologies and histologies (76.7%).

We assessed the utility of the molecular analysis of FNAB samples for the diagnosis of indeterminate thyroid nodules. In the present series, it was not possible to conclude that the molecular status of a FNAB can avoid TC patients from surgery since we present a limited number of indeterminate nodules. However, we verified that all indeterminate nodules reveal to be malignant in the histology, proving that surgery was, for these cases, the right decision.

As previously reported by other studies, we observed that *RAS* mutations were not associated with poor outcome. On contrary, we have confirmed that the presence of *BRAF* mutations are associated with aggressive clinicopathological features. Moreover, the concomitant presence of *TERT*p+*BRAF* mutations show the same behavior. We hypothesize that this cooperation leads to the progression and recurrence of the tumor. However, further studies are necessary to provide new insights on the evolution of these tumors.

Finally, our results indicate that in thyroid cancer there is a dysregulation of the expression levels of miRNAs, potentially influencing their target genes on the promotion of cell differentiation, proliferation and survival. Our miRNAs analysis is an ongoing project, not completed for histology and cytology samples, which is a limitation in our study. By increasing the series, we believe that the correlation between the miRNAs profiling and FNAB molecular analysis will be useful in the early and accurate diagnosis of PTCs and, hopefully, will allow a more efficient treatment of TC.

References

1. Sadler, T.W. *Langman's Medical Embryology*. 12th ed. 2012, Philadelphia, PA: Lippincott Williams & Wilkins.
2. Wartofsky, L., Nostrand, D. V. *Thyroid Cancer: A Comprehensive Guide to Clinical Management*. 2 ed. 2006, Totowa, New Jersey: Humana Press Inc.
3. Mohebati, A., Shaha, A. R. *Anatomy of thyroid and parathyroid glands and neurovascular relations.* Clin Anat, 2012. **25**(1): p. 19-31.
4. Kumar, V., Abbas, A., Aster, J. *Robbins and Cotran Pathologic Basis of Disease*. 9th edition ed. 2015, Philadelphia PA 19103-2899: SAUNDERS ELSEVIER.
5. Mullur, R., Liu, Y. Y., Brent, G. A. *Thyroid hormone regulation of metabolism.* Physiol Rev, 2014. **94**(2): p. 355-82.
6. Sheehan, M.T. *Biochemical Testing of the Thyroid: TSH is the Best and, Oftentimes, Only Test Needed - A Review for Primary Care.* Clin Med Res, 2016. **14**(2): p. 83-92.
7. Le Lièvre, C.S., Le Douarin, N. M. *Mesenchymal derivatives of the neural crest: analysis of chimaeric quail and chick embryos.* J. Embryol. exp. Morph., 1975. **34**(1): p. 125-154.
8. Christ-Crain, M., Morgenthaler, N. G., Müller, B. *Evaluation of Hyperthyroidism and Hyperthyroid Goiter*, in *Surgery of the Thyroid and Parathyroid Glands*, D. Oertli and R. Udelsman, Editors. 2007, Springer.
9. Bray, F., Ferlay, J., Soerjomataram, I., Siegel, R. L., L.A. Torre, et al. *Global cancer statistics 2018: GLOBOCAN estimates of incidence and mortality worldwide for 36 cancers in 185 countries.* CA Cancer J Clin, 2018. **68**(6): p. 394-424.
10. Curado, M.P., Edwards, B., Shin, H. R., Storm, H., Ferlay, J., M. Heanue, and P. Boyle. *Cancer Incidence in Five Continents*. Vol. IX. 2007, Lyon, France: IARC Scientific Publications.
11. Ferlay, J., Colombet, M., Soerjomataram, I., Mathers, C., et al. *Estimating the global cancer incidence and mortality in 2018: GLOBOCAN sources and methods.* Int J Cancer, 2019. **144**(8): p. 1941-1953.
12. GLOBOCAN. *Lyon: International Agency for Research on Cancer/World Health Organization*. 2018; Available from: 2018.//gco.iarc.fr/.
13. RORENO. *Registo Oncológico Nacional 2010. Instituto Português de Oncologia do Porto Francisco Gentil - EPE*. 2016.
14. RORENO. *Projeções da incidência de cancro na Região Norte - 2013, 2015 e 2020. Instituto Português de Oncologia do Porto.* 2013.
15. Girardi, F.M. *Thyroid Carcinoma Pattern Presentation According to Age.* Int Arch Otorhinolaryngol, 2017. **21**(1): p. 38-41.
16. Tuttle, R.M., Ball, D. W., Byrd, D., Dilawari, R. A., Doherty, G. M., et al. *Thyroid carcinoma.* J Natl Compr Canc Netw, 2010. **8**(11): p. 1228-74.
17. Jegerlehner, S., Bulliard, J. L., Aujesky, D., Rodondi, N., et al. *Overdiagnosis and overtreatment of thyroid cancer: A population-based temporal trend study.* PLoS One, 2017. **12**(6): p. e0179387.
18. Mack, W.J., Preston-Martin, S., Dal Maso, L., Galanti, R., et al. *A pooled analysis of case–control studies of thyroid cancer: cigarette smoking and consumption of alcohol, coffee, and tea.* Cancer Causes and Control 2003. **14**: p. 773–785.

19. Pellegriti, G., et al. *Worldwide increasing incidence of thyroid cancer: update on epidemiology and risk factors.* J Cancer Epidemiol, 2013. **2013**: p. 1-10.
20. Cardis, E., Kesminiene, A., Ivanov, V., Malakhova, I., et al. *Risk of thyroid cancer after exposure to 131I in childhood.* J Natl Cancer Inst, 2005. **97**(10): p. 724-32.
21. Liu, Y., Su, L., Xiao, H. *Review of Factors Related to the Thyroid Cancer Epidemic.* Int J Endocrinol, 2017: p. 1-9.
22. Belfiore, A., La Rosa, G. L., La Porta, G. A., Giuffrida, D., et al. *Cancer Risk in Patients With Cold Thyroid Nodules: Relevance of Iodine Intake, Sex, Age, and Multinodularity.* The Americen Journal of Medicine, 1992. **93**: p. 363-369.
23. Kim, H.J., Park, H. K., Byun, D. W., Suh, K., et al. *Iodine intake as a risk factor for BRAF mutations in papillary thyroid cancer patients from an iodine-replete area.* Eur J Nutr, 2018. **57**(2): p. 809-815.
24. Engeland, A., Tretli, S., Akslen, L. A., Bjorge, T. *Body size and thyroid cancer in two million Norwegian men and women.* Br J Cancer, 2006. **95**(3): p. 366-70.
25. Gilliland, F.D., Hunt, W. C., Morris, D. M., Key, C. R. *Prognostic Factors for Thyroid Carcinoma: A Population-Based Study of 15,698 Cases from the Surveillance, Epidemiology and End Results (SEER) Program 1973–1991.* American Cancer Society, 1997. **79**: p. 564-573.
26. Tuttle, R.M., Haugen, B., Perrier, N. D. *Updated American Joint Committee on Cancer/Tumor-Node-Metastasis Staging System for Differentiated and Anaplastic Thyroid Cancer (Eighth Edition): What Changed and Why?* Thyroid, 2017. **27**(6): p. 751-756.
27. Chen, A.Y., Jemal, A., Ward, E. M. *Increasing incidence of differentiated thyroid cancer in the United States, 1988-2005.* Cancer, 2009. **115**(16): p. 3801-7.
28. Haugen, B.R., Alexander, E. K., Bible, K. C., Doherty, G. M., et al. *2015 American Thyroid Association Management Guidelines for Adult Patients with Thyroid Nodules and Differentiated Thyroid Cancer: The American Thyroid Association Guidelines Task Force on Thyroid Nodules and Differentiated Thyroid Cancer.* Thyroid, 2016. **26**(1): p. 1-133.
29. Lloyd, R.V., Osamura, R. Y., Klöppel, G., Rosai, J. *WHO Classification of Tumours of Endocrine Organs*. 4th ed. 2017, Lyon: WHO.
30. Nikiforov, Y.E., Biddinger, P. W., Thompson, L. D. R. *Diagnostic Pathology and Molecular Genetics of the Thyroid: A Comprehensive Guide for practing Thyroid Pathology* 2ed. 2012, Philadelphia: Wolters Kluwer Health | Lippincott Williams & Wilkins.
31. Yassin, F. *Diagnostic criteria of well differentiated thyroid tumor of uncertain malignant potential; a histomorphological and immunohistochemical appraisal.* J Egypt Natl Canc Inst, 2015. **27**(2): p. 59-67.
32. Canberk, S., Baloch, Z. W., Ince, U., Schmitt, F. *Diagnosis of Non-invasive Follicular Tumor with Papillary-like Nuclear Features (NIFTP): A Practice Changer for Thyroid Fine-needle Aspiration Interpretation.* Journal of Basic & Clinical Medicine, 2017. **6**(1): p. 38-43.
33. Nikiforov, Y.E., Seethala, R. R., Tallini, G., Baloch, Z. W., et al. *Nomenclature Revision for Encapsulated Follicular Variant of Papillary Thyroid Carcinoma: A Paradigm Shift to Reduce Overtreatment of Indolent Tumors.* JAMA Oncol, 2016. **2**(8): p. 1023-9.

34. Brown, R.L., De Souza, J. A., Cohen, E. EW. *Thyroid Cancer: Burden of Illness and Management of Disease.* Journal of Cancer, 2011. **2**: p. 193-199.
35. Raposo, L., Morais, S., Oliveira, M. J., Marques, A. P., Bento, M. J. Lunet, N. *Trends in thyroid cancer incidence and mortality in Portugal.* European Journal of Cancer Prevention, 2017. **26**(2): p. 135-143.
36. LiVolsi, V.A. *Papillary thyroid carcinoma: an update.* Mod Pathol, 2011. **24 Suppl 2**: p. S1-9.
37. Jeon, M.J., Kim, T. Y., Kim, W. G., et al. *Differentiating the location of cervical lymph node metastasis is very useful for estimating the risk of distant metastases in papillary thyroid carcinoma.* Clinical Endocrinology, 2014. **81**: p. 593–599.
38. Gharib, H., Goellner, J. R., Johnson, D. A. *Fine-Needle Aspiration Cytology of the Thyroid: A 12-Year Experience With 11,000 Biopsies.* Clinics in Laboratory Medicine, 1993. **13**(3): p. 699-709.
39. Grimm, D. *Current Knowledge in Thyroid Cancer-From Bench to Bedside.* Int J Mol Sci, 2017. **18**(7).
40. Tuttle, R.M., Leboeuf, R., Robbins, R. J., Qualey, R., et al. *Empiric Radioactive Iodine Dosing Regimens Frequently Exceed Maximum Tolerated Activity Levels in Elderly Patients with Thyroid Cancer.* The Journal of Nuclear Medicine, 2006. **47**: p. 1587-1591.
41. Lloyd, R.V., Buehler, D., Khanafshar, E. *Papillary thyroid carcinoma variants.* Head Neck Pathol, 2011. **5**(1): p. 51-6.
42. Cameselle-Teijeiro, J.M., Sobrinho-Simões, M. *New WHO classification of thyroid tumors: A pragmatic categorization of thyroid gland neoplasms.* Endocrinología, Diabetes y Nutrición (English ed.), 2018. **65**(3): p. 133-135.
43. Berho, M., Suster, S. *The Oncocytic Variant of Papillary Carcinoma of the Thyroid: A Clinicopathologic Study of 15 Cases.* Saunders Company, 1997: p. 47-53.
44. Higuchi, M., et al. *Cytological features of solid variants of papillary thyroid carcinoma: a fine needle aspiration cytology study of 18 cases.* Cytopathology, 2017. **28**(4): p. 268-272.
45. Wang, X., Cheng, W., Liu, C., Li, J. *Tall cell variant of papillary thyroid carcinoma: current evidence on clinicopathologic features and molecular biology.* Onco Target, 2016. **7**(26): p. 40792-40799.
46. Wong, K.S., et al. *Tall Cell Variant of Papillary Thyroid Carcinoma: Impact of Change in WHO Definition and Molecular Analysis.* Endocr Pathol, 2019. **30**(1): p. 43-48.
47. Sobrinho-Simões, M., Eloy, C., Magalhães, J., Lobo, C. and T. Amaro. *Follicular thyroid carcinoma.* Mod Pathol, 2011. **24 Suppl 2**: p. S10-8.
48. Maximo, V., et al. *The biology and the genetics of Hurthle cell tumors of the thyroid.* Endocr Relat Cancer, 2012. **19**(4): p. R131-47.
49. Gallardo, E., Medina, J., Sanchez, J. C., Viudez, A., et al. *SEOM clinical guideline thyroid cancer (2019).* Clin Transl Oncol, 2020. **22**(2): p. 223-235.
50. Eloy, C., Ferreira, L., Salgado, C., Soares, P. and M. Sobrinho-Simoes. *Poorly Differentiated and Undifferentiated Thyroid Carcinomas.* Turk Patoloji Derg, 2015. **31 Suppl 1**: p. 48-59.
51. Smallridge, R.C., Ain, K. B., Asa, S. L., Bible, K. C., Brierley, J. D., et al. *American Thyroid Association guidelines for management of patients with anaplastic thyroid cancer.* Thyroid, 2012. **22**(11): p. 1104-39.

52. Wells, S.A., Jr., Asa, S. L., Dralle, H., Elisei, R., et al. *Revised American Thyroid Association guidelines for the management of medullary thyroid carcinoma.* Thyroid, 2015. **25**(6): p. 567-610.
53. Nikiforov, Y.E., Nikiforova, M. N. *Molecular genetics and diagnosis of thyroid cancer.* Nat Rev Endocrinol, 2011. **7**(10): p. 569-80.
54. Cantwell-Dorris, E.R., O'Leary, J. J., Sheils, O. M. *BRAFV600E: implications for carcinogenesis and molecular therapy.* Mol Cancer Ther, 2011. **10**(3): p. 385-94.
55. Lu, Z., Zhang, Y., Feng, D., Sheng, J., W. Yang, and B. Liu. *Targeted next generation sequencing identifies somatic mutations and gene fusions in papillary thyroid carcinoma.* Oncotarget, 2017. **8**(28): p. 45784-45792.
56. Fakhruddin, N., Jabbour, M., Novy, M., Tamim, H., et al. *BRAF and NRAS Mutations in Papillary Thyroid Carcinoma and Concordance in BRAF Mutations Between Primary and Corresponding Lymph Node Metastases.* Sci Rep, 2017. **7**(1): p. 4666.
57. Soares, P., Trovisco, V., Rocha, A. S., Lima, J., Castro, P., et al. *BRAF mutations and RET/PTC rearrangements are alternative events in the etiopathogenesis of PTC.* Oncogene, 2003. **22**(29): p. 4578-80.
58. Tavares, C., Melo, M., Cameselle-Teijeiro, J. M., Soares, P. and M. Sobrinho-Simões. *Genetic predictors of thyroid cancer outcome.* European Journal of Endocrinology, 2016. **174**(4): p. 117-126.
59. Davies, H., Bignell, G. R., Cox, C., Stephens, P., et al. *Mutations of the BRAF gene in human cancer.* Nature, 2002. **417**: p. 949-954.
60. Xing, M. *BRAF mutation in thyroid cancer.* Endocrine-Related Cancer, 2005. **12**: p. 245-262.
61. Zolotov, S. *Genetic Testing in Differentiated Thyroid Carcinoma: Indications and Clinical Implications.* Rambam Maimonides Medical Journal, 2016. **7**(1): p. 1-10.
62. Penna, G.C., Vaisman, F., Vaisman, M., Sobrinho-Simões, M., Soares, P. *Molecular Markers Involved in Tumorigenesis of Thyroid Carcinoma: Focus on Aggressive Histotypes.* Cytogenetic and Genome Research, 2017. **150**: p. 194-207.
63. Soares, P., Sobrinho-Simões, M. *Small papillary thyroid cancers — is BRAF of prognostic value?* Nature Reviews | Endocrinology, 2011. **7**: p. 9-10.
64. Trovisco, V., Vieira de Castro, I., Soares, P., Máximo, V., et al. *BRAF mutations are associated with some histological types of papillary thyroid carcinoma.* Journal of Pathology, 2004. **202**: p. 247-251.
65. Nikiforova, M.N., Ciampi, R., Salvatore, G., Santoro, M., et al. *Low prevalence of BRAF mutations in radiation-induced thyroid tumors in contrast to sporadic papillary carcinomas.* Cancer Letters 2004. **209**: p. 1-6.
66. Lima, J., Trovisco, V., Soares, P., Máximo, V., et al. *BRAF Mutations Are Not a Major Event in Post-Chernobyl Childhood Thyroid Carcinomas.* The Journal of Clinical Endocrinology & Metabolism 2004. **89**(9): p. 4267–4271.
67. Nikiforov, Y.E. *Molecular Diagnostics of Thyroid Tumors.* Arch Pathol Lab Med, 2011. **135**: p. 569-577.
68. Torregrossa, L., Viola, D., Sensi, E., Giordano, M., et al. *Papillary Thyroid Carcinoma With Rare Exon 15 BRAF Mutation Has Indolent Behavior: A Single-Institution Experience.* Clin Endocrinol Metab, 2016. **101**(11): p. 4413-4420.

69. Trovisco, V., Soares, P., Preto, A., Vieira de Castro, I., Lima, J., et al. *Type and prevalence of BRAF mutations are closely associated with papillary thyroid carcinoma histotype and patients' age but not with tumour aggressiveness.* Virchows Arch, 2005. **446**: p. 589-595.
70. Insilla, A.C., Proietti, A., Borrelli, N., Macerola, E., et al. *TERT promoter mutations and their correlation with BRAF and RAS mutations in a consecutive cohort of 145 thyroid cancer cases.* Oncology Letters 2018. **15**: p. 2763-2770.
71. Xing, M., Westra, W. H., Tufano, R. P., Cohen, Y., et al. *BRAF Mutation Predicts a Poorer Clinical Prognosis for Papillary Thyroid Cancer.* The Journal of Clinical Endocrinology & Metabolism, 2005. **90**(12): p. 6373-6379.
72. Abdullah, M.I., Junit, S. M., Leong Ng, K., Jayapalan, J. J., B. Karikalan, and O.H. Hashim. *Papillary Thyroid Cancer: Genetic Alterations and Molecular Biomarker Investigations.* International Journal of Medical Sciences, 2019. **16**(3): p. 450-460.
73. Tidyman, W.E., Rauen, K. A. *Pathogenetics of the RASopathies.* Oxford University Press, 2016: p. 1-29.
74. Howell, G.M., Hodak, S. P., Yip, L. *RAS Mutations in Thyroid Cancer.* The Oncologist 2013. **18**: p. 926-932.
75. Schulten, H.-J., Salama, S., Al-Ahmadi, A., Al-Mansouri, Z., Mirza, Z., et al. *Comprehensive Survey of HRAS, KRAS, and NRAS Mutations in Proliferative Thyroid Lesions from An Ethnically Diverse Population.* Anticancer Research 2013. **33**: p. 4779-4784
76. Volante, M., Rapa, I., Gandhi, M., Bussolati, G., Giachino, D., Papotti, M., Nikiforov, Y. E. *RAS Mutations Are the Predominant Molecular Alteration in Poorly Differentiated Thyroid Carcinomas and Bear Prognostic Impact.* J Clin Endocrinol Metab, 2009. **94**(12): p. 4735–4741.
77. Radkay, L.A., Chiosea, S. I., Seethala, R. R., Hodak, S. P., and S.O. LeBeau, Yip, L., McCoy, K. L., Carty, S. E., Schoedel, K. E., et al. *Thyroid Nodules With KRAS Mutations Are Different From Nodules With NRAS and HRAS Mutations With Regard to Cytopathologic and Histopathologic Outcome Characteristics.* Cancer Cytopathology, 2014: p. 873-882.
78. Hanahan, D., Weinberg, R. A. *Hallmarks of Cancer: The Next Generation.* Cell, 2011. **144**: p. 646-674.
79. Vinagre, J., Pinto, V., Celestino, R., et al. *Telomerase promoter mutations in cancer: an emerging molecular biomarker?* Virchows Arch 2014. **465**: p. 119–133.
80. Pestana, A., Vinagre, J., Sobrinho-Simões, M., Soares, P. *TERT biology and function in cancer: beyond immortalisation.* Journal of Molecular Endocrinology, 2017. **58**: p. 129–146.
81. Kim, N.W., Piatyszek, M. A., Prowse, K. R., Harley, C. B., et al. *Specific Association of Human Telomerase Activity with Immortal Cells and Cancer.* Science, 1994. **266**: p. 2011-2015.
82. Takakura, M., Kyo, S., Kanaya, T., and H. Hirano, Takeda, J., Yutsudo, M., Inoue, M. *Cloning of Human Telomerase Catalytic Subunit (hTERT) Gene Promoter and Identification of Proximal Core Promoter Sequences Essential for Transcriptional Activation in Immortalized and Cancer Cells.* Cancer Research 1999. **59** p. 551–557.

83. Panebianco, F., Nikitski, A. V., Nikiforova, M. N., Nikiforov, Y. E. *Spectrum of TERT promoter mutations and mechanisms of activation in thyroid cancer.* Cancer Medicine, 2019. **8**: p. 5831–5839.
84. Preto, A., Cameselle-Teijeiro, J., Julio Moldes-Boullosa, J., Soares, P., et al. *Telomerase expression and proliferative activity suggest a stem cell role for thyroid solid cell nests.* Modern Pathology, 2004. **17**: p. 819–826.
85. Melo, M., Gaspar da Rocha, A., Vinagre, J., Batista, R., et al. *TERT Promoter Mutations Are a Major Indicator of Poor Outcome in Differentiated Thyroid Carcinomas.* J Clin Endocrinol Metab, , 2014. **99**(5): p. E754–E765.
86. Vinagre, J., Almeida, A., Pópulo, H., et al. *Frequency of TERT promoter mutations in human cancers.* Nature Communications 2013. **4**(2185): p. 1-6.
87. Helena Pópulo, H., Paula Boaventura, P., Vinagre, J., Batista, R., et al. *TERT Promoter Mutations in Skin Cancer: The Effects of Sun Exposure and X-Irradiation.* Journal of Investigative Dermatology 2014. **134**: p. 2251–2257.
88. Penna, G.C., Pestana, A., Cameselle, J. M., Momesso, D., et al. *TERTp mutation is associated with a shorter progression free survival in patients with aggressive histology subtypes of follicular-cell derived thyroid carcinoma.* Endocrine, 2018. **61**: p. 489-498.
89. Bournaud, C., Descotes, F., Decaussin-Petrucci, M., et al. *TERT promoter mutations identify a high-risk group in metastasis-free advanced thyroid carcinoma.* European Journal of Cancer 2019. **108**: p. 41-49.
90. Nikiforova, M.N., Chiosea, S. I., Nikiforov, Y. E. *MicroRNA Expression Profiles in Thyroid Tumors.* Endocr Pathol, 2009. **20**: p. 85–91.
91. Pallante, P., Visone, R., Ferracin, M., et al. *MicroRNA deregulation in human thyroid papillary carcinomas.* Endocrine-Related Cancer, 2006. **13**: p. 497–508.
92. Jin, J., Zhang, J., Xue, Y., et al. *miRNA-15a regulates the proliferation and apoptosis of papillary thyroid carcinoma via regulating AKT pathway.* OncoTargets and Therapy 2019. **12** p. 6217–6226.
93. Marini, F., Luzi, E., Brandi, M. L. *MicroRNA Role in Thyroid Cancer Development.* Journal of Thyroid Research, 2011: p. 1-12.
94. Luzón-Toro, B., Fernández, R. M., Villalba-Benito, L., et al. *Influencers on Thyroid Cancer Onset: Molecular Genetic Basis.* Genes, 2019. **10**(913): p. 1-27.
95. Celano, M., Rosignolo, F., Maggisano, V., et al. *MicroRNAs as Biomarkers in Thyroid Carcinoma.* International Journal of Genomics, 2017: p. 1-11.
96. Nikiforova, M.N., Tseng, G. C., Steward, D., D. Diorio, and Y.E. Nikiforov. *MicroRNA Expression Profiling of Thyroid Tumors: Biological Significance and Diagnostic Utility.* J Clin Endocrinol Metab, 2008. **93**(5): p. 1600–1608.
97. Castagna, M.G., Marzocchi, C., Pilli, T., et al. *MicroRNA expression profile of thyroid nodules in fine-needle aspiration cytology: a confirmatory series.* Journal of Endocrinological Investigation 2019. **42**: p. 97-100.
98. Wei, Z., Gao, AB., Wang, Q., et al. *MicroRNA-221 promotes papillary thyroid carcinoma cell migration and invasion via targeting RECK and regulating epithelial–mesenchymal transition.* OncoTargets and Therapy, 2019. **12** p. 2323–2333.
99. Yoruker, E.E., Terzioglu, D., Teksoz, S., et al. *MicroRNA Expression Profiles in Papillary Thyroid Carcinoma, Benign Thyroid Nodules and Healthy Controls.* Journal of Cancer, 2016. **7**(7): p. 803-809.

100. Wang, J., et al. *Identification of key miRNAs in papillary thyroid carcinoma based on data mining and bioinformatics methods.* Biomed Rep, 2020. **12**(1): p. 11-16.
101. Zhang, Y., et al. *Dynamic monitoring of circulating microRNAs as a predictive biomarker for the diagnosis and recurrence of papillary thyroid carcinoma.* Oncol Lett, 2017. **13**(6): p. 4252-4266.
102. Livak, K.J., Schmittgen, T. D. *Analysis of Relative Gene Expression Data Using Real-Time Quantitative PCR and the 2-ΔΔCT Method.* Methods, 2001. **25**: p. 402–408
103. Ren, H., et al. *Co-existence of BRAF(V600E) and TERT promoter mutations in papillary thyroid carcinoma is associated with tumor aggressiveness, but not with lymph node metastasis.* Cancer Manag Res, 2018. **10**: p. 1005-1013.
104. Melo, M., et al. *TERT, BRAF, and NRAS in Primary Thyroid Cancer and Metastatic Disease.* J Clin Endocrinol Metab, 2017. **102**(6): p. 1898-1907.
105. Kebebew, E., et al. *The prevalence and prognostic value of BRAF mutation in thyroid cancer.* Ann Surg, 2007. **246**(3): p. 466-70; discussion 470-1.
106. Jarwani, P.B., Patel, S. *Fine-needle aspiration cytology (FNAC) of the thyroid: A cytohistologic correlation with critical evaluation of discordant cases.* GCSMC J Med Sci, 2013. **11**.
107. Anand, B., Ramdas, A., Ambroise, M. M., Kumar, N. P. *The Bethesda System for Reporting Thyroid Cytopathology: A Cytohistological Study.* Journal of thyroid Research, 2020: p. 1-8.
108. Bakhos, R., Selvaggi, S.M., DeJong, S., Gordon, D.L., Pitale, S.U., Herrmann, M., Wojcik, E.M. *Fine-Needle Aspiration of the Thyroid: Rate and Causes of Cytohistopathologic Discordance.* Diagnostic Cytophatology, 2000. **23**(4): p. 233-237.
109. Pandey, P., N. Mahajan, and A. Dixit. *Fine-needle aspiration of the thyroid: A cytohistologic correlation with critical evaluation of discordant cases.* Thyroid Research and Practice, 2012. **9**(2).
110. Censi, S., Cavedon, E., Bertazza, L., Galuppini, F., Watutantrige-Fernando, S., De Lazzari, P., et al. *Frequency and Significance of Ras,Tert Promoter, and Braf Mutations in Cytologically Indeterminate Thyroid Nodules: A Monocentric Case Series at a Tertiary-Level Endocrinology Unit.* Frontiers in Endocrinology 2017. **8**: p. 1-7.
111. Bellevicine, C., Migliatico, I., Sgariglia, R., Nacchio, M., Vigliar, E., Pisapia, P., Laccarino, A., Bruzzese, D. *Evaluation of BRAF, RAS, RET/PTC, and PAX8/PPARg Alterations in Different Bethesda Diagnostic Categories: A Multicentric Prospective Study on the Validity of the 7-Gene Panel Test in 1172 Thyroid FNAs Deriving From Different Hospitals in South Italy.* Cancer Cytopathology, 2019: p. 107-118.
112. Decaussin-Petrucci, M., et al. *Molecular testing of BRAF, RAS and TERT on thyroid FNAs with indeterminate cytology improves diagnostic accuracy.* Cytopathology, 2017. **28**(6): p. 482-487.
113. Girardi, F.M., M.B. Barra, and C.G. Zettler. *Variants of papillary thyroid carcinoma: association with histopathological prognostic factors.* Braz J Otorhinolaryngol, 2013. **79**(6): p. 738-44.

114. Henke, L.E., Pfeifer, J. D., Baranski, T. J., DeWees, T., Grigsby, P. W. *Long-term outcomes of follicular variant vs classic papillary thyroid carcinoma.* Endocrine connections, 2018. **7**(12): p. 1226-1235.
115. Estrada-Flórez, A.P., Bohórquez, M. E., Vélez, A., Duque, C. S., Donado, J. H., Mateus, G., Panqueba-Tarazona, C., Polanco-Echeverry, G., et al. *BRAF and TERT mutations in papillary thyroid cancer patients of Latino ancestry.* Endocrine connections, 2019. **8**(9): p. 1310-1317.
116. Liu, X., Zhang, S., Gang, Q., Shen, S., Zhang, J., Lun, Y., Xu, D., Duan, Z., Xin, S. *Interstitial fibrosis in papillary thyroid microcarcinoma and its association with biological behavior.* Oncology Letters 2018. **15**: p. 4937-4943.
117. Liu, R., Xing, M. *Diagnostic and Prognostic TERT Promoter Mutations in Thyroid Fine Needle Aspiration Biopsy.* Endocr Relat Cancer 2014. **21**(5): p. 825–830.
118. Argyropoulou, M., Veskoukis, A. S., Karanatsiou, Pagona-Maria., Manolakelli, A., et al. *Low Prevalence of TERT Promoter, BRAF and RAS Mutations in Papillary Thyroid Cancer in the Greek Population.* Pathology & Oncology Research, 2018.
119. Xing, M., et al. *BRAF V600E and TERT promoter mutations cooperatively identify the most aggressive papillary thyroid cancer with highest recurrence.* J Clin Oncol, 2014. **32**(25): p. 2718-26.
120. Park, J.Y., Kim, W. Y., Hwang, T. S., Lee, S. S., Kim, H., Han H. S., Lim, S. D., et al. *BRAF and RAS Mutations in Follicular Variants of Papillary Thyroid carcinoma.* Endocr Pathol, 2013. **24**: p. 69-76.
121. Lupi, C., Giannini, R., Ugolini, C., Proietti, A., Berti, P., Minuto, M., Materazzi, G., Elisei, R., Santoro, M., Miccoli, P., Basolo, F. *Association of BRAF V600E Mutation with Poor Clinicopathological Outcomes in 500 Consecutive Cases of Papillary Thyroid Carcinoma.* The Journal of Clinical Endocrinology & Metabolism 2007. **92**(11): p. 4085–4090.
122. Medici, M., Kwong, N., Angell, T. E., Marqusee, E., Kim, M. I., Frates, M. C., Benson, C. B., Cibas, E. S., Barletta, J. A., et al. *The variable phenotype and low-risk nature of RAS-positive thyroid nodules.* BMC Medicine, 2015. **13**(184).
123. Suresh, R., Sethi, S., Ali, S., Giorgadze, T., Sarkar, F. H. *Differential Expression of MicroRNAs in Papillary Thyroid Carcinoma and Their Role in Racial Disparity.* J Cancer Sci Ther. , 2015. **7**(5): p. 145–154.
124. Lu, Z., Wu, Z., Hu, J., Wei, W., Ma, B., Wen, D. *MicroRNA-15 regulates the proliferation, migration and invasion of thyroid cancer cells by targeting Bcl-2.* JBUON, 2019 **24**(5): p. 2114-2119.
125. Sheikholeslami, S., et al. *Overexpression of mir-129-1, miR-146b, mir-183, and mir-197 in follicular thyroid carcinoma and adenoma tissues.* Mol Cell Probes, 2020. **51**: p. 1-6.
126. Qiu, Z., et al. *miR-146a and miR-146b in the diagnosis and prognosis of papillary thyroid carcinoma.* Oncol Rep, 2017. **38**(5): p. 2735-2740.
127. Visone, R., Russo, L., Pallante, P., De Martino, I., Ferraro, A., et al. *MicroRNAs (miR)-221 and miR-222, both overexpressed in human thyroid papillary carcinomas, regulate p27Kip1 protein levels and cell cycle.* Endocrine-Related Cancer 2007. **14** p. 791–798.
128. Yang, S.I., Choi, Y. S. *Expressions of miRNAs in Papillary Thyroid Carcinoma and Their Associations with the BRAFV600EMutation and Clinicopathological Features.* Kosin Medical Journal 2020. **35**: p. 1-14.

129. Sun, Y., et al. *Expression of miRNAs in Papillary Thyroid Carcinomas Is Associated with BRAF Mutation and Clinicopathological Features in Chinese Patients.* Int J Endocrinol. **2013**: p. 128735.

Supplementary section

Supplementary table 1. Univariate analysis for *TERT* mutation status and clinicopathological features of PTCs

Clinicopathological characteristics	*TERT*		
	WT	Mutated	p-value
Mean age ± Std (n=65)	52.74 ± 16.94	56.50 ± 11.56	0.546
Mean tumor size ± Std (mm) (n=65)	26.12 ± 14.81	35.00 ± 11.20	0.109
Gender (n=65)			
Male	7 (12.3%)	3 (37.5%)	0.098
Female	50 (87.7%)	5 (62.5%)	
Extrathyroidal invasion (n=56)			
Absent	31 (64.6%)	3 (37.5%)	0.241
Present	17 (35.4%)	5 (62.5%)	
Capsule invasion (n=41)			
Absent	5 (13.9%)	0 (0.0%)	1
Present	31 (86.1%)	5 (100%)	
Vascular invasion (n=63)			
Absent	50 (90.9%)	3 (37.5%)	**0.002**
Present	5 (9.1%)	5 (62.5%)	
Venous invasion (n=56)			
Absent	51 (100%)	3 (60.0%)	**0.006**
Present	0 (0.0%)	2 (40.0%)	
Lymphatic invasion (n=58)			
Absent	39 (76.5%)	6 (85.7%)	1
Present	12 (23.5%)	1 (14.3%)	
Fibrosis (n=64)			
Absent	15 (26.8%)	2 (25.0%)	1
Present	41 (73.2%)	6 (75.0%)	
Inflammatory infiltrate (n=64)			
Absent	33 (58.9%)	4 (50.0%)	0.502
Present	22 (39.3%)	4 (50.0%)	
Chronic	1 (1.8%)	0 (0.0%)	
Tall cell (n=64)			
Absent	47 (83.9%)	5 (62.5%)	0.145
< 50%	8 (14.4%)	2 (25.0%)	
≥ 50%	1 (1.8%)	1 (12.5%)	
Oncocytic component (n=64)			
Absent	36 (64.3%)	3 (37.5%)	0.153
< 75%	17 (30.5%)	5 (62.5%)	
≥ 75%	3 (5.4%)	0 (0.0%)	
Psammoma bodies (n=64)			
Absent	43 (76.8%)	7 (87.5%)	0.673
Present	13 (23.2%)	1 (12.5%)	
Calcification (n=64)			
Absent	39 (69.6%)	7 (87.5%)	0.424
Present	17 (30.4%)	1 (12.5%)	
Necrosis (n=64)			
Absent	54 (96.4%)	8 (100%)	1
Present	2 (3.6%)	0 (0.0%)	
Focality (n=65)			
Unifocal	31 (54.4%)	4 (50.0%)	1
Multifocal	26 (45.6%)	4 (50.0%)	
Laterality (n=65)			
Unilateral	35 (61.4%)	7 (87.5%)	0.242
Bilateral	22 (38.6%)	1 (12.5%)	
Lymph node metastasis (n=38)			
Absent	24 (72.7%)	3 (60.0%)	0.615
Present	9 (27.3%)	2 (40.0%)	

Supplementary table 2. Univariate analysis for *BRAF* mutation status and clinicopathological features of PTCs

Clinicopathological characteristics	*BRAF*		
	WT	Mutated	p-value
Mean age ± Std (n=66)	52.39 ± 17.19	55.05 ± 14.33	0.534
Mean tumor size ± Std (mm) (n=66)	28.61 ± 14.11	24.09 ± 15.29	0.237
Gender (n=66)			
Male	5 (11.4%)	5 (22.7%)	0.281
Female	39 (88.6%)	17 (77.3%)	
Extrathyroidal invasion (n=57)			
Absent	28 (71.8%)	6 (33.3%)	**0.009**
Present	11 (28.2%)	12 (66.7%)	
Capsule invasion (n=41)			
Absent	5 (15.2%)	0 (0.0%)	0.563
Present	28 (84.8%)	8 (100%)	
Vascular invasion (n=64)			
Absent	37 (86.0%)	17 (81.0%)	0.717
Present	6 (14.0%)	4 (19.0%)	
Venous invasion (n=57)			
Absent	38 (97.4%)	17 (94.4%)	0.536
Present	1 (2.6%)	1 (5.6%)	
Lymphatic invasion (n=59)			
Absent	31 (79.5%)	15 (75.0%)	0.746
Present	8 (20.5%)	5 (25.0%)	
Fibrosis (n=65)			
Absent	16 (37.2%)	1 (4.5%)	**0.006**
Present	27 (62.8%)	21 (95.5%)	
Inflammatory infiltrate (n=65)			
Absent	31 (72.1%)	6 (27.3%)	**0.009**
Present	11 (25.6%)	16 (72.7%)	
Chronic	1 (2.3%)	0 (0.0%)	
Tall cell (n=65)			
Absent	39 (90.7%)	14 (63.6%)	**0.001**
< 50%	3 (7.0%)	7 (31.8%)	
≥ 50%	1 (2.3%)	1 (4.5%)	
Oncocytic component (n=65)			
Absent	27 (62.8%)	12 (54.5%)	0.522
< 75%	14 (32.6%)	9 (40.7%)	
≥ 75%	2 (4.7%)	1 (4.5%)	
Psammoma bodies (n=65)			
Absent	38 (88.4%)	13 (59.1%)	**0.011**
Present	5 (11.6%)	9 (40.9%)	
Calcification (n=65)			
Absent	34 (79.1%)	13 (59.1%)	0.142
Present	9 (20.9%)	9 (40.9%)	
Necrosis (n=65)			
Absent	42 (97.7%)	21 (95.5%)	1
Present	1 (2.3%)	1 (4.5%)	
Focality (n=66)			
Unifocal	26 (59.1%)	10 (45.5%)	0.31
Multifocal	18 (40.9%)	12 (54.5%)	
Laterality (n=66)			
Unilateral	27 (61.4%)	16 (72.7%)	0.421
Bilateral	17 (38.6%)	6 (27.3%)	
Lymph node metastasis (n=39)			
Absent	19 (82.6%)	9 (56.3%)	0.146
Present	4 (17.4%)	7 (43.8%)	

Supplementary table 3. Univariate analysis for *NRAS* mutation status and clinicopathological features of PTCs

Clinicopathological characteristics	*NRAS*		
	WT	**Mutated**	**p-value**
Mean age ± Std (n=66)	54.51 ± 16.12	38.20 ± 8.53	**0.03**
Mean tumor size ± Std (mm) (n=66)	26.07 ± 14.49	39.80 ± 8.67	**0.042**
Gender (n=66)			
Male	9 (14.8%)	1 (20.0%)	0.573
Female	52 (85.2%)	4 (80.0%)	
Extrathyroidal invasion (n=57)			
Absent	30 (56.6%)	4 (100%)	0.14
Present	23 (43.4%)	0 (0.0%)	
Capsule invasion (n=41)			
Absent	5 (13.2%)	0 (0.0%)	1
Present	33 (86.8%)	3 (100%)	
Vascular invasion (n=64)			
Absent	49 (83.1%)	5 (100%)	1
Present	10 (16.9%)	0 (0.0%)	
Venous invasion (n=57)			
Absent	50 (96.2%)	5 (100%)	1
Present	2 (3.8%)	0 (0.0%)	
Lymphatic invasion (n=59)			
Absent	42 (76.4%)	4 (100%)	0.566
Present	13 (23.6%)	0 (0.0%)	
Fibrosis (n=65)			
Absent	14 (23.3%)	3 (60.0%)	0.107
Present	46 (76.7%)	2 (40.0%)	
Inflammatory infiltrate (n=65)			
Absent	33 (55.0%)	4 (80.0%)	0.269
Present	26 (43.3%)	1 (20.0%)	
Chronic	1 (1.7%)	0 (0.0%)	
Tall cell (n=65)			
Absent	48 (80.0%)	5 (100%)	1
< 50%	10 (16.6%)	0 (0.0%)	
≥ 50%	2 (3.4%)	0 (0.0%)	
Oncocytic component (n=65)			
Absent	37 (61.7%)	2 (40.0%)	0.323
< 75%	21 (35.0%)	2 (40.0%)	
≥ 75%	2 (3.4%)	1 (20.0%)	
Psammoma bodies (n=65)			
Absent	46 (76.7%)	5 (100%)	0.576
Present	14 (23.3%)	0 (0.0%)	
Calcification (n=65)			
Absent	43 (71.7%)	4 (80.0%)	1
Present	17 (28.3%)	1 (20.0%)	
Necrosis (n=65)			
Absent	58 (96.7%)	5 (100%)	1
Present	2 (3.3%)	0 (0.0%)	
Focality (n=66)			
Unifocal	34 (55.7%)	2 (40.0%)	0.652
Multifocal	27 (44.3%)	3 (60.0%)	
Laterality (n=66)			
Unilateral	41 (67.2%)	2 (40.0%)	0.333
Bilateral	20 (32.8%)	3 (60.0%)	
Lymph node metastasis (n=39)			
Absent	27 (71.1%)	1 (100%)	1
Present	11 (28.9%)	0 (0.0%)	

Supplementary table 4. Univariate analysis for *HRAS* mutation status and clinicopathological features of PTCs

Clinicopathological characteristics	*HRAS*		
	WT	Mutated	p-value
Mean age ± Std (n=66)	53.47 ± 16.10	50.25 ± 20.61	0.704
Mean tumor size ± Std (mm) (n=66)	27.60 ± 14.72	19.50 ± 10.21	0.284
Gender (n=66)			
Male	9 (14.5%)	1 (25.0%)	0.49
Female	53 (85.5%)	3 (75.0%)	
Extrathyroidal invasion (n=57)			
Absent	32 (60.4%)	2 (50.0%)	1
Present	21 (39.6%)	2 (50.0%)	
Capsule invasion (n=41)			
Absent	5 (13.5%)	0 (0.0%)	1
Present	32 (86.5%)	4 (100%)	
Vascular invasion (n=64)			
Absent	51 (85.0%)	3 (75.0%)	0.502
Present	9 (15.0%)	1 (25.0%)	
Venous invasion (n=57)			
Absent	52 (96.3%)	3 (100%)	1
Present	2 (3.7%)	0 (0.0%)	
Lymphatic invasion (n=59)			
Absent	43 (76.8%)	3 (100%)	1
Present	13 (23.2%)	0 (0.0%)	
Fibrosis (n=65)			
Absent	14 (23.0%)	3 (75.0%)	0.052
Present	47 (77.0%)	1 (25.0%)	
Inflammatory infiltrate (n=65)			
Absent	33 (54.1%)	4 (100%)	0.098
Present	27 (44.3%)	0 (0.0%)	
Chronic	1 (1.6%)	0 (0.0%)	
Tall cell (n=65)			
Absent	49 (80.3%)	4 (100%)	1
< 50%	10 (16.4%)	0 (0.0%)	
≥ 50%	2 (3.2%)	0 (0.0%)	
Oncocytic component (n=65)			
Absent	36 (59.0%)	3 (75.0%)	0.798
< 75%	22 (36.0%)	1 (25.0%)	
≥ 75%	3 (4.9%)	0 (0.0%)	
Psammoma bodies (n=65)			
Absent	47 (77.0%)	4 (100%)	0.569
Present	14 (23.0%)	0 (0.0%)	
Calcification (n=65)			
Absent	43 (70.5%)	4 (100%)	0.569
Present	18 (29.5%)	0 (0.0%)	
Necrosis (n=65)			
Absent	59 (96.7%)	4 (100%)	1
Present	2 (3.3%)	0 (0.0%)	
Focality (n=66)			
Unifocal	33 (53.2%)	3 (75.0%)	0.62
Multifocal	29 (46.8%)	1 (25.0%)	
Laterality (n=66)			
Unilateral	40 (64.5%)	3 (75.0%)	1
Bilateral	22 (35.5%)	1 (25.0%)	
Lymph node metastasis (n=39)			
Absent	25 (69.4%)	3 (100%)	0.545
Present	11 (30.6%)	0 (0.0%)	

Supplementary table 5. Univariate analysis for *KRAS* mutation status and clinicopathological features of PTCs

Clinicopathological characteristics	*KRAS*		
	WT	**Mutated**	**p-value**
Mean age ± Std (n=66)	53.50 ± 16.37	46.00 ± 11.31	0.524
Mean tumor size ± Std (mm) (n=66)	27.09 ± 14.62	27.50 ± 17.69	0.969
Gender (n=66)			
Male	9 (14.1%)	1 (50.0%)	0.282
Female	55 (85.9%)	1 (50.0%)	
Extrathyroidal invasion (n=57)			
Absent	33 (58.9%)	1 (100%)	1
Present	23 (41.1%)	0 (0.0%)	
Capsule invasion (n=41)			
Absent	4 (10.0%)	1 (100%)	0.122
Present	36 (90.0%)	0 (0.0%)	
Vascular invasion (n=64)			
Absent	52 (83.9%)	2 (100%)	1
Present	10 (16.1%)	0 (0.0%)	
Venous invasion (n=57)			
Absent	53 (96.4%)	2 (100%)	1
Present	2 (3.6%)	0 (0.0%)	
Lymphatic invasion (n=59)			
Absent	44 (77.2%)	2 (100%)	1
Present	13 (22.8%)	0 (0.0%)	
Fibrosis (n=65)			
Absent	16 (25.4%)	1 (50.0%)	0.458
Present	47 (74.6%)	1 (50.0%)	
Inflammatory infiltrate (n=65)			
Absent	36 (57.1%)	1 (50.0%)	1
Present	26 (41.3%)	1 (50.0%)	
Chronic	1 (1.6%)	0 (0.0%)	
Tall cell (n=65)			
Absent	52 (82.5%)	1 (50.0%)	0.337
< 50%	9 (14.4%)	1 (50.0%)	
≥ 50%	2 (3.2%)	0 (0.0%)	
Oncocytic component (n=65)			
Absent	39 (61.9%)	0 (0.0%)	0.132
< 75%	21 (33.5%)	2 (100%)	
≥ 75%	3 (4.8%)	0 (0.0%)	
Psammoma bodies (n=65)			
Absent	49 (77.8%)	2 (100%)	1
Present	14 (22.2%)	0 (0.0%)	
Calcification (n=65)			
Absent	45 (71.4%)	2 (100%)	1
Present	18 (28.6%)	0 (0.0%)	
Necrosis (n=65)			
Absent	61 (96.8%)	2 (100%)	1
Present	2 (3.2%)	0 (0.0%)	
Focality (n=66)			
Unifocal	35 (54.7%)	1 (50.0%)	1
Multifocal	29 (45.3%)	1 (50.0%)	
Laterality (n=66)			
Unilateral	42 (65.6%)	1 (50.0%)	1
Bilateral	22 (34.4%)	1 (50.0%)	
Lymph node metastasis (n=39)			
Absent	28 (71.8%)	-	-
Present	11 (28.2%)	-	

Supplementary table 6. Association of the presence of *BRAF* mutations in *TERT* negative cases with clinicopathological features of PTCs

Clinicopathological characteristics	*TERT*^{WT}/*BRAF*^{WT}	*TERT*^{WT}/*BRAF*^{Mut}	p-value
Mean age ± Std (n=57)	51.60 ± 17.43	55.41 ± 15.90	0.442
Mean tumor size ± Std (mm) (n=57)	28.15 ± 13.85	21.35 ± 16.31	0.114
Gender (n=57)			
Male	4 (10.0%)	3 (17.6%)	0.415
Female	36 (90.0%)	14 (82.4%)	
Extrathyroidal invasion (n=48)			
Absent	26 (74.3%)	5 (38.5%)	**0.039**
Present	9 (25.7%)	8 (61.5%)	
Capsule invasion (n=36)			
Absent	5 (16.7%)	0 (0.0%)	0.564
Present	25 (83.3%)	6 (100%)	
Vascular invasion (n=55)			
Absent	35 (89.7%)	15 (93.8%)	1
Present	4 (10.3%)	1 (6.3%)	
Venous invasion (n=51)			
Absent	36 (100%)	15 (100%)	-
Present	0 (0.0%)	0 (0.0%)	
Lymphatic invasion (n=51)			
Absent	28 (77.8%)	11 (73.3%)	0.730
Present	8 (22.2%)	4 (26.7%)	
Fibrosis (n=56)			
Absent	14 (35.9%)	1 (5.9%)	**0.023**
Present	25 (64.1%)	16 (94.1%)	
Inflammatory infiltrate (n=56)			
Absent	28 (71.8%)	5 (29.4%)	**0.003**
Present	10 (25.6%)	12 (70.6%)	
Chronic	1 (2.6%)	0 (0.0%)	
Tall cell (n=56)			
Absent	35 (89.7%)	12 (70.6%)	**0.027**
< 50%	3 (7.7%)	5 (29.4%)	
≥ 50%	1 (2.6%)	0 (0.0%)	
Oncocytic component (n=56)			
Absent	26 (66.7%)	10 (58.8%)	0.436
< 75%	11 (28.2%)	6 (35.3%)	
≥ 75%	2 (5.1%)	1 (5.9%)	
Psammoma bodies (n=56)			
Absent	34 (87.2%)	9 (52.9%)	**0.013**
Present	5 (12.8%)	8 (47.1%)	
Calcification (n=56)			
Absent	30 (76.9%)	9 (52.9%)	0.113
Present	9 (23.1%)	8 (47.1%)	
Necrosis (n=56)			
Absent	38 (97.4%)	16 (94.1%)	0.519
Present	1 (2.6%)	1 (5.9%)	
Focality (n=57)			
Unifocal	23 (57.5%)	8 (47.1%)	0.566
Multifocal	17 (42.5%)	9 (52.9%)	
Laterality (n=57)			
Unilateral	24 (60.0%)	11 (64.7%)	0.776
Bilateral	16 (40.0%)	6 (35.3%)	
Lymph node metastasis (n=33)			
Absent	17 (81.0%)	7 (58.3%)	0.230
Present	4 (19.0%)	5 (41.7%)	

Supplementary table 7. Association of the concomitant presence of *TERT* and *BRAF* mutations in association with clinicopathological features of PTCs

Clinicopathological characteristics	*TERT*^{WT}/*BRAF*^{WT}	*TERT*^{Mut}/*BRAF*^{Mut}	p-value
Mean age ± Std (n=45)	51.60 ± 17.43	53.80 ± 7.98	0.636
Mean tumor size ± Std (mm) (n=45)	28.15 ± 13.85	33.40 ± 4.76	0.107
Gender (n=45)			
Male	4 (10.0%)	2 (40.0%)	0.125
Female	36 (90.0%)	3 (60.0%)	
Extrathyroidal invasion (n=40)			
Absent	26 (74.3%)	1 (20.0%)	**0.031**
Present	9 (25.7%)	4 (80.0%)	
Capsule invasion (n=32)			
Absent	5 (16.7%)	0 (0.0%)	1
Present	25 (83.3%)	2 (100%)	
Vascular invasion (n=44)			
Absent	35 (89.7%)	2 (40.0%)	**0.023**
Present	4 (10.3%)	3 (60.0%)	
Venous invasion (n=39)			
Absent	36 (100%)	2 (66.7%)	0.077
Present	0 (0.0%)	1 (33.3%)	
Lymphatic invasion (n=41)			
Absent	28 (77.8%)	4 (80.0%)	1
Present	8 (22.2%)	1 (20.0%)	
Fibrosis (n=44)			
Absent	14 (35.9%)	0 (0.0%)	0.161
Present	25 (64.1%)	5 (100%)	
Inflammatory infiltrate (n=44)			
Absent	28 (71.8%)	1 (20.0%)	0.061
Present	10 (25.6%)	4 (80.0%)	
Chronic	1 (2.6%)	0 (0.0%)	
Tall cell (n=44)			
Absent	35 (89.7%)	2 (40.0%)	**0.010**
< 50%	3 (7.7%)	2 (40.0%)	
≥ 50%	1 (2.6%)	1 (20.0%)	
Oncocytic component (n=44)			
Absent	26 (66.7%)	2 (40.0%)	0.376
< 75%	11 (28.2%)	3 (60.0%)	
≥ 75%	2 (5.1%)	0 (0.0%)	
Psammoma bodies (n=44)			
Absent	34 (87.2%)	4 (80.0%)	0.538
Present	5 (12.8%)	1 (20.0%)	
Calcification (n=44)			
Absent	30 (76.9%)	4 (80.0%)	1
Present	9 (23.1%)	1 (20.0%)	
Necrosis (n=44)			
Absent	38 (97.4%)	5 (100%)	1
Present	1 (2.6%)	0 (0.0%)	
Focality (n=45)			
Unifocal	23 (57.5%)	2 (40.0%)	0.642
Multifocal	17 (42.5%)	3 (60.0%)	
Laterality (n=45)			
Unilateral	24 (60.0%)	5 (100%)	0.144
Bilateral	16 (40.0%)	0 (0.0%)	
Lymph node metastasis (n=25)			
Absent	17 (81.0%)	2 (50.0%)	0.234
Present	4 (19.0%)	2 (50.0%)	

Supplementary table 8. *RAS* mutations in association with clinicopathological features of PTCs

Clinicopathological characteristics	*RAS*		
	WT	**Mutated**	**p-value**
Mean age ± Std (n=66)	55.13 ± 16.08	44.00 ± 14.23	**0.037**
Mean tumor size ± Std (mm) (n=66)	26.49 ± 14.78	30.18 ± 13.64	0.447
Gender (n=66)			
Male	7 (12.7%)	3 (27.3%)	0.351
Female	48 (87.3%)	8 (72.7%)	
Extrathyroidal invasion (n=57)			
Absent	27 (56.3%)	7 (77.8%)	0.288
Present	21 (43.8%)	2 (22.2%)	
Capsule invasion (n=41)			
Absent	4 (12.1%)	1 (12.5%)	1
Present	29 (87.9%)	7 (87.5%)	
Vascular invasion (n=64)			
Absent	44 (83.0%)	10 (90.9%)	1
Present	9 (17.0%)	1 (9.1%)	
Venous invasion (n=57)			
Absent	45 (95.7%)	10 (100%)	1
Present	2 (4.3%)	0 (0.0%)	
Lymphatic invasion (n=59)			
Absent	37 (74.0%)	9 (100%)	0.185
Present	13 (26.0%)	0 (0.0%)	
Fibrosis (n=65)			
Absent	10 (18.5%)	7 (63.6%)	**0.005**
Present	44 (81.5%)	4 (36.4%)	
Inflammatory infiltrate (n=65)			
Absent	28 (51.9%)	9 (81.8%)	0.253
Present	25 (46.3%)	2 (18.2%)	
Chronic	1 (1.9%)	0 (0.0%)	
Tall cell (n=65)			
Absent	43 (79.6%)	10 (90.9%)	0.915
< 50%	9 (16.8%)	1 (9.1%)	
≥ 50%	2 (3.8%)	0 (0.0%)	
Oncocytic component (n=65)			
Absent	34 (63.0%)	5 (45.5%)	0.354
< 75%	18 (33.6%)	5 (45.5%)	
≥ 75%	2 (3.8%)	1 (9.1%)	
Psammoma bodies (n=65)			
Absent	40 (74.1%)	11 (100%)	0.102
Present	14 (25.9%)	0 (0.0%)	
Calcification (n=65)			
Absent	37 (68.5%)	10 (90.9%)	0.265
Present	17 (31.5%)	1 (9.1%)	
Necrosis (n=65)			
Absent	52 (96.3%)	11 (100%)	1
Present	2 (3.7%)	0 (0.0%)	
Focality (n=66)			
Unifocal	30 (54.5%)	6 (54.5%)	1
Multifocal	25 (45.5%)	5 (45.5%)	
Laterality (n=66)			
Unilateral	37 (67.3%)	6 (54.5%)	0.495
Bilateral	18 (32.7%)	5 (45.5%)	
Lymph node metastasis (n=39)			
Absent	24 (68.6%)	4 (100%)	0.309
Present	11 (31.4%)	0 (0.0%)	

1. **Relationship between clinicopathological features and the molecular profile of whole series**

Univariate analysis was performed to determine possible associations between the presence of genetic alterations and the clinicopathological features of the patients/tumors. The presence of *TERT*p mutations was significantly associated with vascular (p=0.004) and venous invasion (p=0.027) (Supplementary table 9 and 10).

BRAF mutations were significantly associated with the presence of extrathyroidal invasion (p=0.01), fibrosis (p=0.004), inflammatory infiltrate (p=0.001), tall cell component (p=0.001) and psammoma bodies (p=0.007) (Supplementary table 9 and 11).

Patients with NRAS mutation are significant associated with younger age (p=0.033) (Supplementary table 9 and 12).

For *HRAS* and *KRAS* mutations and clinicopathological features no statistically significant associations were observed (Supplementary table 13 and 14, respectively).

Looking to the presence of mutations in any *RAS* genes (*NRAS*, *HRAS* and *KRAS*), we found a significant association with the absence of fibrosis (p=0.008) (Supplementary table 9 and 15).

Supplementary table 9. Summary of significant associations between mutations and clinicopathological features of all series

Mutations	Clinicopathological characteristics	WT	Mutated	*p*-value
***TERT*p**	**Vascular invasion** (n=73)			
	Absent	57 (87.7%)	3 (37.5%)	**0.004**
	Present	8 (12.3%)	5 (62.5%)	
	Venous invasion (n=65)			
	Absent	58 (96.7%)	3 (60.0%)	**0.027**
	Present	2 (3.3%)	2 (40.0%)	
BRAF	**Extrathyroidal invasion** (n=67)			
	Absent	35 (71.4%)	6 (33.3%)	**0.01**
	Present	14 (28.6%)	12 (66.7%)	
	Fibrosis (n=72)			
	Absent	19 (38.0%)	1 (4.5%)	**0.004**
	Present	31 (62.0%)	21 (95.5%)	
	Inflammatory infiltrate (n=73)			
	Absent	36 (70.6%)	6 (27.3%)	**0.001**
	Present	14 (27.5%)	16 (72.7%)	
	Chronic	1 (2.0%)	0 (0.0%)	
	Tall cell (n=72)			
	Absent	46 (92.0%)	14 (63.6%)	**0.001**
	< 50%	3 (6.0%)	7 (31.8%)	
	≥ 50%	1 (2.0%)	1 (4.5%)	
	Psammoma bodies (n=72)			
	Absent	45 (90.0%)	13 (59.1%)	**0.007**
	Present	5 (10.0%)	9 (40.9%)	
NRAS	**Mean age ± Std** (n=90)	53.36 ± 15.46	38.20 ± 8.53	**0.033**
***RAS* (*NRAS*, *HRAS* and *KRAS*)**	**Fibrosis** (n=72)			
	Absent	13 (21.3%)	7 (63.6%)	**0.008**
	Present	48 (78.7%)	4 (36.4%)	

Supplementary table 10. Univariate analysis for *TERT* status and clinicopathological features in all series

Clinicopathological characteristics	*TERT*		
	WT	**Mutated**	**p-value**
Mean age ± Std (n=88)	51.94 ± 16.01	56.5 ± 11.56	0.435
Mean tumor size ± Std (mm) (n=81)	26.63 ± 15.54	35.00 ± 11.20	0.143
Gender (n=88)			
Male	12 (15.0%)	3 (37.5%)	0.133
Female	68 (85.0%)	5 (62.5%)	
Extrathyroidal invasion (n=66)			
Absent	38 (65.5%)	3 (37.5%)	0.242
Present	20 (34.5%)	5 (62.5%)	
Capsule invasion (n=49)			
Absent	8 (18.2%)	0 (0.0%)	0.575
Present	36 (81.8%)	5 (100%)	
Vascular invasion (n=73)			
Absent	57 (87.7%)	3 (37.5%)	**0.004**
Present	8 (12.3%)	5 (62.5%)	
Venous invasion (n=65)			
Absent	58 (96.7%)	3 (60.0%)	**0.027**
Present	2 (3.3%)	2 (40.0%)	
Lymphatic invasion (n=65)			
Absent	46 (79.3%)	6 (85.7%)	1
Present	12 (20.7%)	1 (14.3%)	
Fibrosis (n=71)			
Absent	18 (28.6%)	2 (25.0%)	1
Present	45 (71.4%)	6 (75.0%)	
Inflammatory infiltrate (n=72)			
Absent	38 (59.4%)	4 (50.0%)	0.74
Present	25 (39.1%)	4 (50.0%)	
Chronic	1 (1.6%)	0 (0.0%)	
Tall cell (n=71)			
Absent	54 (85.7%)	5 (62.5%)	0.112
< 50%	8 (12.8%)	2 (25.0%)	
≥ 50%	1 (1.6%)	1 (12.5%)	
Oncocytic component (n=71)			
Absent	40 (63.5%)	3 (37.5%)	0.112
< 75%	17 (27.1%)	5 (62.5%)	
≥ 75%	6 (9.5%)	0 (0.0%)	
Psammoma bodies (n=71)			
Absent	50 (79.4%)	7 (87.5%)	1
Present	13 (20.6%)	1 (12.5%)	
Calcification (n=71)			
Absent	46 (73.0%)	7 (87.5%)	0.67
Present	17 (27.0%)	1 (12.5%)	
Necrosis (n=71)			
Absent	60 (95.2%)	8 (100%)	1
Present	3 (4.8%)	0 (0.0%)	
Focality (n=88)			
Unifocal	39 (48.8%)	4 (50.0%)	1
Multifocal	41 (51.2%)	4 (50.0%)	
Laterality (n=88)			
Unilateral	50 (62.5%)	7 (87.5%)	0.251
Bilateral	30 (37.5%)	1 (12.5%)	
Lymph node metastasis (n=45)			
Absent	29 (72.5%)	3 (60.0%)	0.617
Present	11 (27.5%)	2 (40.0%)	

Supplementary table 11. Univariate analysis for *BRAF* status and clinicopathological features in all series

Clinicopathological characteristics	*BRAF*		
	WT	Mutated	p-value
Mean age ± Std (n=90)	51.71 ± 15.91	22 ± 14.33	0.383
Mean tumor size ± Std (mm) (n=83)	28.75 ± 15.13	24.09 ± 15.29	0.22
Gender (n=90)			
Male	10 (14.7%)	5 (22.7%)	0.51
Female	58 (85.3%)	17 (77.3%)	
Extrathyroidal invasion (n=67)			
Absent	35 (71.4%)	6 (33.3%)	**0.01**
Present	14 (28.6%)	12 (66.7%)	
Capsule invasion (n=49)			
Absent	8 (19.5%)	0 (0.0%)	0.322
Present	33 (80.5%)	8 (100%)	
Vascular invasion (n=74)			
Absent	44 (83.0%)	17 (81.0%)	1
Present	9 (17.0%)	4 (19.0%)	
Venous invasion (n=66)			
Absent	45 (93.8%)	17 (94.4%)	1
Present	3 (6.3%)	1 (5.6%)	
Lymphatic invasion (n=66)			
Absent	38 (82.6%)	15 (75.0%)	0.512
Present	8 (17.4%)	5 (25.0%)	
Fibrosis (n=72)			
Absent	19 (38.0%)	1 (4.5%)	**0.004**
Present	31 (62.0%)	21 (95.5%)	
Inflammatory infiltrate (n=73)			
Absent	36 (70.6%)	6 (27.3%)	**0.001**
Present	14 (27.5%)	16 (72.7%)	
Chronic	1 (2.0%)	0 (0.0%)	
Tall cell (n=72)			
Absent	46 (92.0%)	14 (63.6%)	**0.001**
< 50%	3 (6.0%)	7 (31.8%)	
≥ 50%	1 (2.0%)	1 (4.5%)	
Oncocytic component (n=72)			
Absent	31 (62.0%)	12 (54.5%)	0.619
< 75%	14 (28.0%)	9 (40.7%)	
≥ 75%	5 (10.0%)	1 (4.5%)	
Psammoma bodies (n=72)			
Absent	45 (90.0%)	13 (59.1%)	**0.007**
Present	5 (10.0%)	9 (40.9%)	
Calcification (n=72)			
Absent	41 (82.0%)	13 (59.1%)	0.074
Present	9 (18.0%)	9 (40.9%)	
Necrosis (n=72)			
Absent	48 (96.0%)	21 (95.5%)	1
Present	2 (4.0%)	1 (4.5%)	
Focality (n=90)			
Unifocal	34 (50.0%)	10 (45.5%)	0.808
Multifocal	34 (50.0%)	12 (54.5%)	
Laterality (n=90)			
Unilateral	43 (63.2%)	16 (72.7%)	0.453
Bilateral	25 (36.8%)	6 (27.3%)	
Lymph node metastasis (n=46)			
Absent	24 (80.0%)	9 (56.3%)	0.167
Present	6 (20.0%)	7 (43.8%)	

Supplementary table 12. Univariate analysis for *NRAS* status and clinicopathological features in all series

Clinicopathological characteristics	*NRAS*		
	WT	**Mutated**	**p-value**
Mean age ± Std (n=90)	53.36 ± 15.46	38.20 ± 8.53	**0.033**
Mean tumor size ± Std (mm) (n=83)	26.73 ± 15.24	39.80 ± 8.67	0.062
Gender (n=90)			
Male	14 (16.5%)	1 (20.0%)	1
Female	71 (83.5%)	4 (80.0%)	
Extrathyroidal invasion (n=67)			
Absent	37 (58.7%)	4 (100%)	0.152
Present	26 (41.3%)	0 (0.0%)	
Capsule invasion (n=49)			
Absent	8 (17.4%)	0 (0.0%)	1
Present	38 (82.6%)	3 (100%)	
Vascular invasion (n=74)			
Absent	56 (81.2%)	5 (100%)	0.579
Present	13 (18.8%)	0 (0.0%)	
Venous invasion (n=66)			
Absent	57 (93.4%)	5 (100%)	1
Present	4 (6.6%)	0 (0.0%)	
Lymphatic invasion (n=66)			
Absent	49 (79.0%)	4 (100%)	0.577
Present	13 (21.0%)	0 (0.0%)	
Fibrosis (n=72)			
Absent	17 (25.4%)	3 (60.0%)	0.127
Present	50 (74.6%)	2 (40.0%)	
Inflammatory infiltrate (n=73)			
Absent	38 (55.9%)	4 (80.0%)	0.435
Present	29 (42.6%)	1 (20.0%)	
Chronic	1 (1.5%)	0 (0.0%)	
Tall cell (n=72)			
Absent	55 (82.1%)	5 (100%)	1
< 50%	10 (15.0%)	0 (0.0%)	
≥ 50%	2 (3.0%)	0 (0.0%)	
Oncocytic component (n=72)			
Absent	41 (61.2%)	2 (40.0%)	0.285
< 75%	21 (31.5%)	2 (40.0%)	
≥ 75%	5 (7.5%)	1 (20.0%)	
Psammoma bodies (n=72)			
Absent	53 (79.1%)	5 (100%)	0.575
Present	14 (20.9%)	0 (0.0%)	
Calcification (n=72)			
Absent	50 (74.6%)	4 (80.0%)	1
Present	17 (25.4%)	1 (20.0%)	
Necrosis (n=72)			
Absent	64 (95.5%)	5 (100%)	1
Present	3 (4.5%)	0 (0.0%)	
Focality (n=90)			
Unifocal	42 (49.4%)	2 (40.0%)	1
Multifocal	43 (50.6%)	3 (60.0%)	
Laterality (n=90)			
Unilateral	57 (67.1%)	2 (40.0%)	0.335
Bilateral	28 (32.9%)	3 (60.0%)	
Lymph node metastasis (n=46)			
Absent	32 (71.1%)	1 (100%)	1
Present	13 (28.9%)	0 (0.0%)	

Supplementary table 13. Univariate analysis for *HRAS* status and clinicopathological features in all series

Clinicopathological characteristics	*HRAS*		
	WT	**Mutated**	**p-value**
Mean age ± Std (n=90)	52.63 ± 15.40	50.25 ± 20.61	0.766
Mean tumor size ± Std (mm) (n=83)	27.92 ± 15.36	19.50 ± 10.21	0.283
Gender (n=90)			
Male	14 (16.3%)	1 (25.0%)	0.524
Female	72 (83.7%)	3 (75.0%)	
Extrathyroidal invasion (n=67)			
Absent	39 (61.9%)	2 (50.0%)	0.638
Present	24 (38.1%)	2 (50.0%)	
Capsule invasion (n=49)			
Absent	8 (17.8%)	0 (0.0%)	1
Present	37 (82.2%)	4 (100%)	
Vascular invasion (n=74)			
Absent	58 (82.9%)	3 (75.0%)	0.546
Present	12 (17.1%)	1 (25.0%)	
Venous invasion (n=66)			
Absent	59 (93.7%)	3 (100%)	1
Present	4 (6.3%)	0 (0.0%)	
Lymphatic invasion (n=66)			
Absent	50 (79.4%)	3 (100%)	1
Present	13 (20.6%)	0 (0.0%)	
Fibrosis (n=72)			
Absent	17 (25.0%)	3 (75.0%)	0.062
Present	51 (75.0%)	1 (25.0%)	
Inflammatory infiltrate (n=73)			
Absent	38 (55.1%)	4 (100%)	0.183
Present	30 (43.5%)	0 (0.0%)	
Chronic	1 (1.4%)	0 (0.0%)	
Tall cell (n=72)			
Absent	56 (82.4%)	4 (100%)	1
< 50%	10 (14.6%)	0 (0.0%)	
≥ 50%	2 (3.0%)	0 (0.0%)	
Oncocytic component (n=72)			
Absent	40 (58.8%)	3 (75.0%)	0.76
< 75%	22 (32.2%)	1 (25.0%)	
≥ 75%	6 (8.8%)	0 (0.0%)	
Psammoma bodies (n=72)			
Absent	54 (79.4%)	4 (100%)	0.58
Present	14 (20.6%)	0 (0.0%)	
Calcification (n=72)			
Absent	50 (73.5%)	4 (100%)	0.566
Present	18 (26.5%)	0 (0.0%)	
Necrosis (n=72)			
Absent	65 (95.6%)	4 (100%)	1
Present	3 (4.4%)	0 (0.0%)	
Focality (n=90)			
Unifocal	41 (47.7%)	3 (75.0%)	0.355
Multifocal	45 (52.3%)	1 (25.0%)	
Laterality (n=90)			
Unilateral	56 (65.1%)	3 (75.0%)	1
Bilateral	30 (34.9%)	1 (25.0%)	
Lymph node metastasis (n=46)			
Absent	30 (69.8%)	3 (100%)	0.548
Present	13 (30.2%)	0 (0.0%)	

Supplementary table 14. Univariate analysis for *KRAS* status and clinicopathological features in all series

Clinicopathological characteristics	*KRAS*		
	WT	**Mutated**	**p-value**
Mean age ± Std (n=90)	52.67 ± 15.62	46.00 ± 11.31	0.551
Mean tumor size ± Std (mm) (n=83)	27.52 ± 15.28	27.50 ± 17.68	0.999
Gender (n=90)			
Male	14 (15.9%)	1 (50.0%)	0.307
Female	74 (84.1%)	1 (50.0%)	
Extrathyroidal invasion (n=67)			
Absent	40 (60.6%)	1 (100%)	1
Present	26 (39.4%)	0 (0.0%)	
Capsule invasion (n=49)			
Absent	7 (14.6%)	1 (100%)	0.163
Present	41 (85.4%)	0 (0.0%)	
Vascular invasion (n=74)			
Absent	59 (81.9%)	2 (100%)	1
Present	13 (18.1%)	0 (0.0%)	
Venous invasion (n=66)			
Absent	60 (93.8%)	2 (100%)	1
Present	4 (6.3%)	0 (0.0%)	
Lymphatic invasion (n=66)			
Absent	51 (79.7%)	2 (100%)	1
Present	13 (20.3%)	0 (0.0%)	
Fibrosis (n=72)			
Absent	19 (27.1%)	1 (50.0%)	0.481
Present	51 (72.9%)	1 (50.0%)	
Inflammatory infiltrate (n=73)			
Absent	41 (57.7%)	1 (50.0%)	1
Present	29 (40.8%)	1 (50.0%)	
Chronic	1 (1.4%)	0 (0.0%)	
Tall cell (n=72)			
Absent	59 (84.3%)	1 (50.0%)	0.308
< 50%	9 (12.9%)	1 (50.0%)	
≥ 50%	2 (2.8%)	0 (0.0%)	
Oncocytic component (n=72)			
Absent	43 (61.4%)	0 (0.0%)	0.129
< 75%	21 (30.0%)	2 (100%)	
≥ 75%	6 (8.6%)	0 (0.0%)	
Psammoma bodies (n=72)			
Absent	56 (80.0%)	2 (100%)	1
Present	14 (20.0%)	0 (0.0%)	
Calcification (n=72)			
Absent	52 (74.3%)	2 (100%)	1
Present	18 (25.7%)	0 (0.0%)	
Necrosis (n=72)			
Absent	67 (95.7%)	2 (100%)	1
Present	3 (4.3%)	0 (0.0%)	
Focality (n=90)			
Unifocal	43 (48.9%)	1 (50.0%)	1
Multifocal	45 (51.1%)	1 (50.0%)	
Laterality (n=90)			
Unilateral	58 (65.9%)	1 (50.0%)	1
Bilateral	30 (34.1%)	1 (50.0%)	
Lymph node metastasis (n=46)			
Absent	33 (71.7%)	0 (0.0%)	-
Present	13 (28.3%)	0 (0.0%)	

Supplementary table 15. Univariate analysis for *RAS* status and clinicopathological features in all series

Clinicopathological characteristics	*RAS*		
	WT	**Mutated**	**p-value**
Mean age ± Std (n=90)	53.71 ± 15.41	44.00 ± 14.23	0.051
Mean tumor size ± Std (mm) (n=83)	27.11 ± 15.49	30.18 ± 13.64	0.536
Gender (n=90)			
Male	12 (15.2%)	3 (27.3%)	0.384
Female	67 (84.8%)	8 (72.7%)	
Extrathyroidal invasion (n=67)			
Absent	35 (60.3%)	7 (77.8%)	0.466
Present	23 (39.7%)	2 (22.2%)	
Capsule invasion (n=49)			
Absent	7 (17.1%)	1 (12.5%)	1
Present	34 (82.9%)	7 (87.5%)	
Vascular invasion (n=74)			
Absent	51 (81.0%)	10 (90.9%)	0.676
Present	12 (19%)	1 (9.1%)	
Venous invasion (n=66)			
Absent	52 (92.9%)	10 (100%)	1
Present	4 (7.1%)	0 (0.0%)	
Lymphatic invasion (n=66)			
Absent	44 (77.2%)	9 (100%)	0.186
Present	13 (22.8%)	0 (0.0%)	
Fibrosis (n=72)			
Absent	13 (21.3%)	7 (63.6%)	**0.008**
Present	48 (78.7%)	4 (36.4%)	
Inflammatory infiltrate (n=73)			
Absent	33 (53.2%)	9 (81.8%)	0.242
Present	28 (45.2%)	2 (18.2%)	
Chronic	1 (1.6%)	0 (0.0%)	
Tall cell (n=72)			
Absent	50 (82.0%)	10 (90.9%)	0.887
< 50%	9 (14.7%)	1 (9.1%)	
≥ 50%	2 (3.2%)	0 (0.0%)	
Oncocytic component (n=72)			
Absent	38 (62.3%)	5 (45.5%)	0.258
< 75%	18 (29.5%)	5 (45.5%)	
≥ 75%	5 (8.2%)	1 (9.1%)	
Psammoma bodies (n=72)			
Absent	47 (77.0%)	11 (100%)	0.107
Present	14 (23.0%)	0 (0.0%)	
Calcification (n=72)			
Absent	44 (72.1%)	10 (90.9%)	0.271
Present	17 (27.9%)	1 (9.1%)	
Necrosis (n=72)			
Absent	58 (95.1%)	11 (100%)	1
Present	3 (4.9%)	0 (0.0%)	
Focality (n=90)			
Unifocal	38 (48.1%)	6 (54.5%)	0.755
Multifocal	41 (51.9%)	5 (45.5%)	
Laterality (n=90)			
Unilateral	53 (67.1%)	6 (54.5%)	0.502
Bilateral	26 (32.9%)	5 (45.5%)	
Lymph node metastasis (n=46)			
Absent	29 (69.0%)	4 (100%)	0.313
Present	13 (31.0%)	0 (0.0%)	

2. Relationship between clinicopathological features and the presence of lymph node metastasis (LNM)

For 46 cases, information regarding the presence of LNM was available (Supplementary table 16). 13 cases (28.3%) presented LNM at diagnosis. Six (13%) patients were male and 40 (87%) were female. No significant associations were found with age, tumor size nor gender. The presence of extrathyroidal and vascular invasion were significantly associated with the presence of LNM (p=0.0003, p=0.021, respectively). A significant association was also obtained regarding the presence of venous invasion (p=0.049). The presence of lymphatic invasion and inflammatory infiltrate have a significant association with the presence of LNM (p=0.0002 and p=0.017, respectively).

When we compared the presence of genetic alterations with the presence of LNM, we saw a significant association with the presence of *BRAF* mutation for cytology samples (p=0.017) (data not shown) and a tendency for significance when *TERT*p was mutated (p=0.062) (data not shown). No statistical significance was found in histology.

Supplementary table 16. Analysis of clinicopathological features with the presence or absence of LNM

Clinicopathological characteristics	Lymph node metastasis (n=46)		
	Absent	Present	p-value
Mean age ± Std (n=46)	50.06 ± 15.01	56.54 ± 18.89	0.283
Mean tumor size ± Std (mm) (n=45)	24.79 ± 12.99	32.83 ± 19.54	0.206
Gender (n=46)			
Male	5 (15.2%)	1 (7.7%)	0.659
Female	28 (84.8%)	12 (92.3%)	
Extrathyroidal invasion (n=42)			
Absent	22 (73.3%)	1 (8.3%)	**0.0003**
Present	8 (26.7%)	11 (91.7%)	
Capsule invasion (n=25)			
Absent	2 (9.1%)	0 (0.0%)	1
Present	20 (90.9%)	3 (100%)	
Vascular invasion (n=42)			
Absent	30 (93.8%)	6 (60.0%)	**0.021**
Present	2 (6.3%)	4 (40.0%)	
Venous invasion (n=39)			
Absent	30 (100%)	7 (77.8%)	**0.049**
Present	0 (0.0%)	2 (22.2%)	
Lymphatic invasion (n=42)			
Absent	28 (87.5%)	2 (20.0%)	**0.0002**
Present	4 (12.5%)	8 (80.0%)	
Fibrosis (n=41)			
Absent	9 (30.0%)	0 (0.0%)	0.083
Present	21 (70.0%)	11 (100%)	
Inflammatory infiltrate (n=41)			
Absent	19 (63.3%)	2 (18.2%)	**0.017**
Present	10 (33.3%)	9 (81.8%)	
Chronic	1 (3.3%)	0 (0.0%)	
Psammoma bodies (n=41)			
Absent	23 (76.7%)	7 (63.6%)	0.445
Present	7 (23.3%)	4 (36.4%)	
Calcification (n=41)			
Absent	22 (73.3%)	6 (54.5%)	0.280
Present	8 (26.7%)	5 (45.5%)	
Necrosis (n=41)			
Absent	29 (96.7%)	9 (81.8%)	0.170
Present	1 (3.3%)	2 (18.2%)	
Focality (n=46)			
Unifocal	21 (63.6%)	7 (53.8%)	0.738
Multifocal	12 (36.4%)	6 (46.2%)	
Laterality (n=46)			
Unilateral	27 (81.8%)	8 (61.5%)	0.248
Bilateral	6 (18.2%)	5 (38.5%)	

FACULDADE DE **MEDICINA**